Synthesis, Dyeing Potential, Antibacterial Activity and Docking Study of Azo Dye Derivatives

By

RUTH SAHILU

A Thesis Submitted to

The department of Applied Chemistry

School of Applied Natural Sciences

Presented in Partial Fulfillment of the Requirements for Master of Science Degree in Applied Chemistry (Specialization in Synthetic Organic Chemistry)

Office of Graduate Studies

Adama Science and Technology University

June, 2021

Adama, Ethiopia

Synthesis, Characterization, Dyeing Potential, Antibacterial Activity and Docking Study of Azo Dye Derivatives

By

RUTH SAHILU

Major Advisor: Prof. Aman Dekebo

Co-Advisor: Dr. Endale Mulugeta

A Thesis Submitted to

The department of Applied Chemistry

School of Applied Natural Sciences

Presented in Partial Fulfillment of the Requirements for Master of Science Degree in Applied Chemistry (Specialization in Synthetic Organic Chemistry)

Office of Graduate Studies

Adama Science and Technology University

June, 2021

Adama, Ethiopia

DECLARATION

I hereby declare that this Master Thesis entitled “Synthesis, Dyeing Potential, Antibacterial Activity and Docking Study of Azo Dye Derivatives” is my original work. That is, it has not been submitted for the award of any academic degree, diploma or certificate in any other university. All sources of materials that are used for this thesis have been duly acknowledged through citation.

_____	_____	_____
Name of the student	Signature	Date

RECOMMENDATION

I/we, the advisor(s) of this thesis, hereby certify that I/we have read the revised version of the thesis entitled “Synthesis, Dyeing Potential, Antibacterial Activity and Docking Study of Azo Dye Derivatives” prepared under my/our guidance by Ruth Sahilu submitted in partial fulfillment of the requirements for the degree of Masters of Science Synthetic Organic Chemistry.

Therefore, I/we recommend the submission of revised version of the thesis to the department following the applicable procedures.

Prof. Aman Desta		_____
Major Advisor	Signature	Date
_____	_____	_____
Co-advisor	Signature	Date

APPROVAL OF BOARD OF EXAMINERS

we, the advisors of the thesis entitled “Synthesis, Dyeing Potential, Antibacterial Activity and Docking Study of Azo Dye Derivatives” and developed by Ruth Sahilu, hereby certify that the recommendation and suggestions made by the board of examiners are appropriately incorporated into the final version of the thesis.

Prof. Aman Dekebo _____ _____

Major Advisor Signature Date

_____ _____ _____

Co-advisor Signature Date

We, the undersigned, members of the Board of Examiners of the thesis by Ruth Sahilu have read and evaluated the thesis entitled “Synthesis, Dyeing Potential, Antibacterial Activity and Docking Study of Azo Dye Derivatives” and examined the candidate during open defense. This is, therefore, to certify that the thesis is accepted for partial fulfillment of the requirement of the degree of Master of Science in Synthetic Organic Chemistry.

_____ _____ _____

Chairperson Signature Date

_____ _____ _____

Internal Examiner Signature Date

Mesfin Getachew (PhD) _____ _____

External Examiner Signature Date

Final approval and acceptance of the thesis is contingent upon submission of its final copy to the Office of Postgraduate Studies (OPGS) through the Department Graduate Council (DGC) and School Graduate Committee (SGC).

_____ _____ _____

Department Head Signature Date

_____ _____ _____

School Dean Signature Date

_____ _____ _____

Office of Postgraduate Studies, Dean Signature Date

ACKNOWLEDGMENTS

First, I would like to thank the Almighty God for providing health and strength to conduct this piece of work.

I would like to express my deepest gratitude to my advisors Prof. Aman Dekebo and Dr. Endale Mulugeta for their constructive advice, useful discussion, continuous guidance, friendly treatment, encouragement and careful supervision of the research project at all time.

I would like to acknowledge Adama Science and Technology University Department of Applied Chemistry for supporting materials required for this research and for giving me the opportunity to pursue my M.Sc. study.

I am thankful to the staff of Chemistry Department of Addis Ababa University, for their cooperation in running of NMR spectroscopy sample analysis. My thanks also go to Dr. Rajalakshmanan. E for assisting molecular docking study.

Last but not least my acknowledgment goes to my families, friends and all of those who contributed an idea give a bit of suggestion and helped me in a technical way.

TABLE OF CONTENTS

LIST OF ABBERVIATIONS AND ACRONMYS

CC: Column Chromatography

$CDCl_3$: Deuterated chloroform

^1H NMR: Proton Nuclear Magnetic Resonance

^{13}C NMR: Carbon Nuclear Magnetic Resonance

DEPT: Distortionless Enhancement by polarization transfers

DMSO: Dimethyl sulphoxide

MHA: Mueller Hinton agar

MRSA: Methicillin-resistant *Staphylococcus aurous*

RF: Retention factor

SAR: Structure activity relationship

TLC: Thin Layer Chromatography

UV: Ultraviolet

LIST OF SCHEMES

LIST OF TABLES

LIST OF FIGURES

LIST OF APPENDIXES

ABSTRACT

*Azo dyes are compounds containing electron-donating (D) and electron-accepting (A) functional groups through an azo p-conjugated linker. Most azo dyes are synthesized by diazotization of an aromatic primary amine, followed by coupling with one or more electron-rich nucleophiles such as amino and hydroxyl group. Azo dyes are found to possess different pharmacological activities such as antitumor, anti-inflammatory, antimycotic, antimicrobial as well as antioxidant were previously reported. In this work, four p-nitroaniline azo dye derivatives (**46**, **47**, **48** and **49**) and four aniline azo dye derivatives (**50**, **51**, **52** and **53**) were synthesized by reacting diazonium salt with 2-naphthol (1-naphthol, resorcinol and phenol). The structures of the compounds were characterized using spectroscopic techniques (UV-Vis, ^{1}H, ^{13}C and DEPT-135 NMR).*

*Dyeing action of azo dyes was evaluated in terms of dye exhaustion and fixation on cotton, wool, silk and polyester by using cold and hot methods. The better exhaustion and fixation values of dyes are all the four types of fibers in cold dyeing method than hot method reveals high suitability of cold dyeing method. The synthesized dye compounds were screened for their antibacterial activities against Escherichia coli and Staphylococcus aureus at different concentration (50, 75, and 100 mg/mL) and the result revealed that compound **46** showed potent activity against E.coli and S. aureus with 13.1± 0.76 and 13 ± 0 zone of inhibitions at 100 mg/mL concentrations respectively and compared to standard drug Penicillin (19.8 ± 0.28). Compounds **48** and **49** also showed higher activity against S. aureus (14 ± 0.5) and E.coli (14 ± 0.5) at 100 mg/mL respectively. Compound **52** and **53** showed no activity on S. aureus and E.coli respectively. Molecular docking of isolated compounds was done using Autodock vina version 4.2 software. Among the investigated ligands dye compound **46** and **47** exhibited better docking efficiency with DNA gyrase with binding affinity -7.4kcal/mol.*

***Key words**:* Azo dyes; Diazotization; Antibacterial Activity; Dyeing Potential; Docking study

1. INTRODUCTION

1.1. Background

Dyeing may be defined as "The process of coloring fibers, yarn or fabric by using a liquid containing coloring matter for imparting a particular due to a substance". Dyes are used in a wide range of industrial applications for example; textiles (the most significant), food products, cosmetics, pharmaceuticals and paper printing. Dyes are extensively used in the textile industry not only for cotton, but also wool and polyamides because of their wide variety of color shades, high wet fastness, ease of application and brilliant colors. A steady increase in the dye usage has been observed as a result of the increased cotton use worldwide (Rizk *et al*., 2015)

Dyes can be classified based on their source. Natural dye is a colorant (dye or pigment) obtained from vegetable or animal matter without any chemical processing (Sousa *et al*., 2008). The title 'natural dye' covers all the dyes derived from nature may be cellulosic, protein or mineral. Alizarin and indigo are examples of natural dyes. The other one is synthetic dyes, were readily accepted because of their very distinct advantage over natural dyes in respect to application, color range, color fastness and availability (Yazdanbakhsh and Moradi-e-Rufchahi, 2009). Mauve, magenta, and the azo dyes are some examples of synthetic dyes. Dyes can be also classified according to their solubility and chemical as disperse dyes and reactive dyes. Disperse dyes are water insoluble unlike to this reactive dyes are water soluble (El-Harfi *et al*., 2017).

Properties Several groups of dyes can be distinguished on the basis of their compound structure (e.g., phthalocyanins, anthraquinones, quinone-imines and xanthenes). However, the most commonly used dyes are azo dyes, because they are easier and more cost effective to synthesize than natural dyes (Fernández *et al*., 2010).

Azo dyes are compounds containing electron-donating (D) and electron-accepting (A) functional groups through azo pi-conjugated linker and the D-π-A system has various electronic structures which can bring full range of colors (Li *et al.*, 2015). Hence, azo dyes are widely used in dyeing of natural and synthetic fibers as well as industrially important chromophores (Tskhovrebov *et al*., 2015). Azo dyes are one of the most important classes of synthetic dyes because they are easily synthesized and have broad color spectrum (Raposo *et al*., 2011). In general, azo dyes are classified into monoazo dyes, disazo dyes, trisazo dyes and polyazo dyes, but the monoazo compounds account for the great majority of them. Azo dyes

also have versatile applications in many fields such as optical data storage, non-linear optics, dye-sensitized solar cells, ink jet printers and metallochromic indicators. Even though some azo dyes have been reported poisonous, they are found to possess pharmacological properties. These are also used as indicators in chemical laboratories and find applications in dyeing food stuffs in food technology and preservative for food grains (Geng *et al*., 2015).

Although azo and heterocyclic diazo compounds have been extensively used as disperse dyes but reactive dyes which form homopolar bond with textile substrate, claim the greatest interest at the present time. The brilliance of reactive dyeing due to uncomplicated simple structure of the dye molecules and good wet fastness due to stable linkage between dye and textile fiber in both alkaline and acid media have led to their preponderance over dyes of other classes (Aziz and El-Mallah, 2009).

The azo groups are generally connected to benzene and naphthalene rings, also attached to aromatic heterocycles or enolizable aliphatic groups. These side groups are necessary for imparting the color of the dye, with many different shades and intensities being possible. A common example of an azo dye is shown in **Figure 1**. When describing a dye molecule, nucleophiles are referred to as *auxochromes*, while the aromatic groups are called *chromophores*. Together, the dye molecule is often described as a *chromogen* (Al-Rubaie and Mhessn, 2012).

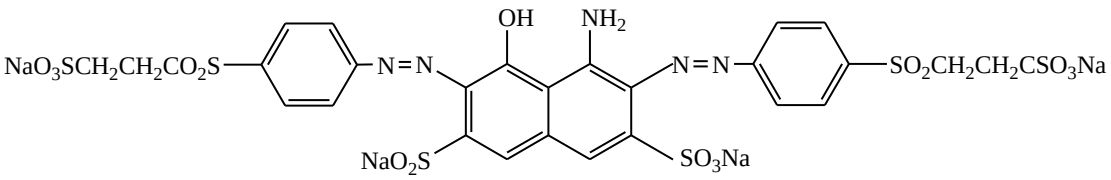

1

Figure 1: Chemical structure of an azo dye structure

The azo dye sulfonamides (**1**) antibacterial drugs were the first effective chemotherapeutic agents that could be used systematically for the cure of bacterial infection in humans (Tacic *et al*., 2017). A series of azo dyes containing the sulfonamide functional group were synthesized as potential antimicrobial agents, sulfonamide was classified into three different types; that are aniline-substituted sulfonamides, prodrug that react to generate active sulfanilamides and nonanilin sulfonamides. There are also other commonly used drugs that are azo dyes sulfonamides or sulfanilamides (the diuretic furosemide,the diuretic chlorthlidone and the oral hypoglycemic drug tolbutamide). Today, there are a few sulfonamides and especially sulfonamide–trimethoprim combination that are used extensively for opportunistic infection in the patients with AIDS (Beale *et al*., 2011).

1.2. Statement of the problem

Azo dyes are found to possess different pharmacological activities such as antitumor (Parimi and Kolli,2012), anti-inflammatory (Hutchinson *et al.,* 2011), antimycotic (Padmavathi and Shanmugapriya, 2009), antimicrobial (Mamhidir *et al.,* 2007) as well as antioxidant (Shridhar, 2012). Due to the increasing number of multi-drug resistant microbial pathogens, the treatment of infectious disease has become a challenging problem in hospital and community. Therefore, it is important to find compounds of antibiotics with different modes of action to combat drug resistance pathogens. Azo dyes are also used as indicators in chemical laboratories and as dyeing agent in textile industry. Nowadays industries need dyes which has suitable color, fastness properties, such as fastness to light and fixing of itself to fabrics. This research designed to synthesize some azo dye derivatives and to evaluate the dyeing potential, antibacterial activity and molecular docking studies.

1.3. Objectives

1.3.1. General objective

To synthesize and investigate the dyeing potential, antibacterial and *in silico* molecular docking analysis of azo dye derivatives.

1.3.2. Specific objectives

The specific objectives are to:

- To synthesize azo dye derivatives using diazotization of aniline.
- To elucidate the structures of synthesized compounds by some physical (digital melting point apparatus) and spectroscopic methods including UV-Vis, ^{1}H, ^{13}C and DEPT-135 NMR.
- To study the dyeing properties of compounds with respect to cotton, wool, polyester and silk fibers.
- To evaluate antibacterial properties of compounds using disk diffusion method against *Escherichia coli* and *Staphylococcus aureus.*
- To conduct *in silico* molecular docking analysis of the synthesized azo dyes against *E.coli* DNA gyrase-B.

1.4. Significance of the study

The study serves as a springboard for researchers who are interested to conduct further studies in related areas. The study on the synthesis of azo dye para red and other derivatives may help to arrive at synthetic dyes. Furthermore, the synthesized compounds might be uses as antibacterial agents.

2. LITERATURE REVIEW

2.1. Synthesis

Azo dyes are generally synthesized in two steps: the diazotization of aromatic primary amines, followed by the coupling reaction between diazonium salts and activated aromatic compounds (phenols or aromatic amines) (Safari and Zarnegar, 2015).

2.1.1. Synthesis of azo dyes using diazonium salts

Synthesis of most azo dyes involves diazotization of a primary aromatic amine, followed by coupling with one or more nucleophiles. Amino- and hydroxy- groups are commonly used coupling components. Because of the diversity of dye components available for synthesis, a large number of structurally different azo dyes exist and are used in industry (Stolz, 2001). Diazonium salts are precursors of the synthesis of azo dyes and they are also widely used in organic synthesis such as Sand Meyer reaction, Balz-Schiemann reaction, carbon-carbon coupling reaction and modification of polymeric materials and Nano-materials (Christoforou and Koutentis, 2006).

Labd-alredha *et al.* (2011) synthesized azo dyes para red (**2)**. The diazonium salt reacts as an electrophile with an electron-rich coupling component, like a *β*-naphthol and naphthaline derivative through an electrophilic aromatic substitution. The hydroxyl group (such as *β*-naphthol) direct the aryl diazonium ion to the para site unless that position is occupied, in which case the ion attaches ortho (Kucharski *et al*, 1999). The studies confirm para red was prepared from the reaction of diazonium salt of *p*-nitroaniline with *β*-naphthol

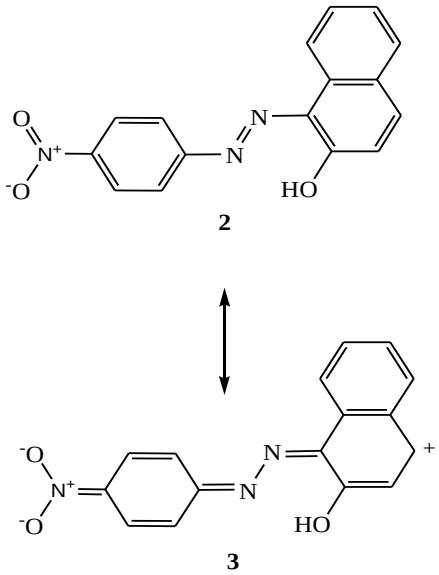

Figure 2: Represent the hyper conjugation system of para red molecule

Another study also made by Jinjing *et al.* (2017) synthesized a new synthetic strategy for industrially important deep-shade disperse azo dyes (85-96.1%). The study is to prepare stable solid diazonium salts of weakly basic amines in the absence of concentrated sulfuric acid. Because Solid diazonium salts are very dangerous and have the tendency to explode because of their very poor thermal stability (Garel and Saint-Jalmes, 2006). Thus, the diazotization of amines with sodium nitrite is usually carried out in the presence of excess hydrochloric or sulfuric acid solution and the obtained diazonium salt solution is directly poured into the coupling system to synthesize azo dyes resulting in large amounts of waste water containing strong liquid acid.

Diazotization by tert-butyl nitrite in ethyl acetate was allowed to proceed in the presence of equivalent 1,5-naphthalenedisulfonic acid as stabilizer of diazonium salts and donor of hydrogen ion for the reaction. The separated solid diazonium salts exhibited good thermal stability. The corresponding disperse azo dyes were subsequently synthesized through the azo-coupling of the prepared solid diazonium salts with a range of aromatic tertiary amines. The azo dyes were produced in short reaction time, excellent yields, mild reaction conditions, simple experimental procedure and low energy consumption (Al-Rubaie and Mhessn, 2012).

Clean synthesis of azo dyes based on weakly basic amines is still a great challenge because they are very difficult to be diazotized due to their extremely weak alkalinity. Weakly basic amines with two or three strong electron withdrawing groups are the main raw materials on the preparation of dark disperse azo dyes with excellent color fastness's (Valizadeh *et al.*, 2012). However, their diazotization reactions using sodium nitrite are difficult to be carried out in hydrochloric or sulfuric acid solution because of their low reaction activity and solubility.

In industrial production, the diazotization of weakly basic amines is always conducted in more than 10 times the molar quantity of concentrated sulfuric acid (Hooker *et al.*, 2002) and has to use nitrosyl sulfuric. Subsequently, the concentrated acid solution of diazonium salt is poured into the coupling system. Due to the strong dilution heat effect of concentrated sulfuric acid, large amounts of ice were used to maintain low temperature of the system to avoid the decomposition of the diazonium salt. Meanwhile, it is difficult to handle the high acid content waste water.

Herein, the study prepared method of disperse azo dyes based on the novel stable solid diazonium salts of weakly basic amines. After the reactions of weakly basic amines with tertbutyl nitrite carried out in organic solution without any sulfuric acid in the presence of equivalent 1,5-naphthalenedisulfonic acid, the stable solid diazonium salts were obtained by simple filtration because of their very low solubility in organic solvent. This study show how can avoid the strong heat effect coming from the dilution of concentrated sulfuric acid in the traditional coupling process.

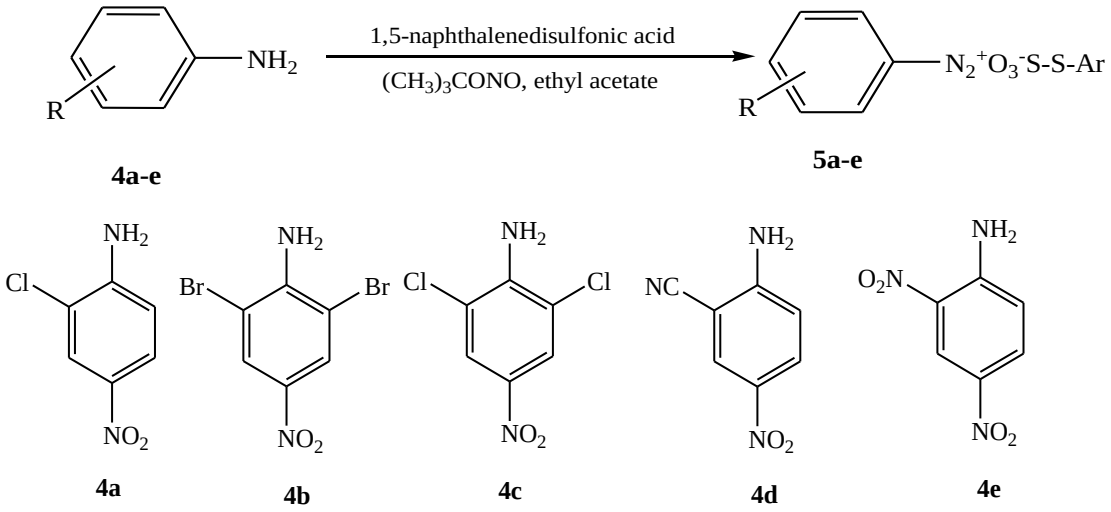

Scheme 1: Preparation of stable diazonium salts in organic solvent**.**

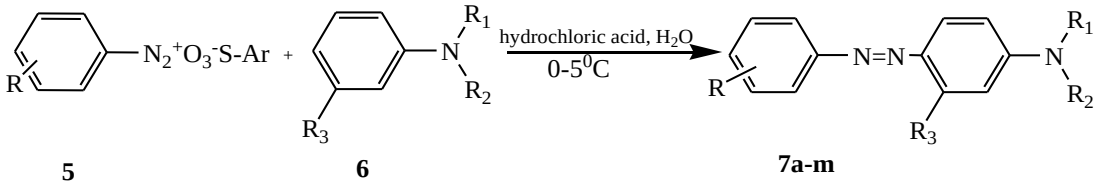

7a-e: $R_1 = R_2 = CH_2CH_3$, R_3 =H

7f-h: $R_1 = CH_2CH_2CN$, $R_2 = CH_2CH_3$, R_3 =H

7i, j: $R_1 = R_2 = CH_2CH_2CN$, R_3 = H

7k-m: $R_1 = R_2 = CH_2CH_3$, $R_3 = NHCOCH_3$

Scheme 2: Azo-coupling of stable diazonium salts with tertiary aniline derivatives

Compounds **4a**, **4c**, and **4d** were chosen as objects of study and prepared with different temperatures. The yield indicates no significant reducing of the yield during temperature increase. These results show that this new technology is of great significance for the realization of energy saving and emission reduction in the production of disperse azo dyes based on weakly basic amines (Qiu *et al*., 2017).

2.1.2. Synthesis of azo dye and its derivatives using polymer-supported reagents

The recent technological advancements in polymer-supported reactions have led to the propagation of combinatorial chemistry as a method for the rapid and efficient preparation of novel functionalized molecules. An interesting and fast growing branch of this area is polymer-supported reagents. The application of combinatorial methods for the generation of novel chemical libraries, for use in the pharmaceutical and agrochemical industries, is now common place increasingly, these methods are also being adopted by other sectors of the chemical industry in order to prepare novel materials for application in many diverse areas, especially catalysis (Caldarelli *et al*., 2000).

The original work in the area of combinatorial chemistry (Stanková and Lebl, 1996) involved reactions on compounds covalently attached to polystyrene supports on which high reaction yields could be obtained through the use of high reactant concentrations, the excess of which could be removed after the reaction by thorough matrix washing. An alternative to supported solid phase synthesis for a parallel combinatorial approach to new compounds is the use of polymer-supported reagents and scavengers. Polymer supported reagents are materials ionically associated with, or covalently immobilised to insoluble matrices which can be added to a solution phase reaction, and later removed by filtration. Solid phase synthesis is still a widely used technique but it has its disadvantages, which include the extra steps involved in substrate attachment to and detachment from the resin as well as the effects of the matrix environment on the outcome and kinetics of the reaction.

Study by James *et al.* (2002) synthesized resin supported diazonium salts. These were observed to be stable to storage and to provide a convenient means of compound handling and were employed in the solution synthesis of a 6 x 6 azo dye library. Preparation of stable ion-exchange resin supported diazonium species, using two macroporous polystyrene allowing the use of aqueous based chemistry; Amberlyst A-15, which is a sulfonate acid based resin and Amberlyst A-26, which is functionalised with tetra alkyl ammonium groups.

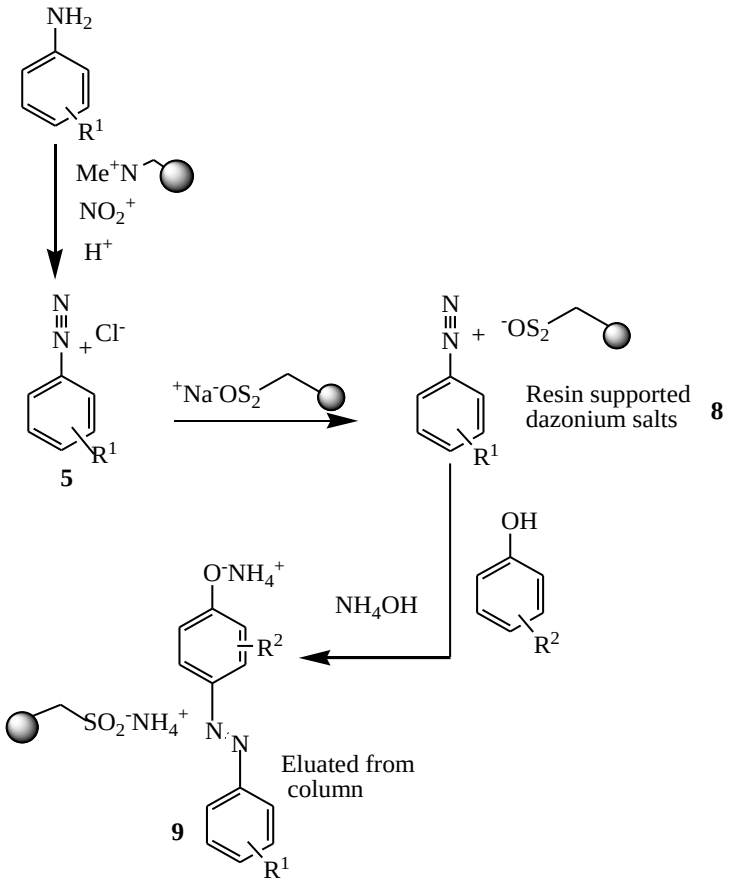

Scheme 3: Azo dye preparation

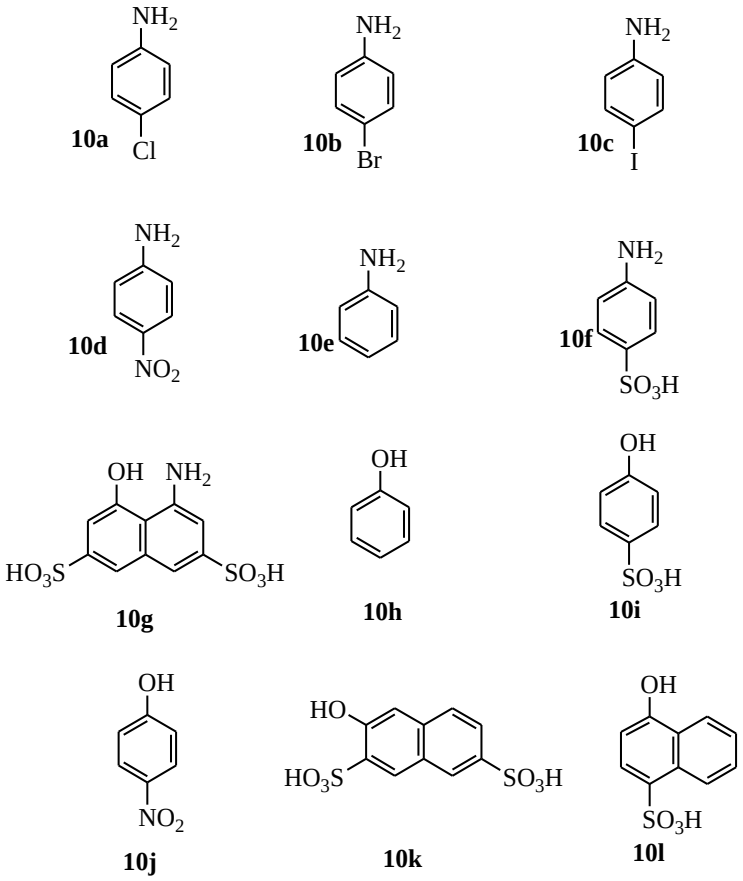

Figure 3: Phenols **10g-l**, aromatic amines **10a-f**

Samples were removed over time and treated with phenol, and the azo dye generated was quantified by HPLC. The material was not observed to lose reactivity over an 8-day period. However, after 12 weeks a reduction of 79% in yield was observed. High purity was observed in series **10g**, **10h** and **10k**, in accordance with the nucleophilicity of the phenols used in those series. The 4-hydroxybenzenesulfonic acid (series **10i**) gave low purities/ reaction yields possibly due to poor accessibility into the Amberlyst A-15 sulfonic acid based resin.

As expected no reaction was observed with 4-nitrophenol (series **10j**) due to their poor reactivity. The library synthesis demonstrates the use of polymer-supported diazonium salts as powerful agents for introducing diversity into azo dye libraries (Merrington *et al*.,2002).

Another study also made by Marina *et al***.** (2000) synthesized azo dyes (85-98%) using polymer supported reagent. The most common process for their preparation involves the diazotisation of an aromatic primary amine and the coupling of the resultant diazonium salt with a phenol or an aromatic amine. This is traditionally achieved using conventional wet chemistry which leads to large quantities of down-stream waste. With the ever increasing environmental restrictions and control on the release of effluent the ability to effect a clean and efficient synthesis of the azo-compound is of considerable environmental and commercial importance.

The study chosen to adopt a different strategy which allow to synthesize a large number of compounds in solution, in a linear (Yasuda and Ley, 2002) or convergent fashion (Habermann *et al*., 1999) through the sequential use of polymer-supported reagents in a multi-step process. The advantage of this approach includes the ease of reaction monitoring (*i.e.* TLC, LC-MS) and the fact that with the appropriate design of sequences, clean products may be obtained using only simple filtrations rather than conventional work-up purification techniques.

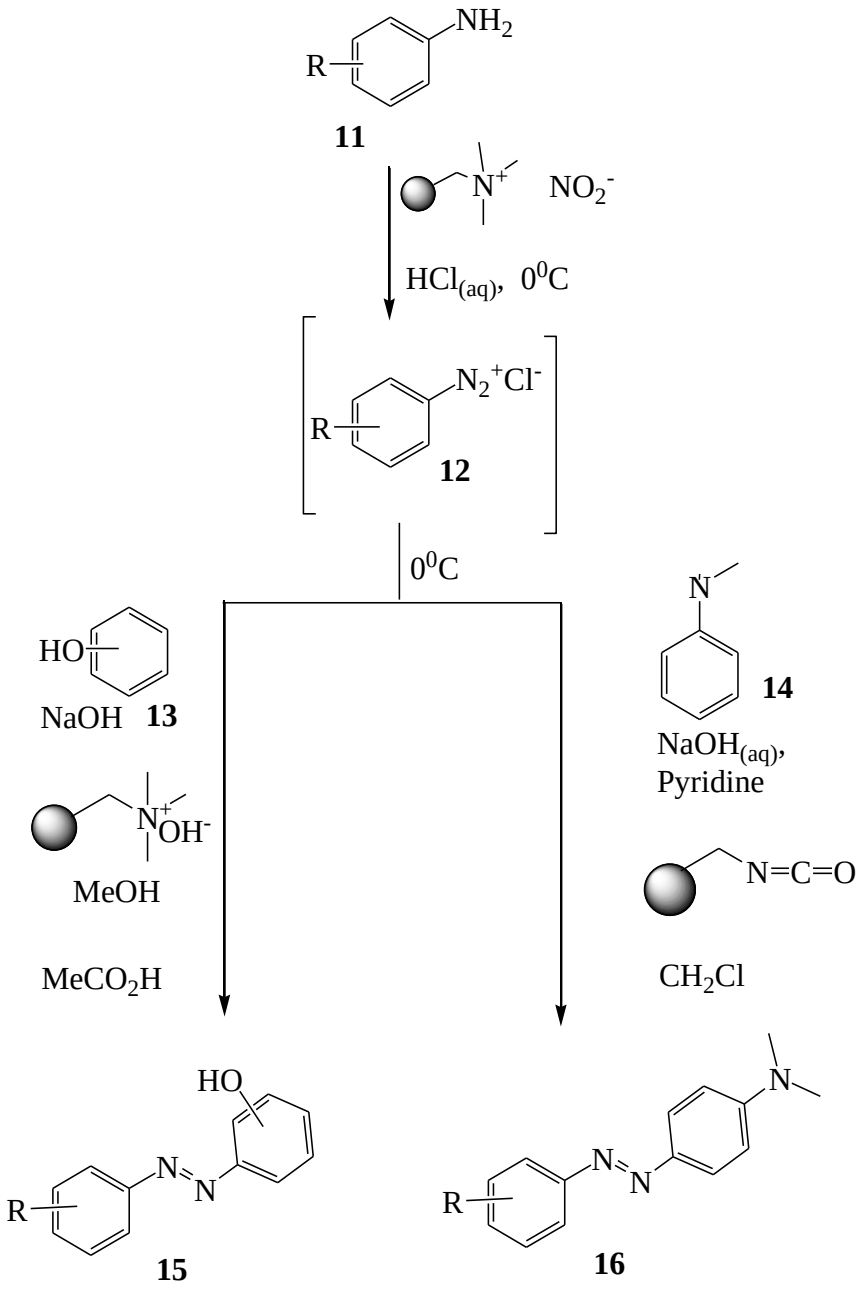

Scheme 4: Preparation of the azo dyes

Table 1 : Diazo dyes derived from phenolic coupling.

Entry	Compound	Yield [a](%)	Purity [b](%)	LC-MS	P^H=0	P^H=14
17	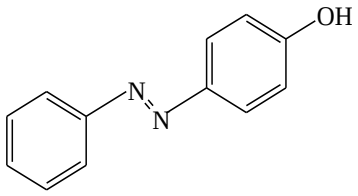	90	>98	109.1o (-)	Yellow	Yellow
18	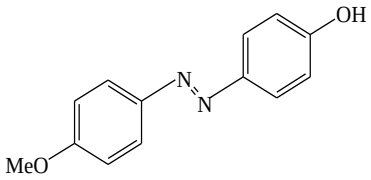	62	85	229.31 (+)	Orange	Orange
19	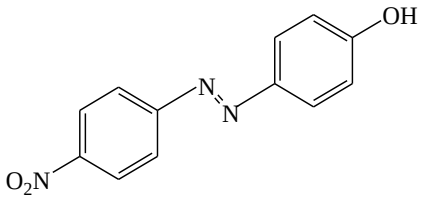	80	>98	224.15 (-)	Yellow	Red
20	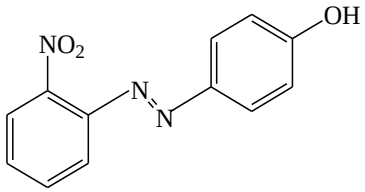	Quant.	>98	242.13 (-)	Yellow	Orange
21	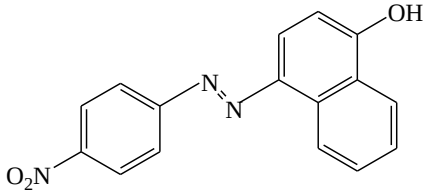	78	80	292.19 (-)	Orange	Blue
22	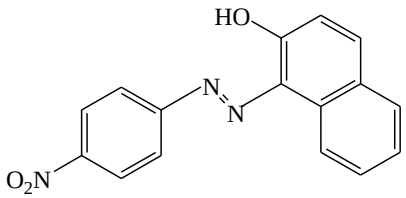	Quant.	>98	292.16 (-)	Yellow	Violet

[a]yields are based on the amount of phenolic derivatives used [b] purity was determined by 400MHz ^{1}H NMR spectroscopy

An attempt to couple the diazonium salt derived from 4-methoxyaniline with dimethylaniline gave no product. This result is in accordance with data for the relative rates of coupling for diazonium salts of aniline derivatives: 4-NO_2: H: 4-CH_3O. As expected the products obtained acted as indicators and showed the characteristic change of colour at extremes of P^H (Caldarelli *et al*., 2000).

2.1.3. Green synthesis of azo dyes

In recent years, organic color chemistry has been undergoing very exciting developments as a result of the opportunities presented by dye applications in modern technology fields such as linear and non-linear optics, reprography, electronic devices, sensors and biomedical uses (Valizadeh *et al*., 2012). On the other side, more attention has been directed toward the application of solid acids in organic synthesis because such reagents not only simplify purification processes but also help prevent release of reaction residues into the environment (Okuhara, 2002). Azo dye compounds are the most widely used class of synthesized organic dyes. Due to the importance of the azo dyes, continuous efforts have been made to achieve simple and ecofriendly methodologies for the synthesis of these compounds.

Recently, various heterogeneous solid acids have been used for the preparation of azo dyes (Dabbagh *et al*., 2007). Although satisfactory yields of products have usually obtained, nano structure solid acids have attracted great interest in recent years due to their particular physical and chemical properties. The properties of these materials mainly depend on their shape, size, and structure which are strongly determined by the synthetic processes (Jortner and Rao, 2002). Nanostructure solid acids exhibit higher activity and selectivity than their corresponding bulk materials. As the diameter of the particle decreases to the nanometer scale, external surface area becomes available for chemical transformations.

This green methodology aims to overcome the limitations and drawbacks of the previously reported methods such as low temperature, use of acids, alkalis and toxic solvents, instability of diazonium salts at room temperature, modest yields, and long reaction times (Rahimizadeh *et al*., 2012). Moreover, various solid acids have been used for the preparation of azo dyes compounds ((Dabbagh *et al*., 2007).

Javad *et al.* (2015) study a solvent-free, efficient and green approach for the synthesis of azo dyes (83-92%) has been developed by the diazo coupling reactions of aromatic amines with β-naphthol in the presence of sulfonic acid functionalized magnetic Fe_3O_4 nanoparticles (Fe_3O_4@SiO_2-SO_3H) by a grinding method at room temperature. Magnetically recyclable catalysts are unique due to their inherent properties such as biocompatibility, thermal stability against degradation, easy renewability and recovery by magnetic separation, higher catalytic activity due to the higher loading of active sites and large surface area (Mobaraki *et al*., 2014).

Convenient and green one-pot procedure for diazotization and diazo coupling reactions using Fe_3O_4@SiO_2-SO_3H as a proficient, mild, environmentally friendly, non-toxic and powerful magnetic nanostructure solid acid catalyst with good stability (**Scheme 5**).

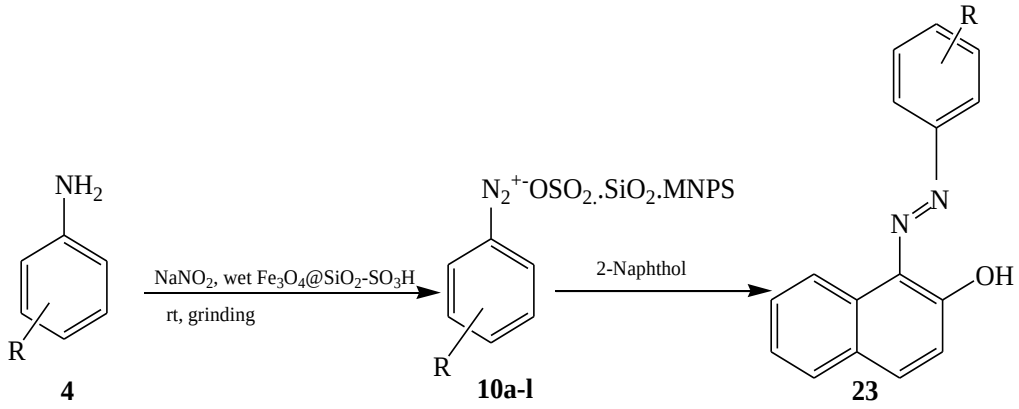

Scheme 5: One-pot method for diazotization and diazo coupling reactions using Fe_3O_4@SiO_2-SO_3H under solvent-free conditions

Table 2: The synthesis azo dyes in the presence of Fe_3O_4@SiO_2-SO_3H by grinding method under solvent free system.

Entry	R	Time(min)	Product	Yield (%)
4f	H	25	**10a**	88
4g	2-NO_2	30	**10b**	83
4h	2-Cl	30	**10c**	85
4i	4-NO_2	25	**10d**	90
4j	4-Br	20	**10e**	90
4k	4-Cl	20	**10f**	90
4l	4-CH_3CH_2	15	**10g**	85
4m	4-CH_3	15	**10h**	85
4n	4-OH	10	**10i**	90
4o	4-OMe	10	**10j**	92
4p	4-CH_3CH_2O	10	**10k**	91
4q	4-NH_2	15	**10l**	88

The poor thermal stability of diazonium salts, strong acidic conditions, and the difficulty to separate the acidic catalysts from the reaction medium limit the application of these compounds and azo dyes are usually synthesized around 0–10°C, because temperatures above 5°C cause the decomposition of diazonium salts and conversion to side products before coupling reactions. this is the main reason for the modest yield of the products (Bamoniri *et al*., 2014). Magnetically recyclable catalysts to solve these problems by developing a green and facile procedure for the synthesis of azo dyes in the presence of a magnetic solid acid catalyst. The rate of diazotization in the presence of Fe_3O_4@SiO_2-SO_3H was much higher than the other catalysts. The small size of nanoparticles and large surface to volume ratio in Fe_3O_4@SiO_2-SO_3H can be the reason for the greater stability of the diazonium salt in comparison to that supported on the bulk acid catalyst.

After completion of the reaction, the separated catalyst can be reused after washing with acetone and ethanol and drying at 70°C. The catalyst could be reused for the next cycle without great loss of catalytic activity (Safari and Zarnegar, 2015).

Abdolhamid *et al.* (2014) also study a series of azo dyes (80-92%) were efficiently synthesized by mixing aromatic amines and $NaNO_2$ in the presence of nano silica supported boron trifluoride (nano $BF_3{\cdot}SiO_2$) and then diazo coupling with 1-naphthol under solvent-free conditions at room temperature. BF_3SiO_2 and its nano structural form are excellent proton sources and convenient and inexpensive catalysts, which can be used for the promotion of many acid-catalyzed organic reactions (Mirjalili *et al*., 2008). In this method, it is not necessary to provide special cold conditions for stabilization of the diazonium salt.

The reaction easily takes place at room temperature, and the resulting diazonium salt can remain on the solid substrate for several months. All aryl diazonium salts prepared with this procedure were nonexplosive because their reactivity decreased when they were supported on nano BF_3SiO_2 as a solid acid. Diazotization method was detected to be safe, and the grinding of these aryl diazonium salts was not found to behazardous.

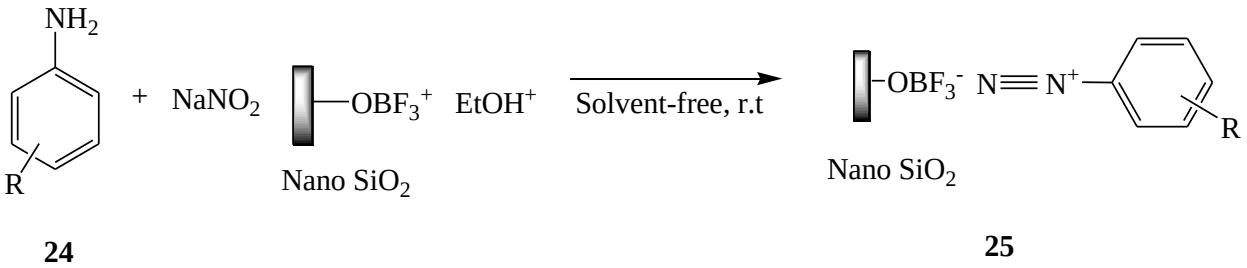

24 **25**

Scheme 6: Diazotization of aromatic amines in the presence of nano BF_3SiO_2.

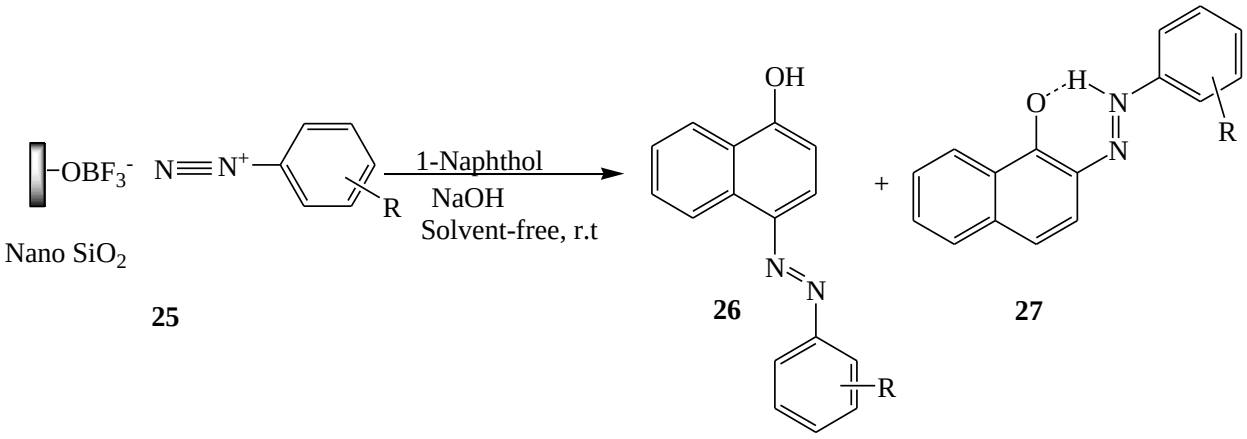

25 **26** **27**

Scheme 7: Diazo coupling of aryl diazonium salts with 1-naphthol under solvent-free conditions

Table 3: Solvent-free synthesis of aryl azo-1-naphthol derivatives at room temperature.

Entry	Amine	2-arylazo-1-naphthol (a)	4-arylazo-1-naphthol (b)	Yield [a] (%)	MP found(lit) in (a) found (lit) in (b) ^{0}C
28	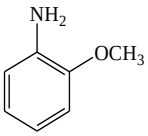	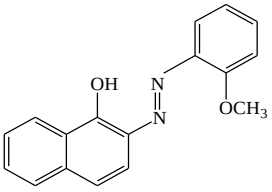	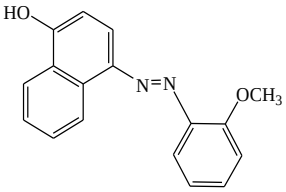	88	181-183(180.5-181)/176-178(177-178)
29	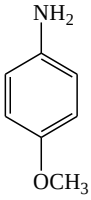	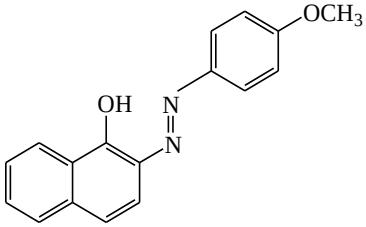	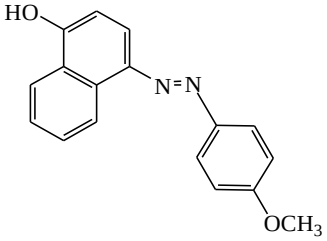	89	127-129(127.5-128)/173-175 (173)
30	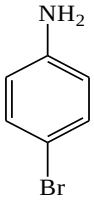	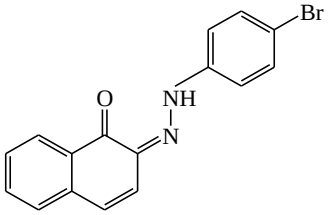	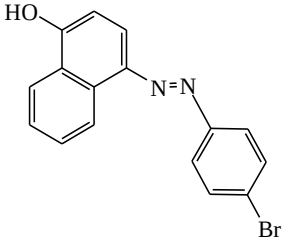	92	196-198/237-239(237-238)
31	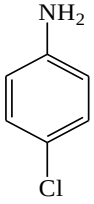	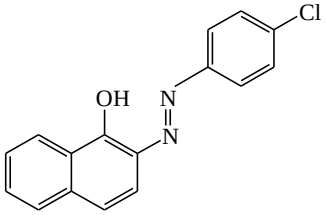	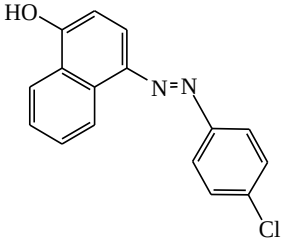	90	187-189(187)229-231(229.5)
32	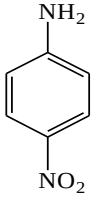	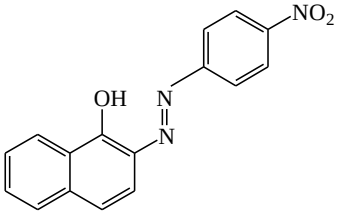	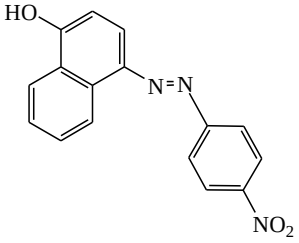	80	235-237 (235-236)/281-283 (281-282)

[a](Ogolev and Stepano, 1965)

[b] (Morgan, 1961)

This green protocol avoids the use of toxic liquid acids and solvents, prevents the generation of side products, and has a distinct advantage by stabilizing diazonium salts supported on nano $BF_3 \cdot SiO_2$, having a short reaction time and high conversion.

The presence of water causes the formation of some phenoxide salt after the addition of diazonium salt. In continuation, phenoxide nucleophilic attack to diazonium salt forms phenolic azo dyes as side products. To prevent this problem, the reaction was performed under solvent-free conditions toward green chemistry. Then, we ground solid 1-naphthol with some NaOH in a mortar. The moisture absorbed by the reaction mixture during the grinding seems to be sufficient for the formation of a homogeneous mixture (Bamoniri *et al*., 2014).

2.2. Dyeing properties of azo dyes

Over the past few decades, azo dyes have been extensively studied in the field of material chemistry as well as dye industry. Azo dyes are an important class of organic colorants which contain at least a conjugated azo chromophore (\ N=N\ ). They are also considered as the largest and the most versatile class of dyes. Azo compounds are the most widely used class of dyes having applications in various fields, such as dyeing textiles (Yazdanbakhsh *et al*., 2010).

Reactive dyes are well known and applied in dyeing of different materials. The combination of two different functional (reactive) groups in the dye's molecule improves their dyeing ability (Kiran and Mehta, 2012). Most of the recent researches are focused on structural variations of existing types, for example variations in substituent, especially on the side chains of the coupling components. The use of heterocyclic coupling component and diazo components in the synthesis of azo dyes is well established, and the resultant dyes exhibit good pictorial strength and brighter dyeing than those derived from aniline-based components. Heterocyclic based dyes are found to have excellent properties as dyes for polyester, cotton, and wool textiles (Wadia and Patel, 2008). Especially, reactive dyes containing reactive groups can provide great opportunity for efficient dye-fiber reaction due to the reactive system, which may cover a wide range of application and retention of color on the polyester, wool and cotton depending on many factors like the structural characteristics of the colorant molecule and fiber, attachment of colorant molecule with fibers, the percentage of fixation of colorant on fibers (Iftikhar *et al*., 2001).

Reactive dyes contain functional groups capable of forming covalent bonds with cellulosic materials. In addition, they are unique being the only class of dye that actually forms covalent bonds with cellulosic (Chopde *et al*., 2010). In reactive dyeing, the dyeing process can be broadly divided into two phases, namely exhaustion and fixation which are used to study the ability and duration of dyes after and before further treatments. The characteristic structural features of typical reactive dyes are the reactive system, enabling the dyes to form covalent bonds between the dye and the substrate; the chromophoric grouping, contributes to the colour and much to the substantivity for cellulose a bridging group that links the reactive system to the chromophore and solubilising groups (Matyjas and Rybicki, 2003).

2.3. Biological properties of azo dyes derivatives

The azo dye containing heterocyclic ring has received much attention in pharmaceuticals industry compared to those with the simple carbocyclic aromatic system due to their extraordinary colouring properties, tentorial strength, brightness, fastness properties and distinct bathochromic effect. Among the various heterocyclic azo dyes, those containing nitrogen atom are actively involved in the different pharmacological activities such as antitumor (Maradiya *et al*., 2012), anti-inflammatory (Bradshaw *et al.,* 2001), antimycotic (Padmavathi *et al*., 2012), antimicrobial (Mahran *et al*., 2007) as well as antioxidant (Shridhar *et al*., 2016).

A study made by Raghavendra *et al.* (2013**)** synthesis of some novel azo dyes starting from 3-nitro salicylic acid. The synthesized dyes were investigated for their redox potentials, evaluated for their dying ability on cotton fabrics, resistivity against the fungi Seeds. The anti-fungal activities of the synthesized compounds have been tested with the seeds of jowar and green gram. (Raghavendra and Ajay, 2013).

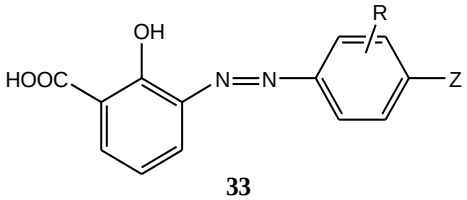

33

33a: Z=NH_2, R=H;

33b: Z=NH_2, R=2-CH_3

33c: Z=NH_2, R=3'-NO_2

33d: Z=OH, R=H

33e: Z=OH, R=2'-CH_3

33f: Z=OH, R=3'NO_2

Figure 4: Some novel azo dyes starting from 3-nitro salicylic acid

The experimental result indicates that the synthesized compounds possess good antifungal activities against many of the fungi species. It was observed that the variation of the compounds concentration remarkably influences the growth of the fungal organisms.

Another study also made by Yazdanbakhsh *et al.* (2012) synthesized a number of new azo disperse dyes were by coupling 4,6-dihydroxypyrimidine with diazonium salts derived from 4-methoxy aniline, N-(4-amino phenyl) acetamide, 3- and 4-methyl aniline, 2-trifluoromethyl aniline, 4- flouoroaniline, 4-cyanoaniline, 4-amino acetophenone, 4-nitroaniline, 2-bromo-4-methyl aniline and 4-amino azobenzene. The antibacterial activity of compounds synthesized was measured against *Salmonella typhimurium* (ST), *Micrococcus luteus* (ML), *Bacillus subtilis* (BS) and *Pseudomonas aeruginosa* (PS) (Yazdanbakhsh *et al*., 2012).

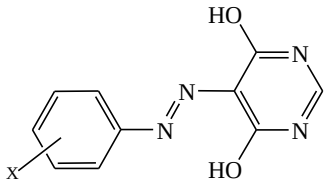

34

34a: X = *p*-OCH_3
34b: X = *P*-$NHCOCH_3$
34c: X = *P*-CH_3
34d: X = *m* -CH_3
34e: X = *m*-CF_3
34f: X = *P*-F
34g: X = *P*-CN
34h: X = *P*-$COCH_3$
34i: X = *P*-NO_2
34j: X = *O*-Br, *P*-CH_3
34k: X = *P*-N=N-PH

Figure 5: Some new azo dyes derived from 4,6-dihydroxypyrimidine

It appears that electron accepting groups, except for dye **34a**, are more active against *S. typhimurium*. Among electron accepting groups, dyes **34i**, **34j** and **34k** have no effect on, respectively, *B. subtilis*, *P. aeruginosa* and *S. typhimurium*. Electron donating dyes **34a-34d** are inactive against *B. subtilis* and *P. aeruginosa*. In general, *B. subtilis* and *P. aeruginosa* were more resistant to dyes than *S. typhimurium* and *M. luteus*. The resistance shown by *B. subtilis* and *P. aeruginosa* to the synthesized compounds, and the selected antibiotics, is not surprising as these bacteria are well known for being resistant to a wider range of antibiotics than most other bacteria.

It should be noted that the concentration of the dyes used in the assays was only 4.38 µg/well, which was much lower than that of the standard antibiotics (15 µg/well for erythromycin and 30 µg/well for tetracycline). Nevertheless, the dyes at these lower concentrations seem to have similar levels of antibiotic activity against these two bacteria. It is also noteworthy that *S. typhimurium* was much more sensitive to all the dyes than to either of the two control antibiotics.

Rizk *et al.* (2015) synthesized reactive dyes having pyrazole moiety and study their fastness properties, color assessment and antimicrobial activity. The biological screening showed that most of the tested compounds display promising antimicrobial activities against the tested microorganisms. The microorganisms used in this study included *Staphylococcus aureus*, (Gram positive bacterium), *Serratia marcescens*, *Shigella dysenteriae*, *Enterobacter cloacae*, *Escherichia coli* (Gram negative bacteria) and *Candida albicans* (fungus). Bacteria were cultured on nutrient agar and the fungus was cultured on sabaroud agar slopes. Antimicrobial activity of the synthesized compounds was tested in vitro on nutrient agar at 30°C after 24 hr by the cut-plug method.

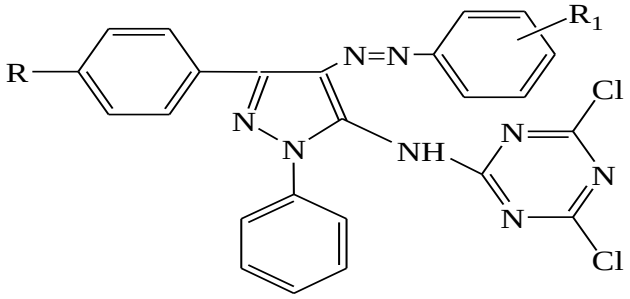

35

35a: R=H, R_1=4-SO_3H

35b: R=Cl, R_1=4-SO_3H

35c: R=CH_3, R_1=4-SO_3H

35d: R=H, R_1=2-COOH

35e: R=Cl, R_1=2-COOH

35f: R=CH_3, R_1=2-COOH

Figure 6: Some azo reactive dyes having pyrazole moiety

The antibacterial and anti-fungal activities of the synthesized dyes were determined against five bacteria *S. aureus* (Gram positive bacterium), *S. marcescens, S. dysenteriae, E. cloacae, E. coli* (Gram negative bacteria) and *C. albicans* (fungus).

The tested compounds except **35e** exhibited strong activity against all strain of tested organisms. For the antifungal activity among the compounds tested only **35a-c** exhibited activity against *C. albicans*. The minimal inhibitory concentration (MIC) for **35a** and **35b** showed a relatively good antimicrobial activity towards most of the tested organisms. The present data showed that the most sensitive microorganism to both compounds was *S. marcescens*. The MIC values were 60.5 and 61.5 for compounds **35a** and **35b**, respectively. The dilutions of both samples and standards were performed by a double fold dilution The antimicrobial activity of the synthesized dyes showed that compounds **35a-c** showed the highest activities against the tested organisms (Rizk *et al*., 2015).

3. MATERIALS AND METHODS

3. 1. Chemicals and cloths

Substituted aniline, concentrated HCl, $NaNO_2$, NaOH solution, 1-Naphthol, 2-Naphthol, Resorcinol, Phenol, *P*- Nitroaniline, *O*- Toluidine and *P*- Chloroaniline, *n*-Hexane, Ethyl acetate, Petroleum ether, Methanol, Ethanol, Dichloromethane and silica gel (60-120 mesh) were used in this work. Cloths used in this work Cotton, wool, silk and polyester cloths were obtained for dyeing studies.

3.2. Physical and spectroscopic methods

Melting point was determined in an open capillaries using digital melting point apparatus. Reaction progress was monitored using silica gel pre-coated TLC plates and spots were visualized using UV lamp at 254 nm and 365nm. Purification of the synthesized compounds were done using silica gel column chromatography. The column was subjected to gradient elution by increasing gradient of ethyl acetate in petroleum ether and spots were visualized under UV light (254 nm and 365nm). The synthesized compounds were characterized on the basis of physical and spectral analysis. The UV-Vis spectra of compounds were recorded on Double-beam UV-Vis spectrophotometer using water and methanol as blank solvents and λ_{max} values were expressed by nm. The ^{1}H and ^{13}C NMR spectra of the compounds were recorded on Bruker avance 400 MHz NMR spectrophotometer using Chloroform-*d* or Methanol-d_4 as the solvent and the values are expressed in δ ppm.

3.3. Synthesis of compounds

The azo dyes, were synthesized by following (Al-Rubaie and Mhessn, 2012) experimental protocol.

3.3.1. Preparation of diazonium salt

Solution of 1 mL of concentrated hydrochloric acid in 10 mL of distilled water was added in a round bottom flask. While stirring, 1 g (7 mmol) of *p*-nitroaniline (aniline derivatives) was added with stirring in ice bath. Then solution of 0.5 g (7 mmol) of sodium nitrite in 2 mL of distilled water were added slowly (Al-Rubaie and Mhessn, 2012).

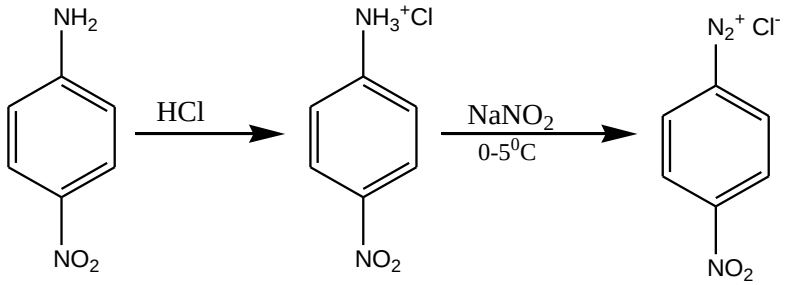

36 **37** **38**

Scheme 8: Preparation of diazonium salt

3.3.2. Synthesis of azo dye

Solution of 1 g (7 mmol) of 2-naphthol (1- naphthol, phenol and resorcinol) in 10 mL of 2.5 M sodium hydroxide was added into the flask with the diazonium salt in an ice bath, with vigorously stirring for a few minutes. The mixture was acidified with 1M hydrochloric acid. The resulting solution formed a coloured precipitate which was filtered by suction and the product was dried under vacuum-oven at 50 ^{o}C for 2 hr.

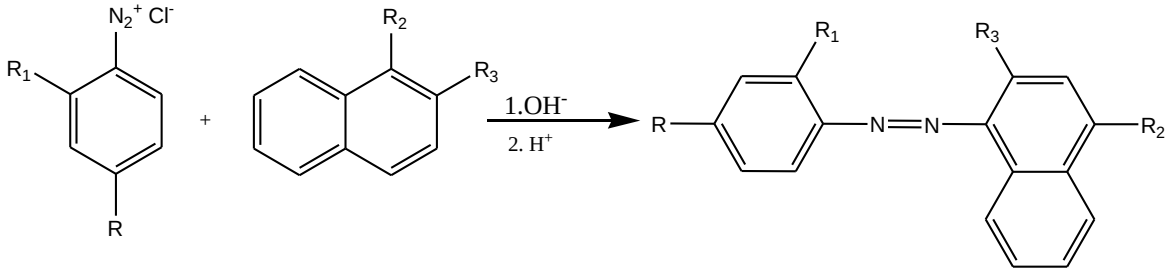

39: R= NO_2, R_1 = H

40: R= H, R_1 = CH_3

41: R= Cl, R_1 = H

42: R_2= H, R-3= OH

43: R_2= OH, R-3=H

46: R = NO_2, R_1 = H, R_2= H, R_3 = OH

47: R = NO_2**,** R_1 = H, R_2= OH, R_3 = H

50: R = H, R_1 = CH_3, R_2= H, R_3 = OH

51: R = Cl, R_1 = H, R_2= H, R_3 = OH

Scheme 9: Synthesis of azo dye **1**

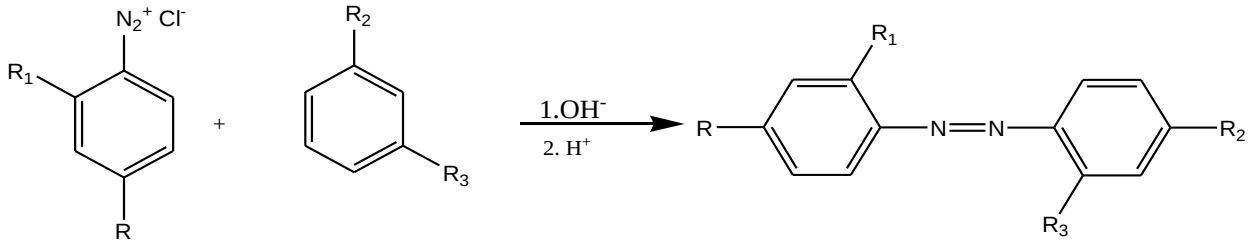

39: R= NO_2, R_1 = H

40: R= H, Cl, R_1 = CH_3

41: R= H, Cl, R_1 = CH_3

44: R_2 = OH, R_3=OH

45: R_3 = R_2 = OH, R_3= H

48: R = NO_2, R_1 = H, R_2 = OH, R_3=OH

49: R = NO_2, R_1 = H, R_2 = OH, R_3= H

52: R = H, R_1 = CH_3, R_2 = OH, R_3=OH

53: R = Cl, R_1 = H, R_2 = OH, R_3=OH

Scheme 10: Synthesis of azo dye **2**

3.4. Test for purity and purification of compounds

Purity of synthesized compounds were monitored using TLC analysis. The pre coated TLC plates (20x20 cm) coated with silica gel with gypsum binder were activated by heating in oven at approximately 60ºC before loading the samples. A sample was loaded on oven dried TLC plates was developed in rectangular glass chambers with ground-in-lids by ascending technique. To obtain reproducible results the development chambers were pre-saturated with solvent before use. When development have proceeded for about ¾ th of the plates, they were removed from the chamber. The spots on TLC plates were visualized in iodine vapors and UV lamp at 254 nm and 365nm.

Silica gel column chromatography was conducted for separation of the mixture of the synthesized compounds (by increasing gradient of ethyl acetate in petroleum ether) depending on the TLC profile and availability of chemicals.

3.5. Preparation of solutions and spectrophotometric measurements

Solution of each azo dye was prepared by dissolving appropriate quantity of the compound (10 mg) directly in MeOH-H_2O (1:3 v/v) for λ_{max} determination. From 200nm – 600nm, optical density was measured to determine λ_{max} of each sample.

For quantitative studies standard solutions of azo dyes was prepared by dissolving known quantities of samples in known volumes of solvent (methanol-water (1:3 v/v)), for finding out necessary H_2SO_4 conc. for producing maximum color intensity of each dye. Six equiconcentrate solutions of each dye sample was prepared in methanol-water (1:3 v/v) solvent containing different quantities of acid and optical density values was measured at λ_{max} of each dye. From the highest value of optical density of dye at its λ_{max} requisite concentration of acid necessary for producing maximum color was determined. For the preparation of calibration curves optical density of each dye solution at different concentrations containing requisite quantity of acid producing maximum color intensity was measured.

3.5.1. Dyeing and post-dyeing treatment

Two of the four prewashed white cloth pieces of appropriate size (8 cm x 8 cm) of silk, wool, polyester and cotton were dipped in suitable volume of (10 ml) dye solution of appropriate concentration (500 ppm) in each test tube at room temperature and 90±5 ^{o}C containing necessary concentration of H_2SO_4 separately and were left for 45 min, squeezed and dried in sunlight. One of the two pieces of each fiber, dyed dry clothes using cold and hot methods, was washed with water and dried in sunlight.

3.5.2. Determination of total dye exhaustion and fixation of dye

For determination of total dye exhaustion one piece of each fiber was dyed by each method was squeezed and optical density of extracted solution of each dye was measured to find out concentration from its calibration curve was prepared under similar conditions of temperature and solvent; from the concentration of extract total dye exhaustion was calculated. Dye dry clothes was dipped in 20 ml water and was left for 30 minutes and then was squeezed and optical density of extract was measured and concentration was determined from calibration curve to know the fixation of dye on each of fiber. Dye exhaustion (% E) and fixation (% F) were calculated using the following equations (Mustafa and Turner, 2011).

$$\%E = \frac{(D_0 - D_f)}{D_0} \times 100$$ for extent of exhaustion

$$\%F = \frac{(D_0 - D_f - D_e)}{D_0 - D_f} \times 100$$ for extent of fixation

Where D_0, D_f and D_e are concentration of dye before and after dyeing and amount of extracted dyes respectively.

3.6. Anti-bacterial activity

The synthesized compounds were tested *in vitro* for their antibacterial activity by using the paper disc diffusion technique (Yadav *et al*., 2011). Antibacterial activity of the compounds was tested against two important bacteria, *Escherichia coli* and *Staphylococcus aureus,* using nutrient agar medium. Penicillin, a standard drug, was used as reference in bacterial inhibition. From inhibition zone data correlations of structures with antibacterial activity of compounds were critically examined.

3.6. 1. Preparation of Inoculums

The bacterial cultures were inoculated into the nutrient broth (inoculation medium) and incubated overnight at 37ºC. Inoculated medium containing 24 hrs grown culture were added aseptically to the nutrient medium and mixed thoroughly to get a uniform distribution. The solution was poured approximately 20 mL of sterile MHA in sterile culture plates and allowed to attain room temperature. Sterile agar-disc diffusion previously soaked in a known concentration (100, 75 and 50 mg/mL per disc) synthesized compounds and standard drugs was prepared in DMSO using nutrient agar tubes and carefully placed at the center of the labeled seeded plate. The zones of growth inhibition around the disks were measured after 24 hrs of incubation at 37°C for bacteria. The inhibition zones were measured with a ruler and compared with the positive control disk (disk containing Penicillin).

3.6.2. Molecular docking study of synthesized compounds against DNA gyrase

Molecular docking studies were performed in order to predict the interaction of synthesized compounds with the binding sites of DNA-Gyrase-B. Topoisomerases are interesting antibacterial drug targets, since bacteria express in two forms, DNA gyrase and topoisomerase IV, which were both required for maintenance of proper DNA topology during transcription and replication (Vina, 2011).

The chemical structure of NMR identified compounds **46-53** were drawn using Chem Bio Draw tool (Chem Bio Office Ultra 14.0 suite) assigned with proper 2D orientation, and structure of each was checked for structural drawing error. Energy of each molecule was minimized using ChemBio3D. The energy minimized ligand molecules were then used as input for AutoDock Vina version 4.2 software, in order to carry out the docking simulation. The protein data bank (PDB) used crystal structure of the enzyme as receptor molecule. All the water molecules were removed from the receptor. The graphical user interface program, molecular graphics lab tool was used to set the grid box for docking simulations. The grid was set so that it surrounds the region of interest in the macromolecule. The grid box volume was set to 8, 14, and 14 Å for x, y, and z dimensions, respectively, and the grid center was set to 3.194, 43.143, and 69.977 for x, y, and z center, respectively, which covered all the ten amino acid residues in the considered active pocket. The docking algorithm provided with AutoDockVina version 4.2 software was used to search for the best docked conformation between ligand and protein. During the docking process, a maximum of ten conformers were considered for each ligand. The ligands are represented in different color, H-bonds with their respective distances are represented with yellow color and the interacting residues are represented in ball and stick model representation (Vina, 2011).

4. RESULTS AND DISCUSSION

4.1. Synthesis of azo dyes derivatives

The synthesis of azo dye derivatives was carried out by reaction of diazonium ion and 2-Naphthol (1-Naphthol or Resorcinol or Phenol) to yield compounds from **46** to **53** with 68.3% to 97.7%. Diazonium ion was prepared by diazotization of *p*-nitro aniline (*o*-toluidine or *p*-chloroaniline) using $NaNO_2$ in the presence of hydrochloric acid.

4.2. Reaction mechanism

The plausible mechanism of the reaction starts with diazotization reaction of *p*-Nitroaniline (*o*-Toluidine or *p*-Chloroaniline) with $NaNO_2$ in the presence of hydrochloric acid as shown in the following mechanism.

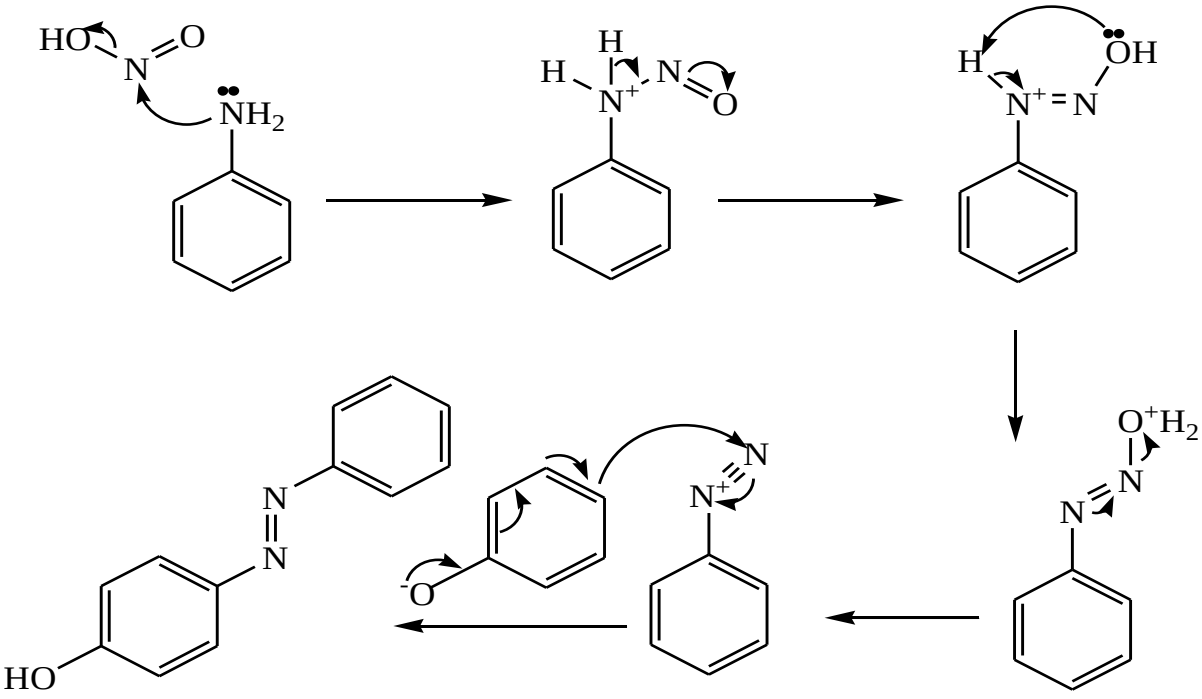

Scheme 11: Reaction mechanism of azo dyes

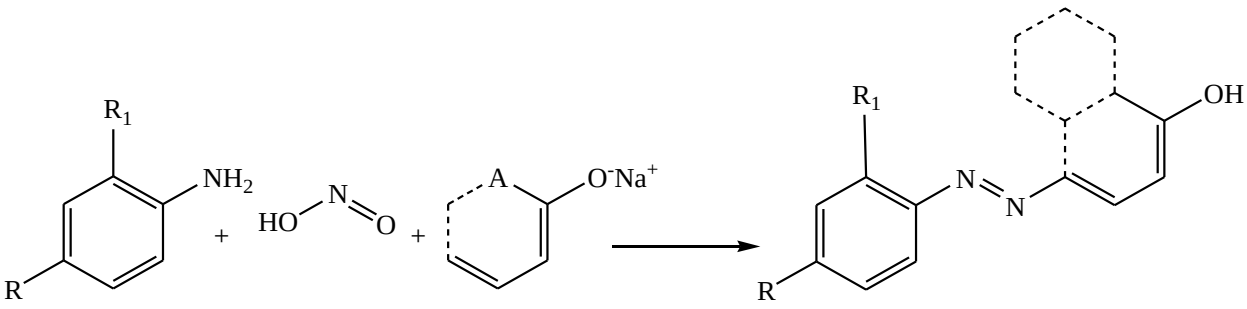

39-41 **42-45** **46-53**

Scheme 12: General scheme for azo dye synthesis

39-41: **39**, R (NO_2), R_1 (H); **40**, R (H), R_1 (CH_3); **41**, R (Cl), R_1 (H).

42-45: **42**, A (2-Naphthol); **43**, A (1-Naphthol); **44**, A (Resorcinol), **45**, A (Phenol).

46-53: 46, a, R (NO_2), R_1 (H), A (2-Naphthol);

47, a, R (NO_2), R_1 (H), A (1-Naphthol);

48, a, R (NO_2), R_1 (H), A (Resorcinol);

49, a, R (NO_2), R_1(H), A (Phenol);

50, b, R (H), R_1 (CH_3), A (2-Naphthol);

51, c, R (Cl), R_1(H), A (2-Naphthol);

52, b, R (H), R_1 (CH_3), A (Resorcinol);

53, c, R (Cl), R_1(H), A (Resorcinol)

4.3. Characterization of synthesized compounds

4.3.1. Physical properties of synthesized compounds

The synthesized azo dye derivatives were obtained as solid crystal with their melting point, percent of yield, molecular weight and color in **Table 4.**

Table 4: Physical characterization and % yield of the synthesized compounds.

Compound	Molecular formula	Color	M.p (°C)	Yield (%)	R_f	TLC solvent system
46	$C_{16}H_{11}N_3O_3$	Red solid	272-275	86.7	**0.28**	5:1 (Petrol /$CHCl_3$)
47	$C_{16}H_{11}N_3O_3$	Red-brown solid	283-285	92.0	**0.74**	2:3 (Petrol /EtOAc)
48	$C_{12}H_9N_3O_4$	Dark red solid	188-190	74.1	**0.74**	1:4 (Petrol /EtOAc)
49	$C_{12}H_9N_3O_3$	Pale yellow solid	232-235	68.3	**0.62**	4:1 (Petrol /EtOAc)
50	$C_{17}H_{14}N_2O$	Red solid	166-168	97.7	**0.25**	4:1 (Petrol /$CHCl_3$)
51	$C_{16}H_{11}ClN_2O$	Orange solid	168-172	73.58	**0.37**	4:1 (Petrol /$CHCl_3$)
52	$C_{13}H_{12}N_2O_2$	Light red solid	185-188	96.0	**0.28**	1:4 (Petrol /$CHCl_3$)
53	$C_{12}H_9ClN_2O_2$	Black solid	189-192	71.0	**0.28**	1:4 (Petrol /$CHCl_3$)

4.3.2. Characterization of synthesized compounds

The ^{1}H and ^{13}C-NMR spectrum was recorded on a Bruker Avance DMX400-FT-NMR spectrometer and the chemical shifts are given in δ (ppm) downfield from tetramethylsilane (TMS) which served as an internal standard.

4.3.2.1. Characterization of 1-((4-Nitrophenyl) Azo)-2-Naphthol (**46**)

Compound **46** was obtained as red crystalline with melting point of 272-275 °C (274-277°C lit (Eissa and Mohamed, 2018)), R_f 0.28 in Petrol/ $CHCl_3$ (5:1) solvent system and 86.7% yield.

The UV-Vis spectrum (200-600 nm, Methanol and water) showed maximum absorption at 405 nm and 379 nm, attributable to (N=N) and (C=C) $n\rightarrow\pi^*$ and $\pi\rightarrow\pi^*$ transitions, respectively (**Appendix 1**). The ^{1}H NMR spectrum (400 MHz, $CDCl_3$, **Table 5**) showed a singlet signals which resonates at δ 16.00 (*s*, OH) corresponding to a hydroxyl proton and doublet signal which resonates at δ 7.14 (*d, J = 7.25* Hz, H-6) corresponding to an aromatic proton. A pair of doublets at δ 8.30 (*d, J = 7.98* Hz, H-9, H-11) and δ 7.64 (*d, J = 7.98* Hz, H-8, H-12) suggest the presence of AA'XX' spin system phenyl ring confirming para substituted aromatic ring. The multiple peaks observed at δ 7.76-7.71 (*m*, 3H, H-5, H-14, H-15) and doublet peaks at δ 7.32 (*d, J = 7.96* Hz, H-13) confirms presence of aromatic ring (**Appendix 2**).

The ^{13}C NMR spectrum (100 MHz, $CDCl_3$, **Table 6**) showed peak at δ 156.6 attributed SP^2 oxygenated quaternary carbon attached to hydroxyl group (C-1). The peak observed at δ 121.6, 153.4 and 150.8 suggest presence of a carbon attached to nitrogen group (C-2, C-7 and C-10). The signal observed at δ 126.5 (C-8, C-12) and 127.7 (C-9, C-11) suggests the AA'XX' spin system aromatic ring suggesting 1,4 substitution pattern. The signals observed at δ 144.4,122.4, 124.7, 122.5, 126.4 and 129.8 indicates the SP^2 methines (C-5, C-6, C-13, C-14, C-15 and C-16) (**Appendix 3**). In DEPT-135 NMR spectrum there is no signals at δ 156.6, 121.6, 125.7, 129.3,153.4 and 150.8, which suggests the six quaternary carbon (C-1, C-2, C-3, C-4, C-7 and C-10) (**Appendix 4**). Based on ^{1}H NMR and ^{13}C-NMR recorded data (**Table 5**) and comparison with literature spectral data (Eissa and Mohamed, 2018), the structure of synthesized compound was fully elucidated as follows.

Table 7: ^{1}H, ^{13}C- NMR and DEPT-135 spectral data of compound **46** in $CDCl_3$.

Position	**46**			Eissa and Mohamed, 2018	
	^{1}H	^{13}C	DEPT-135	^{1}H	^{13}C
1	16.00 (1H, *s*, OH)	156.6	-	12.25 (1H, *s*, OH)	156.0
2	-	121.6	-	-	120.0
3	-	125.7	-	-	125.9
4	-	129.3	-	-	129.1
5	-	144.4	144.4	-	145.0
6	7.14 (1H, *d*, *J = 7.25* Hz)	122.4	122.4	7.20 (1H, *d*, Ar)	122.5
7	-	153.4	-	-	154.0
8,12	7.64 (2H, *d*, *J = 7.98* Hz)	126.5	126.5	7.80 (2H, *d*, Ar)	127.2
9,11	8.30 (2H, *d*, *J = 7.98* Hz)	127.7	127.7	8.45 (2H, *d*, Ar)	124.9
10	-	150.8	-	-	149.8
13	7.32 (1H, *d*, *J = 7.96* Hz, Ar)	124.7	124.7	7.45 (2H, *m*, Ar)	126.1
14	7.76-7.71 (3H, *m*, H-5, H-14, H-15)	122.7	122.5	8.05-8.25 (3H, *m*, Ar)	122.5
15	-	126.4	126.4	-	126.1
16	-	129.8	129.8	-	129.1

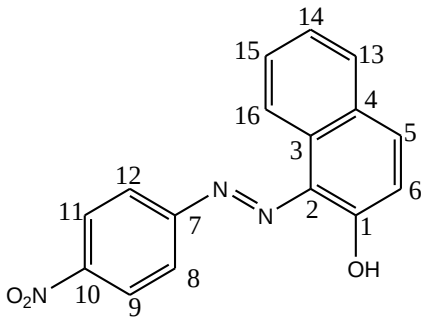

46

4.3.2.2. Characterization of 4-((4-Nitrophenyl) Azo)-1-Naphthol (47)

Compound **47** was obtained as Red-brown solid crystalline with melting point of 283-285°C (281-283°C lit. (Eissa and Mohamed, 2018)), R_f 0.74 in Petrol / EtOAc (2:3) solvent system and 92.0% yield.

The UV-Vis spectrum (200-600 nm, Methanol and water) showed maximum absorption at 450 nm and 325 nm, attributable to (N=N) and (C=C) n→π* and π→π* transitions, respectively (**Appendix 5**). The ^{1}H NMR spectrum (400 MHz, $CDCl_3$, **Table 6**) showed signals a pair of doublet at δ 9.05 (*d, J = 7.98* Hz, H-2) and 7.96 (*d, J = 7.98* Hz, H-3) corresponding to an aromatic proton. A pair of doublet each at δ 7.50 (*d, J = 8.20* Hz, H-9, H-11) and δ 7.42 (*d, J = 8.20* Hz, H-8, H-12) suggest the presence of AA'XX' spin system confirming 1,4 substituted phenyl ring. The multiple peak observed at δ 8.10-8.30 (*m*, H-13, H-14, H-15) confirms presence of aromatic ring (**Appendix 6**).

The ^{13}C NMR spectrum (100 MHz, $CDCl_3$, **Table 6**) showed peak at δ 156.7 attributed to SP^2 oxygenated carbon attached to hydroxyl group (C-1). The peak observed at δ 143.2, 154.8 and 149.5 suggest presence of a carbon attached to nitrogen group (C-4, C-7 and C-10). The signal observed at δ 125.9 (C-8, C-12) and 127.4 (C-9, C-11) suggests SP^2 methines confirming AA'XX' spin system aromatic ring (**Appendix 7**). The signals observed at δ 107.1, 115.9, 123.3, 120.0, 127.0 and 128.4 indicates aromatic methines (C-2, C-3, C-13, C-14, C-15 and C-16).

In DEPT-135 NMR spectrum there is no signals at δ 156.7, 143.2, 123.9, 124.3, 154.8 and 149.5, which suggests the six quaternary carbons (C-1, C-4, C-5, C-6, C-7 and C-10) (**Appendix 8**). Based on ^{1}H NMR and ^{13}C-NMR recorded data (**Table 6**) and comparison with literature spectral data (Eissa and Mohamed, 2018), the structure of synthesized compound was fully elucidated as follows.

Table 8: ^{1}H, ^{13}C- NMR and DEPT-135 spectral data of compound **47** in $CDCl_3$**.**

Position	**47**			Eissa and Mohamed, 2018	
	^{1}H	^{13}C	DEPT-135	^{1}H	^{13}C
1	-	156.7	-	11.95 (1H, *s*, OH)	156.8
2	9.05 (1H, *d*, *J = 7.98* Hz)	107.1	107.0	8.95 (1H, *d*, Ar)	108.9
3	7.96 (1H, *d*, *J = 7.98* Hz)	115.9	115.9	8.65 (1H, *d*, Ar)	115.0
4	-	143.2	-	-	143.0
5	-	123.9	-	-	120.0
6	-	124.3	-	-	124.9
7	-	154.8	-	-	155.0
8,12	7.42 (2H, *d*, *J = 8.20* Hz)	125.9	125.8	7.35 (2H, *d*, Ar)	123.9
9,11	7.50 (2H, *d*, *J = 8.20* Hz)	127.4	129.0	7.50 (2H, *d*, Ar)	127.2
10	-	149.5	-	-	150.5
13	8.10-8.30 (3H, *m*, H-13, H-14, H-15)	123.3	123.1	8.15-8.30 (3H, *m*, Ar)	123.7
14	-	120.0	120.7	-	-
15	-	127.0	127.4	-	127.1
16	-	128.4	127.8	7.15 (1H, *d*, Ar)	-

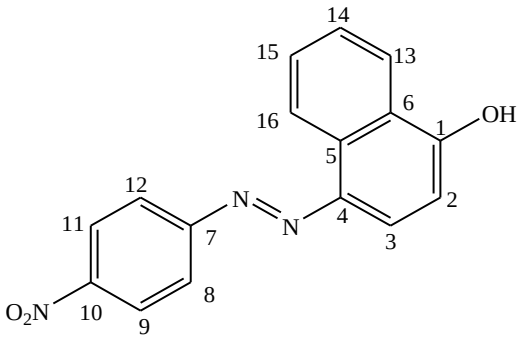

47

4.3.2.3. Characterization of 1-((4-Nitrophenyl) Azo)-Resorcinol (48)

Compound **48** was obtained as Dark red solid crystalline with melting point of 188-190°C (183-185 °C lit (Valizadeh et al., 2015)), R_f 0.74 in Petrol / EtOAc (1:4) solvent system and 74.1% yield.

The UV-Vis spectrum (200-600 nm, Methanol and water) showed maximum absorption at 452 nm and 260 nm, attributable to (N=N) and (C=C) $n \rightarrow \pi^*$ and $\pi \rightarrow \pi^*$ transitions, respectively (**Appendix 9**). The ^{1}H NMR spectrum (400 MHz, $CDCl_3$,**Table 9**) showed a singlet signal at δ 6.01 (s, OH) corresponding to a hydroxyl proton. A doublet signals which resonates at δ 5.54 (*d, J = 2.41* Hz) proton attached to aromatic carbon. A pair of doublet peaks observed at δ 6.82 (*d, J = 8.20* Hz, H-8, H-12) and δ 7.48 (*d, J = 8.20* Hz, H-9, H-11) suggest the presence of AA'XX' aromatic ring confirming 1,4-substitution pattern (**Appendix 10**).

The ^{13}C NMR spectrum (100 MHz, $CDCl_3$, **Table 10**) showed peak at δ 159.9 and 164.6 attributed to carbons attached to hydroxyl group (C-1 and C-3). The peak observed at δ 143.8, 151.8 and 148.2 suggest presence of a carbon attached to nitrogen group (C-4, C-7 and C-10). The signal observed at δ 119.8 (C-8, C-12) and 123.9 (C-9, C-11) suggests SP^2 methines confirming AA'XX' spin system aromatic ring. The upfield chemical shift value of C-2 appearing at δ 102.3 indicates 1,3- diorthooxygenation pattern due to two hydroxyl groups at C-1 and C-2 positions responsible for upfield chemical shift values due to delocalization from lone pair oxygen of hydroxyl groups and the signals observed at δ 128.0 (C-5) and 110.8(C-6) suggest ABX spin system of aromatic ring (**Appendix 11**). In DEPT-135 NMR spectrum there is no signals at δ 159, 164.6, 143.8, 151.8 and 148.2 which suggests the five quaternary carbon (C-1, C-3, C-4, C-7 and C-10) (**Appendix 12**). Based on ^{1}H NMR and ^{13}C-NMR recorded data (**Table 7**) and comparison with literature spectral data (Valizadeh *et al*., 2015), the structure of synthesized compound was fully elucidated as follows.

Table 11: ^{1}H, ^{13}C- NMR and DEPT-135 spectral data of compound **48** in $CDCl_3$.

Position	**48**			Valizadeh *et al*., 2015	
	^{1}H	^{13}C	DEPT-135	^{1}H	^{13}C
1	6.01 (*s*, OH)	159.9	-	8.92 (*s*, OH)	149.7
2	5.54 (1H, *d, J = 2.41* Hz)	102.3	107.3	6.32 (1H, *d*, Ar)	105.8
3	-	164.6	-	12.03 (*s*, OH)	156.2
4	-	143.8	-	-	130.9
5	-	128.0	129.6	7.74 (1H, *d*, Ar*)*	128.3
6	-	110.8	115.7	6.62 (1H, *dd*, Ar)	110.6
7	-	151.8	-	-	148.1
8,12	6.82 (2H, *d, J = 8.20* Hz)	119.8	124.7	7.83 (2H, *d*, Ar)	120.9
9,11	7.48 (2H, *d, J = 8.20* Hz)	123.9	128.9	7.85 (2H, *d*, Ar)	127.3
10	-	148.2	-	-	146.1

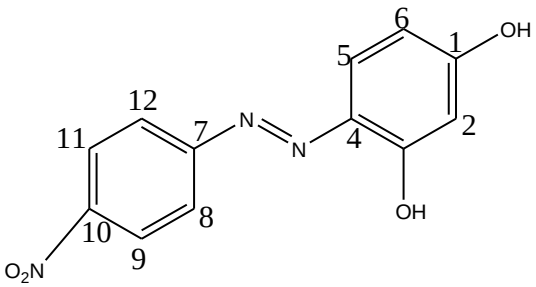

48

4.3.2.4. Characterization of 1-((4-Nitrophenyl) Azo)- Phen-4-ol (49)

Compound **49** was obtained as Pale yellow solid crystalline with melting point of 232-235°C (235-237°C lit. (Eissa and Mohamed, 2018)), R_f 0.62 in Petrol /EtOAc (4:1) solvent system and 68.3% yield.

The UV-Vis spectrum (200-600 nm, Methanol and water) showed maximum absorption at 403 nm and 270 nm, attributable to (N=N) and (C=C) n→π* and π→π* transitions, respectively (**Appendix 13**).

The ^{1}H NMR spectrum (400 MHz, $CDCl_3$, **Table 12**) showed a singlet signal which resonates at δ 5.95 (*s*, 1H OH) corresponding to a hydroxyl proton. The four doublet peaks observed at δ 5.85 (*d, J = 7.95* Hz, H-2, H-6), δ 6.34 (*d, d, J = 7.95* Hz, H-3, H-5), δ 6.76 (*d, J = 8.02* Hz, H-8, H-12) and δ 6.84 (*d, J = 8.02* Hz, H-9, H-11) confirms presence of two aromatic rings with AA'XX' spin system suggesting the presence of two 1,4- substituted phenyl ring (**Appendix 14**).

The ^{13}C NMR spectrum (100 MHz, $CDCl_3$, **Table 13**) showed a total of 12 well resolved signals. The signal resonating at δ 160.1 attributed to SP^2 quaternary carbon attached to hydroxyl group (C-1). The peak observed at δ 144.0, 152.7 and 148.9 suggest presence of a carbon attached to nitrogen group (C-4, C-7 and C-10). The signal observed at δ 126.8 (C-2, C-6), 129.7 (C-3, C-5), 119.8 (C-8, C-12) and 128.8 (C-9, C-11) suggests the presence of four equivalent aromatic carbons suggesting two phenyl rings with AA'XX' spin system (**Appendix 15**). In DEPT-135 NMR spectrum there is no signals at δ 160.1, 144.0, 152.7 and 148.9 which suggests the four quaternary carbon (C-1, C-4, C-7 and C-10) (**Appendix 16**). Based on ^{1}H NMR and ^{13}C-NMR recorded data (**Table 8**) and comparison with literature spectral data (Eissa and Mohamed, 2018), the structure of synthesized compound was fully elucidated as follows.

Table 14: ^{1}H, ^{13}C- NMR and DEPT-135 spectral data of compound **49** in $CDCl_3$.

Position	**49**			Eissa and Mohamed, 2018	
	^{1}H	^{13}C	DEPT-135	^{1}H	^{13}C
1	5.95 (1H, *s*, OH)	160.1	-	11.35 (1H, *s*, OH)	160.0
2,6	5.85 (2H, *d, J = 7.95* Hz)	126.8	126.8	7.55-7.70 (4H, *m*, Ar)	-
3,5	6.34 (2H, *d, J = 7.95* Hz)	129.7	129.7	-	123.8
4	-	144.0	-	-	143.9
7	-	152.7	-	-	152.1
8,12	6.76 (2H, *d, J = 8.02* Hz)	119.8	119.8	7.00 (2H, *d*, Ar)	119.5
9,11	6.84 (2H, *d, J = 8.02* Hz)	128.8	128.5	8.25 (2H, *d*, Ar)	123.6
10	-	148.9	-	-	148.9

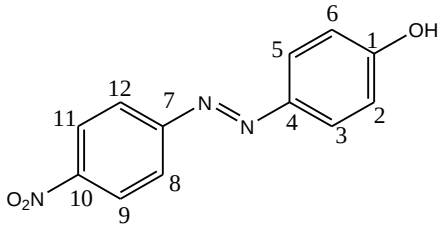

49

4.3.2.5. Characterization of 1-((*O*-toluidine) Azo)-2-Naphthol (50)

Compound **50** was obtained as red solid crystalline with melting point of 166-168°C (169-171 °C lit. (Ajani *et al.*, 2013)). R_f 0.25 in Petrol /$CHCl_3$ (4:1) solvent system and 97.7 % yield.

The UV-Vis spectrum (200-600 nm, Methanol and water) showed maximum absorption at 391 nm and 329 nm, attributable to (N=N) and (C=C) n→π* and π→π* transitions, respectively (**Appendix 17**). The ^{1}H NMR spectrum (400 MHz, MeOD, **Table 15**) showed singlet signals which resonates at δ 6.76 (*s*, OH) and 2.45 (*s*, 3H) corresponding to a hydroxyl proton and a methyl proton respectively. Doublet peaks observed at δ 8.46 (*d*, *J = 7.87* Hz, H-5) and δ 7.59 (*d*, *J = 7.80* Hz, H-9, H-10) corresponding to an aromatic proton. One multiple peaks observed at δ 7.35 – 6.93 (*m*, H-14, H-15, H-16) confirms presence of aromatic ring (**Appendix 18**).

The ^{13}C NMR spectrum (100 MHz, MeOD, **Table 16**) showed peak at δ 152.2 attributed SP^2 quaternary carbon attached to hydroxyl group (C-1). The peak observed at δ 145.8 and 147.6 suggest presence of carbon attached to nitrogen group (C-2, C-7). The peak observed at δ 16.4 suggest presence of methyl group (C-13) (**Appendix 19**). In DEPT-135 NMR spectrum there is no signals at δ 152.2, 145.8, 130.3, 131.6, 147.6 and 133.2 which suggests the six quaternary carbon (C-1, C-2, C-3, C-4, C-7 and C-12) (**Appendix 20**). Based on ^{1}H NMR and ^{13}C-NMR recorded data (**Table 9**) and comparison with literature spectral data (Ajani *et al*., 2013), the structure of synthesized compound was fully elucidated as follows.

Table 17: ^{1}H, ^{13}C- NMR and DEPT-135 spectral data of compound **50** in MeOD.

Position	**50**			Ajani *et al*., 2013	
	^{1}H	^{13}C	DEPT-135	^{1}H	^{13}C
1	6.76 (1H, *s*, OH)	152.2	-	-	149.0
2	-	145.8	-	-	148.6
3	-	130.3	-	-	130.4
4	-	131.6	-	-	-
5	8.46 (1H, *d, J = 7.87* Hz)	133.8	133.6	8.56-8.54 (1H, *d*, Ar)	134.5
6	-	119.2	119.2	6.96-6.94 (1H, *d*, Ar)	125.7
7	-	147.6	-	-	148.6
8	-	126.9	126.9	-	128.5
9	7.59 (2H, *d, J = 7.80* Hz, H-9, H-10)	130.8	130.9	-	-
10	-	135.4	136.3	-	-
11	-	132.3	132.6	-	-
12	-	133.2	-	-	-
13	2.45 (3H, *s*)	16.4	16.0	-	-
14	7.35 – 6.93 (3H, *m*, H-14, H-15, H-16)	128.7	128.8	8.10- 8.07 (1H, *d*, Ar)	130.7
15	-	125.4	125.4	7.48-7.44 (1H, *d*, Ar)	126.6
16	-	127.7	127.7	7.51-7.49 (1H, *d*, Ar)	128.1
17	-	127.3	-	7.97-7.95 (1H, *d*, Ar)	127.5

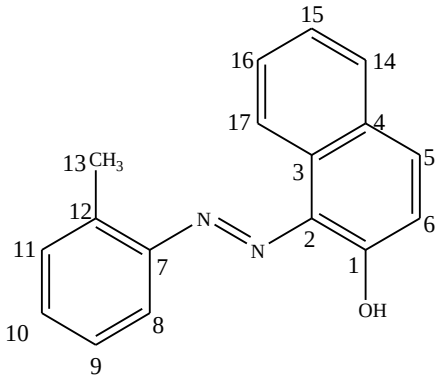

50

4.3.2.6. Characterization of 1-((4-Chlorophenyl) Azo)-2-Naphthol (**51**)

Compound **51** was obtained as orange solid crystalline with melting point of 168-172°C (169-171 lit. (Ajani *et al*., 2013)). R_f 0.37 in Petrol /$CHCl_3$ (4:1) solvent system and 73.58% yield.

The UV-Vis spectrum (200-600 nm, Methanol and water) showed maximum absorption at 413 nm and 380 nm, attributable to (N=N) and (C=C) n→π* and π→π* transitions, respectively (**Appendix 21**). The ^{1}H NMR spectrum (400 MHz, MeOD, **Table 18**) showed a pair of doublet signals at δ 8.56 (*d, J = 7.67 Hz,* H-5) and 6.86 (*d, J = 7.67* Hz, H-6) corresponding to an aromatic proton. A pair of doublet peaks observed at δ 7.18 (*d*, H-8, H-12) and δ 7.58 (*d*, H-9, H-11) confirms presence of AA'XX' spin system suggesting 1,4 substituted phenyl ring. Two triplet signals which resonates at δ 7.66 (t, H-14) and 7.31 (t, H-15) and one doublet signal at δ 7.50 (*d, J = 7.67* Hz, H-16) corresponding to an aromatic proton (**Appendix 22**).

The ^{13}C NMR spectrum (100 MHz, MeOD, **Table 19**) showed peak at δ 150.9 attributed to SP^2 carbon attached to hydroxyl group (C-1). The peak observed at δ 145.8 and 147.2 suggest presence of carbon attached to nitrogen group (C-2, C-7). The signal observed at δ 127.2 (C-8, C-12) and 128.7 (C-9, C-11) suggests the presence of AA'XX' spin pattern phenyl ring. The peak observed at δ 135.3 suggest presence of a carbon attached to halogen group (C-10) (**Appendix 23**). In DEPT-135 NMR spectrum there is no signals at δ 150.9, 145.8, 130.4, 131.7, 147.2 and 135.3 which suggests the six quaternary carbon (C-1, C-2, C-3, C-4, C-7 and C-10) (**Appendix 24**). Based on ^{1}H NMR and ^{13}C-NMR recorded data (**Table 10**) and comparison with literature spectral data (Ajani *et al*., 2013), the structure of synthesized compound was fully elucidated as follows.

Table 20: ^{1}H, ^{13}C- NMR and DEPT-135 spectral data of compound 51 in MeOD.

Position	**51**			Ajani *et al*., 2013	
	^{1}H	^{13}C	DEPT-135	^{1}H	^{13}C
1	-	150.9	-	-	149.0
2	-	145.8	-	-	148.6
3	-	130.4	-	-	130.4
4	-	131.7	-	-	130.4
5	8.56 (1H, *d*, *J* = *7.67* Hz)	133.9	133.4	8.56-8.54 (1H, *d*, Ar)	134.5
6	6.86 (1H, *d*, *J* = *7.67* Hz)	119.5	119.4	6.96-6.94 (1H, *d*, Ar)	125.7
7	-	147.2	-	-	148.6
8,12	7.18 (2H, *d*, *J* = *7.80* Hz)	127.2	127.2	7.64-7.60 (2H, *m*, Ar)	128.5
9,11	7.58 (2H, *d*, *J* = *7.80* Hz)	128.7	128.8	7.81-7.79 (2H, *d*, Ar)	132.1
10	-	135.3	-	-	138.4
13	-	129.5	129.9	8.10- 8.07 (1H, *d*, Ar)	130.7
14	7.66 (1H, *t*, *J* = *7.28* Hz)	125.9	126.2	7.48-7.44 (1H, *d*, Ar)	126.6
15	7.31 (1H, *t*, *J* = *7.32* Hz)	128.5	128.6	7.51-7.49 (1H, *d*, Ar)	128.1
16	7.50 (1H, *d*, *J* = *7.67* Hz)	127.8	127.6	7.97-7.95 (1H, *d*, Ar)	127.5

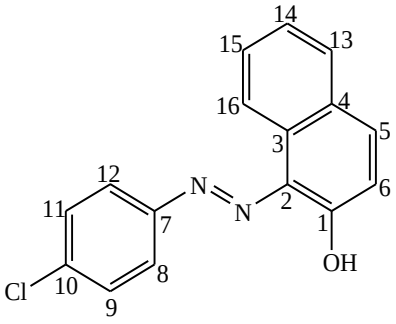

51

4.3.2.7. Characterization of 1- ((*O*-toluidine) Azo)-Resorcinol (52)

Compound **52** was obtained as light red solid crystalline with melting point of 185-188°C (183-185 lit. (Valizadeh *et al.*, 2015), R_f 0.28 in Petrol/ $CHCl_3$ (1:4) solvent system and 96.0% yield.

The UV-Vis spectrum (200-600 nm, Methanol and water) showed maximum absorption at 437 nm and 321 nm, attributable to (N=N) and (C=C) $n \rightarrow \pi^*$ and $\pi \rightarrow \pi^*$ transitions, respectively (**Appendix 25**). The ^{1}H NMR spectrum (400 MHz, MeOD, **Table 21**) showed three singlet signals which resonates at δ 7.14 (*s*, OH), δ 14.30 (*s*, OH) and δ 2.37 (*s*, 3H) corresponding to two hydroxyl protons and methyl protons. Three doublet peaks observed at δ 6.20 (*d*, *J = 2.41* Hz, H-2), 7.52 (*d*, *J = 8.15* Hz, H-5) and δ 6.39 (*dd*, *J = 8.15* and *2.41* Hz, H-6) confirms presence ABX spin pattern of aromatic ring (**Appendix 26**).

The ^{13}C NMR spectrum (100 MHz, MeOD, **Table 22**) showed peak at δ 158.2 and 163.3 attributed to carbons attached to hydroxyl group (C-1, C-3). The peak observed at δ 115.0 and 147.3 suggest presence of a carbon attached to nitrogen group (C-4, C-7) (**Appendix 27**). The signals observed at δ 106.5 indicates the carbon attached to two carbons which contain hydroxyl group (C-2). The signals observed at δ 129.3 and 109.4 indicates the two resorcinol carbons (C-5 and C-6). The signals observed at δ 16.9 and 133.8 indicates the methyl group and SP^2 quaternary carbon attached to methyl group (C-12 and C-13) respectively. In DEPT-135 NMR spectrum there is no signals at δ 158.2, 163.3, 115.0, 147.3 and 133.8 which suggests the five quaternary carbon (C-1, C-3, C-4, C-7 and C-12) (**Appendix 28**). Based on ^{1}H NMR and ^{13}C-NMR recorded data (**Table 11**) and comparison with literature spectral data (Valizadeh *et al.*, 2015), the structure of synthesized compound was fully elucidated as follows.

Table 23: ^{1}H, ^{13}C- NMR and DEPT-135 spectral data of compound **52** in MeOD.

Position	**52**			Valizadeh *et al.,* 2015	
	^{1}H	^{13}C	DEPT-135	^{1}H	^{13}C
1	7.14 (*s*, OH)	158.2	-	8.92 (*s*, OH)	149.7
2	6.20 (1H, *d, J = 2.41* Hz)	106.5	106.5	6.32 (1H, *d*, Ar)	105.8
3	14.30 (*s*, OH)	163.3	-	12.03 (*s*, OH)	156.2
4	-	115.0	-	-	130.9
5	7.52 (1H, *d, J = 8.15* Hz)	129.3	129.3	7.74 (1H, *d*, Ar)	128.3
6	6.39 (1H, *dd, J = 8.15* and *2.41* Hz)	109.4	109.4	6.62 (1H, *dd*, Ar)	110.6
7	-	147.3	-	-	148.1
8	-	126.6	126.6	7.83 (2H, *d*, Ar)	120.9
9	-	130.9	130.9	7.85 (2H, *d*, Ar)	127.3
10	-	134.7	134.7	-	146.1
11	-	132.9	129.6	-	-
12	-	133.8	-	-	-
13	2.37 (*s*, 3H)	16.9	16.9	-	-

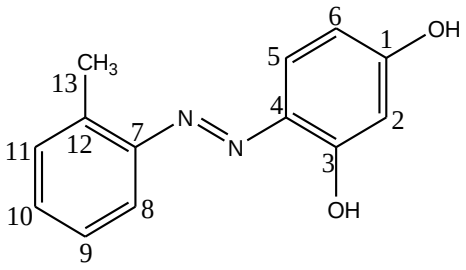

52

4.3.2.8. Characterization of 1-((4-Chlorophenyl) Azo)-Resorcinol (53)

Compound **53** was obtained as black solid crystalline with melting point of 189-192°C (183-185 lit. (Valizadeh *et al.,* 2015)), R_f 0.28 in Petrol/ $CHCl_3$ (1:4) solvent system and 71.0% yield.

The UV-Vis spectrum (200-600 nm, Methanol and water) showed maximum absorption at 489 nm and 452 nm, attributable to (N=N) and (C=C) n→π* and π→π* transitions, respectively (**Appendix 29**).

The ^{1}H NMR spectrum (400 MHz, MeOD, **Table 24**) showed a singlet and doublet of doublet signals which resonates at δ 7.87 (*s*, OH) corresponding to a hydroxyl proton. Three pair of doublet signals at δ 6.22 (*d, J = 2.41* Hz, H-2), δ 7.55 (*d, J = 8.15* Hz, H-5) and δ 6.42 (*dd, J = 8.15* and *2.41* Hz, H-6) conform presence of ABX spin system of aromatic ring. A pair of doublet peaks observed at δ 7.36 (*d, J = 8.20* Hz, H-8, H-12) and δ 7.64 (*d, J = 8.20* Hz, H-9, H-11) confirms presence AA'XX' spin system of 1,4 substituted phenyl ring (**Appendix 30**).

The ^{13}C NMR spectrum (100 MHz, MeOD, **Table 25**) showed peak at δ 167.3 and 160.2 attributed to carbons attached to hydroxyl group (C-1 and C-3). The peak observed at δ 136.3 and 153.0 suggest presence of a carbon attached to nitrogen group (C-4, C-7). The signal observed at δ 126.3 (C-8, C-12) and 133.0 (C-9, C-11) suggests the presence of AA'XX' spin system of phenyl ring. The signals observed at δ 106.6 indicates the carbon attached to two carbons which contain hydroxyl group (C-2). The signals observed at δ 138.0 and 112.9 indicates the SP^2 methines (C-5 and C-6). The signals observed at δ 139.0 indicates the carbon attached to halogen group (C-10) (**Appendix 31**). In DEPT-135 NMR spectrum there is no signals at δ 167.3, 160.2, 136.3, 153.0 and 139.0 which suggests the five quaternary carbon (C-1, C-3, C-4, C-7 and C-10) (**Appendix 32**). Based on ^{1}H NMR and ^{13}C-NMR recorded data (**Table 12**) the formation of the target compound has been assured.

Table 26: ^{1}H, ^{13}C- NMR and DEPT-135 spectral data of compound **53** in MeOD.

Position	**53**			Valizadeh *et al.*, 2015	
	^{1}H	^{13}C	DEPT-135	^{1}H	^{13}C
1	7.87 (*s*, OH)	167.3	-	8.92 (*s*, OH)	156.2
2	6.22 (1H, *d, J = 2.41* Hz)	106.6	106.5	6.32 (1H, d, Ar)	105.8
3	-	160.2	-	12.03 (*s*, OH)	149.7
4	-	136.3	-	-	130.9
5	7.55 (1H, *d, J = 8.15* Hz)	138.0	138.0	7.74 (1H, *d*, Ar)	128.3
6	6.42 (1H, *dd, J = 8.15* and *2.41* Hz)	112.9	112.9	6.62 (1H, *dd*, Ar)	110.6
7	-	153.0	-	-	148.1
8,12	7.36 (2H, *d, J = 8.20* Hz)	126.3	127.3	7.83 (2H, *d*, Ar)	120.9
9,11	7.64 (2H, *d, J = 8.20* Hz)	133.0	128.3	7.85 (2H, *d*, Ar)	127.3
10	-	139.0	-	-	146.1

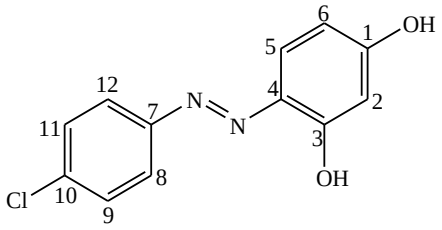

53

4.4. Dyeing studies

The stability and color intensity of Azo dyes being acid (pH) dependent, H_2SO_4 concentration necessary for producing maximum color intensity by each dye has been determined as 2663ppm, 2130ppm, 1597ppm and 3195ppm for **46- 53** dyes respectively. Dye exhaustion and fixation data (**Table 16 and 17**) clearly show that all the eight dyes used have highest dyeing potential in cold dyeing treatment for all the four types of fibers owing to their highest exhaustion and fixation on the fibers probably because of maximum reaction of dye molecules with fiber material and high stability of reaction products at room temperature. The different colors on diverse fibers of these dyes could be accounted for in terms of different structures of their reaction products with the fibers. Fiber wise order in dyeing potential of all the dyes is cotton > polyester > silk > wool. Dyeing properties of these compounds were in good agreement with those reported in literature (Upadhyay *et al*., 2011)

Table 27: Optical density of dye solutions at different wave lengths.

S.No.	wave length (nm)	optical density of dyes							
		46	**47**	**48**	**49**	**50**	**51**	**52**	**53**
1	200	-	-	-	-	-	-	-	-
2	264	-	0.825	0.623	1.170	-	-	0.354	-
3	329	-	0.532	0.420	0.884	1.720	-	0.218	-
4	403	1.932	0.456	0.754	1.414	0.617	0.877	0.472	2.121
5	405	1.934	0.454	0.777	1.413	0.618	0.881	0.483	2.135
6	413	1.915	0.443	0.874	1.372	0.621	0.888	0.526	2.174
7	437	1.511	0.420	1.167	0.980	0.581	0.785	0.599	2.164
8	450	1.182	0.398	1.229	0.756	0.545	0.691	0.573	2.431
9	452	1.132	0.394	1.236	0.727	0.541	0.676	0.566	2.823
10	500	0.548	0.278	0.414	0.299	0.506	0.341	0.207	1.887
11	550	0.446	0.243	-	0.103	0.446	0.247	0.124	0.577
12	600	0.388	0.225	-	-	0.332	0.226	0.096	0.443
	λ_{max}	405	264	452	403	329	413	437	452

Dyes:

46 = 1-((4-Nitrophenyl) azo)-2-Naphthol

47 = 4-(4-Nitrophenylazo)-1-Naphhthol

48 = 1-((4-Nitrophenyl) azo)-Resorcinol

49 = 1-((4-Nitrophenyl) azo)- Phen-4-ol

50 = 1-((*O*-toluidine) azo)-2-Naphthol

51 = 1-((4-Chlorophenyl) azo)-2-Naphthol

52 = 1- ((*O*-toluidine) azo)-Resorcinol

53 = 1-((4-Chlorophenyl) azo)-Resorcinol

Table 28: Optical density at varying concentrations of H_2SO_4 at λ_{max} of dyes.

S.No.	Conc. of H_2SO_4 (ppm)	Optical density dyes							
		46	**47**	**48**	**49**	**50**	**51**	**52**	**53**
1	1065	0.037	0.335	0.426	0.043	0.210	0.131	0.716	0.080
2	1597	0.040	0.329	0.464	0.037	0.179	0.126	0.762	0.084
3	2130	0.040	0.352	0.443	0.033	0.148	0.125	0.703	0.084
4	2663	0.043	0.344	0.448	0.038	0.170	0.150	0.718	0.087
5	3195	0.042	0.338	0.468	0.036	0.199	0.141	0.728	0.089
6	3728	0.042	0.313	0.480	0.033	0.185	0.132	0.680	0.086
	λ_{max}	405 100ppm	264 100ppm	452 100ppm	403 100ppm	329 100ppm	413 100ppm	437 100ppm	452 100ppm

Values in parenthesis are concentrations of dyes

Table 29: Optical density at λ_{max} in varying in concentrations of dyes with appropriate concentrations of acid.

S. No	Dye conc. (ppm)	Optical density at λ_{max}							
		46	**47**	**48**	**49**	**50**	**51**	**52**	**53**
1	20	0.027	0.111	0.098	0.026	0.114	0.056	0.174	0.040
2	30	0.030	0.098	0.092	0.036	0.087	0.051	0.180	0.036
3	40	0.041	0.118	0.145	0.039	0.084	0.048	0.241	0.046
4	50	0.044	0.133	0.166	0.027	0.095	0.080	0.338	0.032
5	60	0.045	0.026	0.233	0.030	0.121	0.077	1.304	0.058
6	70	0.045	0.223	0.300	0.043	0.073	0.084	0.493	0.061
	λ_{max}	405 2663 ppm	264 2130 ppm	452 3728 Ppm	403 1065 ppm	329 1065 ppm	413 2663 ppm	437 1597 ppm	452 3195 Ppm

Values in parenthesis are concentrations of H_2SO_4

Table 30: Dye exhaustion data.

Dye	Method of dyeing	Dye conc. before dyeing (ppm)	Dye conc. after dyeing (ppm)				Dye Exhaustion by fiber (%)			
			Cotton	Wool	Silk	Polyester	Cotton	Wool	Silk	Polyester
46	Cold Hot	500 500	149 260	260 217	154 272	211 251	70.2 48.0	48.0 56.6	69.2 45.6	57.8 49.8
47	Cold Hot	500 500	344.2 136	391 295	357 258	331 292	31.2 72.8	21.8 41.0	28.5 48.4	33.8 41.6
48	Cold Hot	500 500	55 232	26 203	75 222	77 196	89.0 53.6	94.8 59.4	84.8 55.6	84.6 60.8
49	Cold Hot	500 500	96 136	125 115	117 121	110 152	80.8 72.8	75.0 77.0	76.6 75.8	78.0 69.6
50	Cold Hot	500 500	408 138	286 127	346 146	360 156	18.4 72.4	42.8 74.6	30.8 71.0	28.0 68.8
51	Cold Hot	500 500	293 182	235 192	264 320	284 215	41.4 63.6	53.0 61.6	47.2 36.0	43.2 57.0
52	Cold Hot	500 500	153 53	164 70	152 157	173 154	69.4 89.4	67.2 86.0	69.6 68.6	65.4 69.2
53	Cold Hot	500 500	238 222	297 231	264 250	261 269	52.4 55.6	40.6 53.8	47.2 50.0	47.8 46.2

Table 31: Dye fixation data.

Dye	Method of dyeing	After washing conc. of dye (ppm)				Fixation of dye on fiber (%)				Color
		Cotton	Wool	Silk	Polyester	Cotton	Wool	Silk	Polyester	
46	Cold Hot	99 36	54 98	32 66	19 74	71.5 85.0	77.5 65.3	90.7 83.7	93.4 70.2	red solid
47	Cold Hot	96 169	87 109	73 97	46 96	38.4 53.5	19.4 46.8	48.5 59.9	72.7 53.8	Red-brown solid
48	Cold Hot	13 34	16 54	17 137	39 132	97.0 87.3	96.4 81.8	95.9 50.7	90.7 56.7	Dark red solid
49	Cold Hot	14 47	33 37	24 29	31 38	96.5 87.0	91.2 90.3	93.7 90.2	92.0 89.3	Pale yellow solid
50	Cold Hot	62 71	46 69	31 27	30 58	32.6 80.3	78.5 81.5	79.8 92.3	77.6 83.1	Red solid
51	Cold Hot	24 23	15 18	13 15	19 8	88.4 92.7	94.3 93.8	94.4 91.6	91.2 97.1	Orange solid
52	Cold Hot	34 81	48 173	42 90	72 203	90.2 81.8	85.7 59.7	87.9 73.7	94.5 41.6	Light red solid
53	Cold Hot	28 46	65 46	37 34	37 36	89.3 83.4	67.9 82.8	84.3 86.4	84.5 84.4	Black solid

In the following figures **(Figure 7-14**) the symbols represent, cotton in cold method (CC), cotton in hot method (HC), wool in cold method (CW) and wool in cold method (HW), silk in cold method (CS), silk in hot method (HS), polyester in cold method (CP), polyester in hot method (HP), respectively for all **46, 47, 48, 49, 50, 51, 52** and **53** as follow.

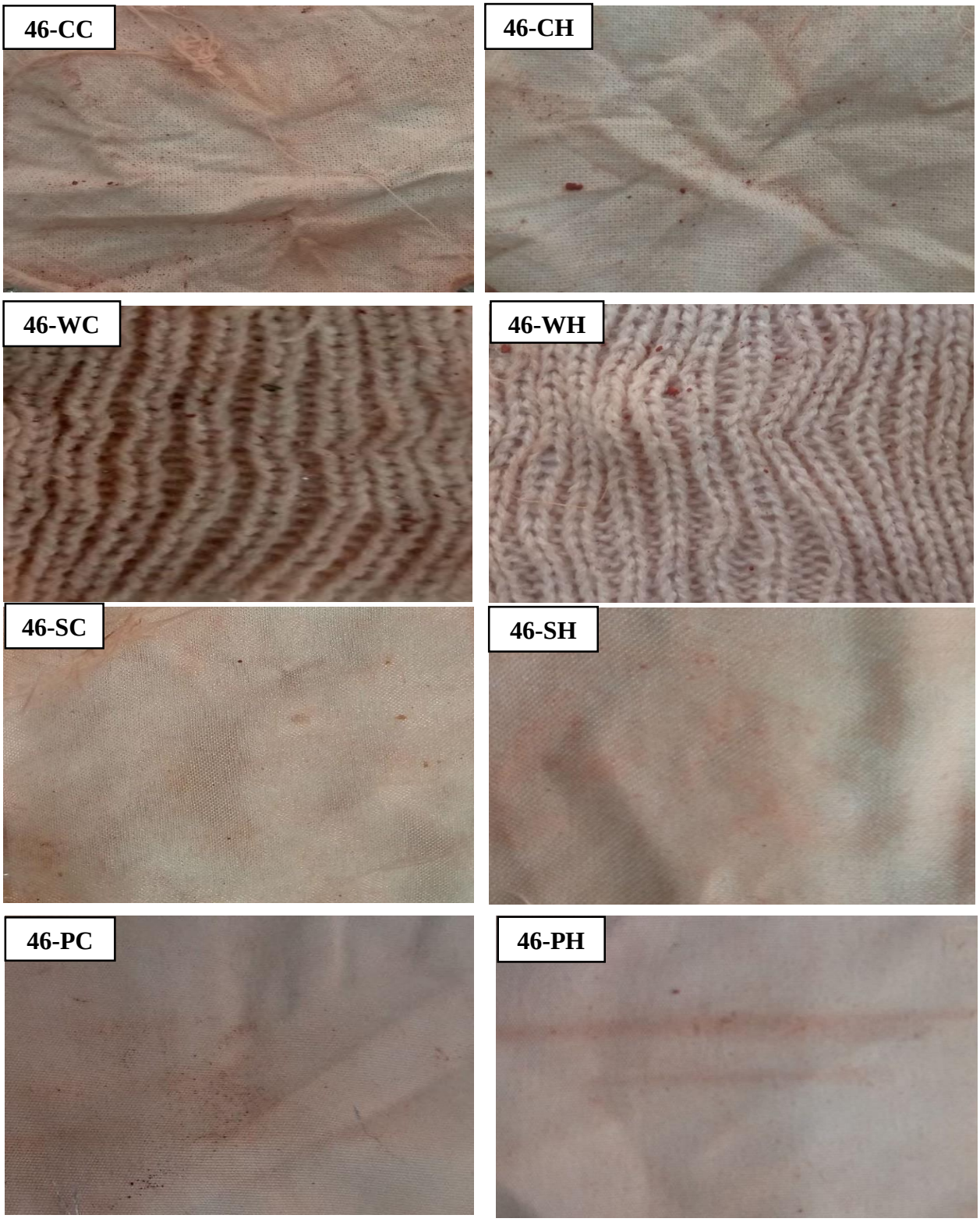

Figure 7: Fiber colors dyed with dye **46**

Figure 8: Fiber colors dyed with dye **47**

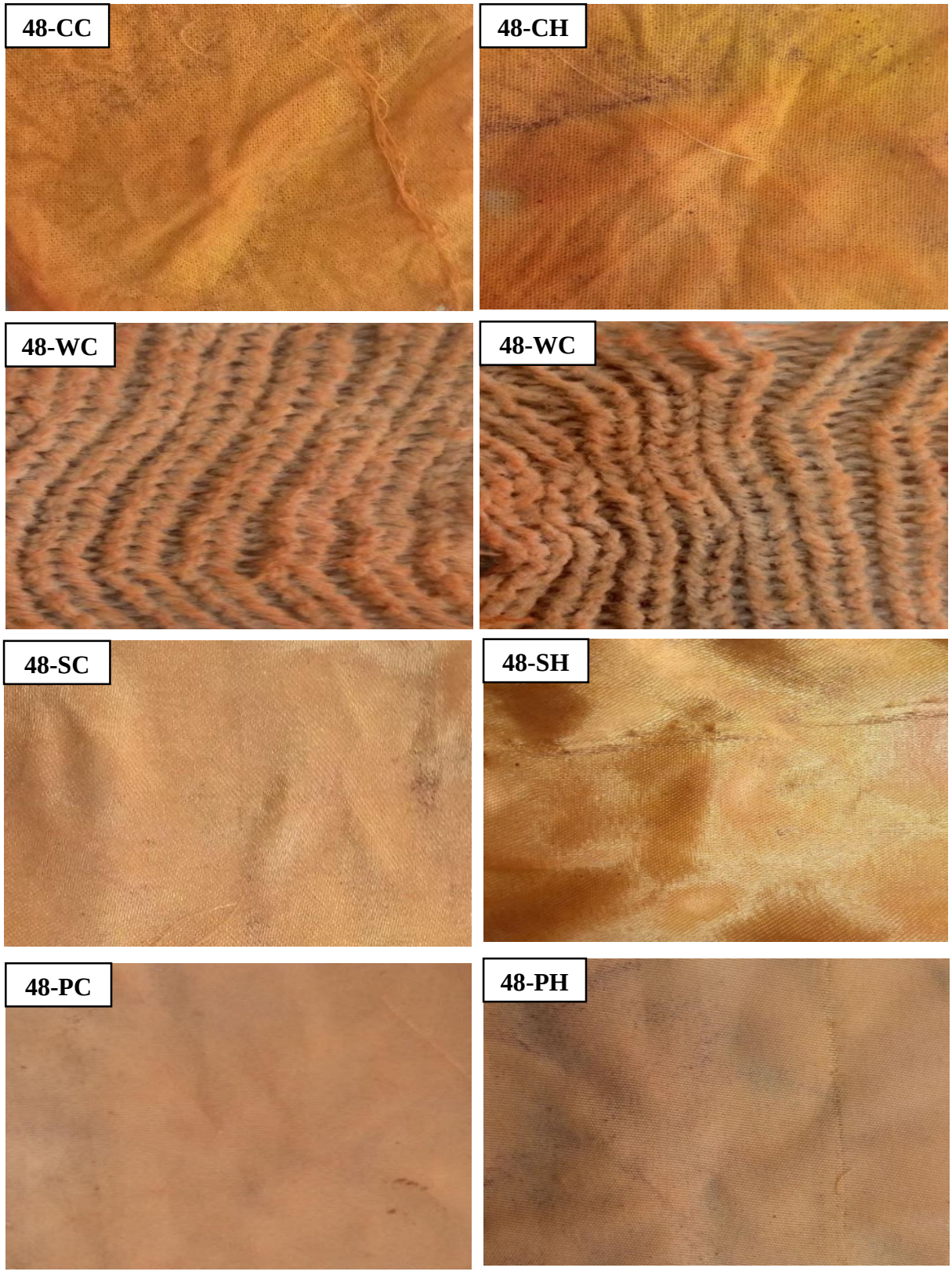

Figure 9: Fiber colors dyed with dye **48**

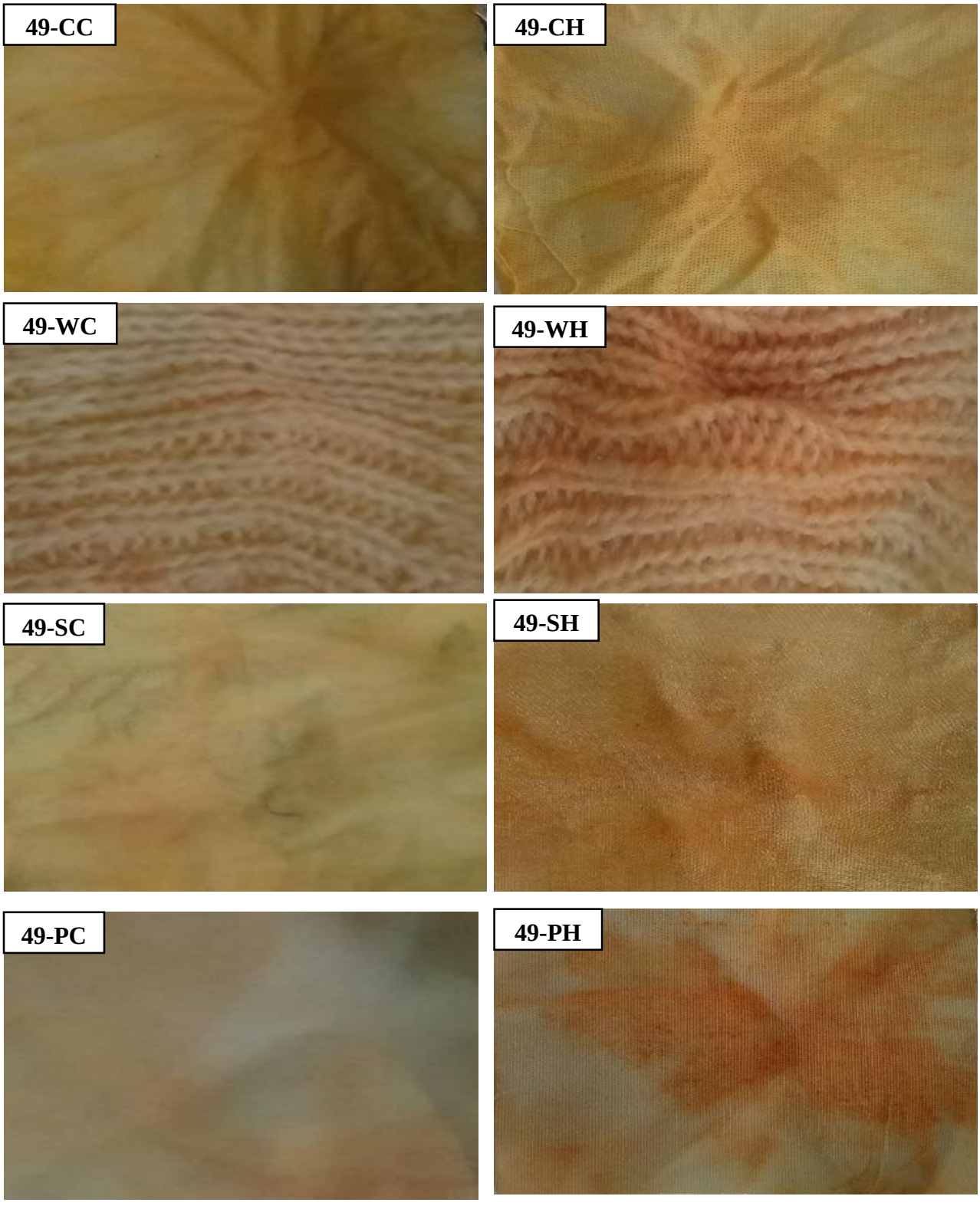

Figure 10: Fiber colors dyed with dye **49**

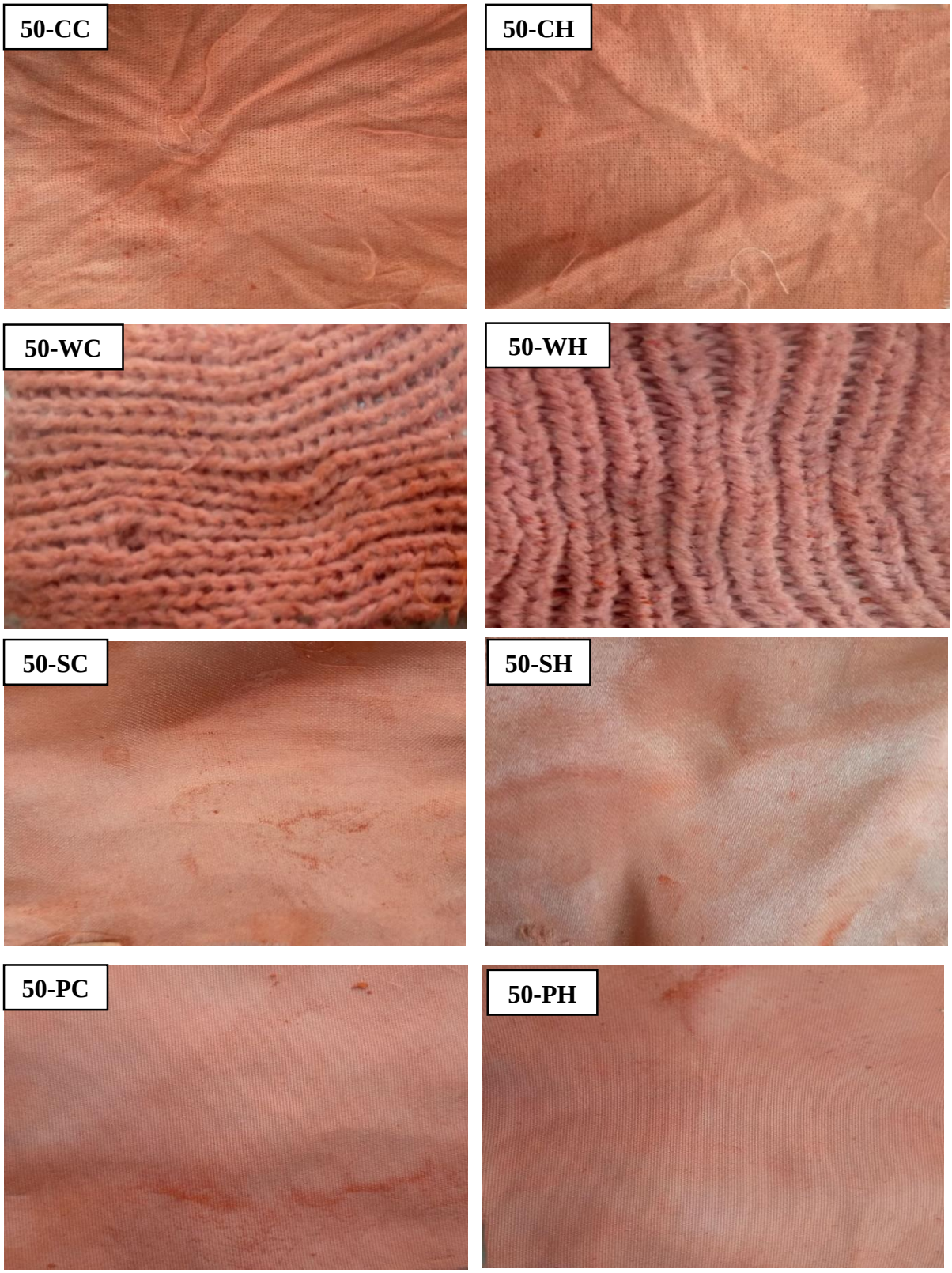

Figure 11: Fiber colors dyed with dye **50**

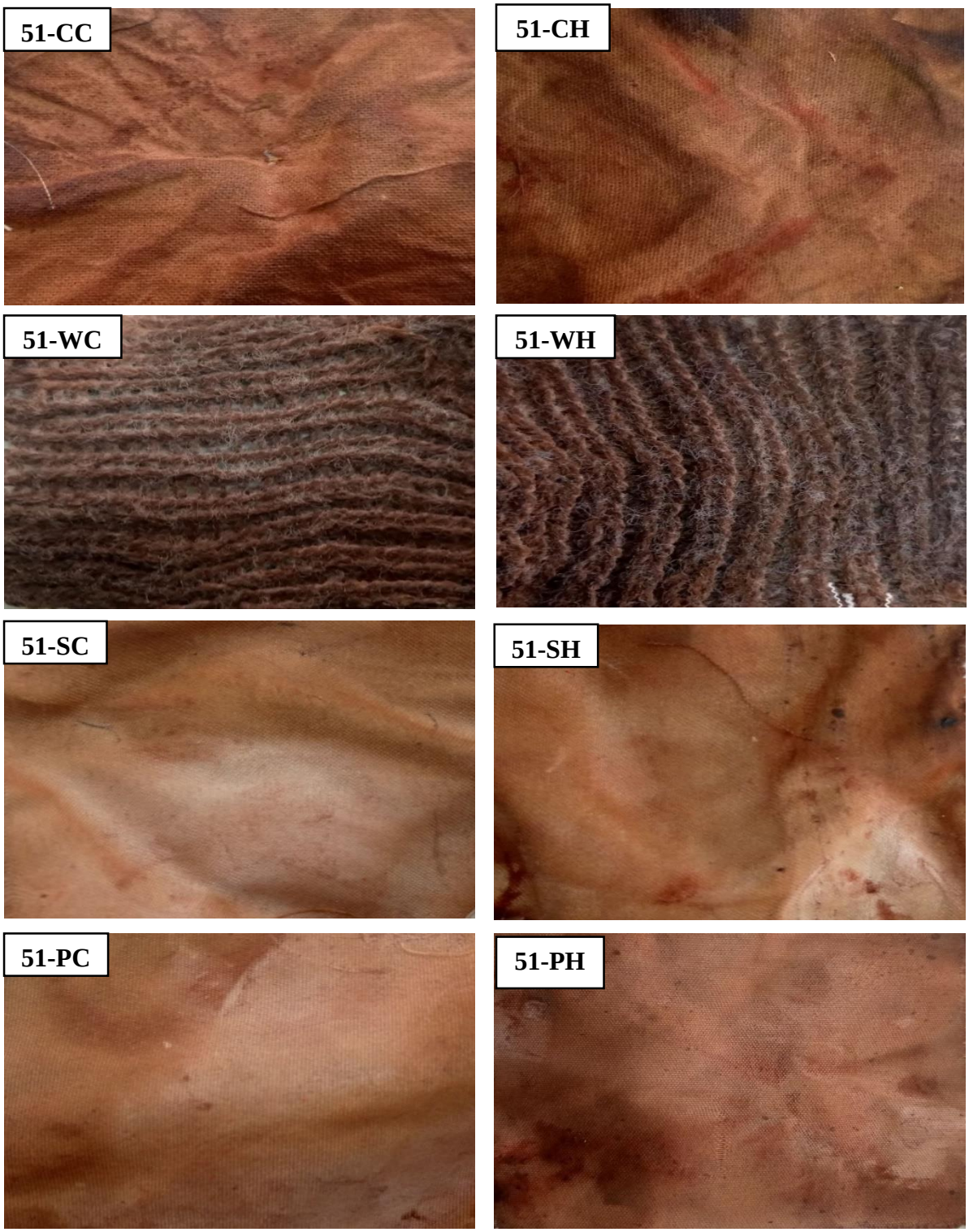

Figure 12: Fiber colors dyed with dye **51**

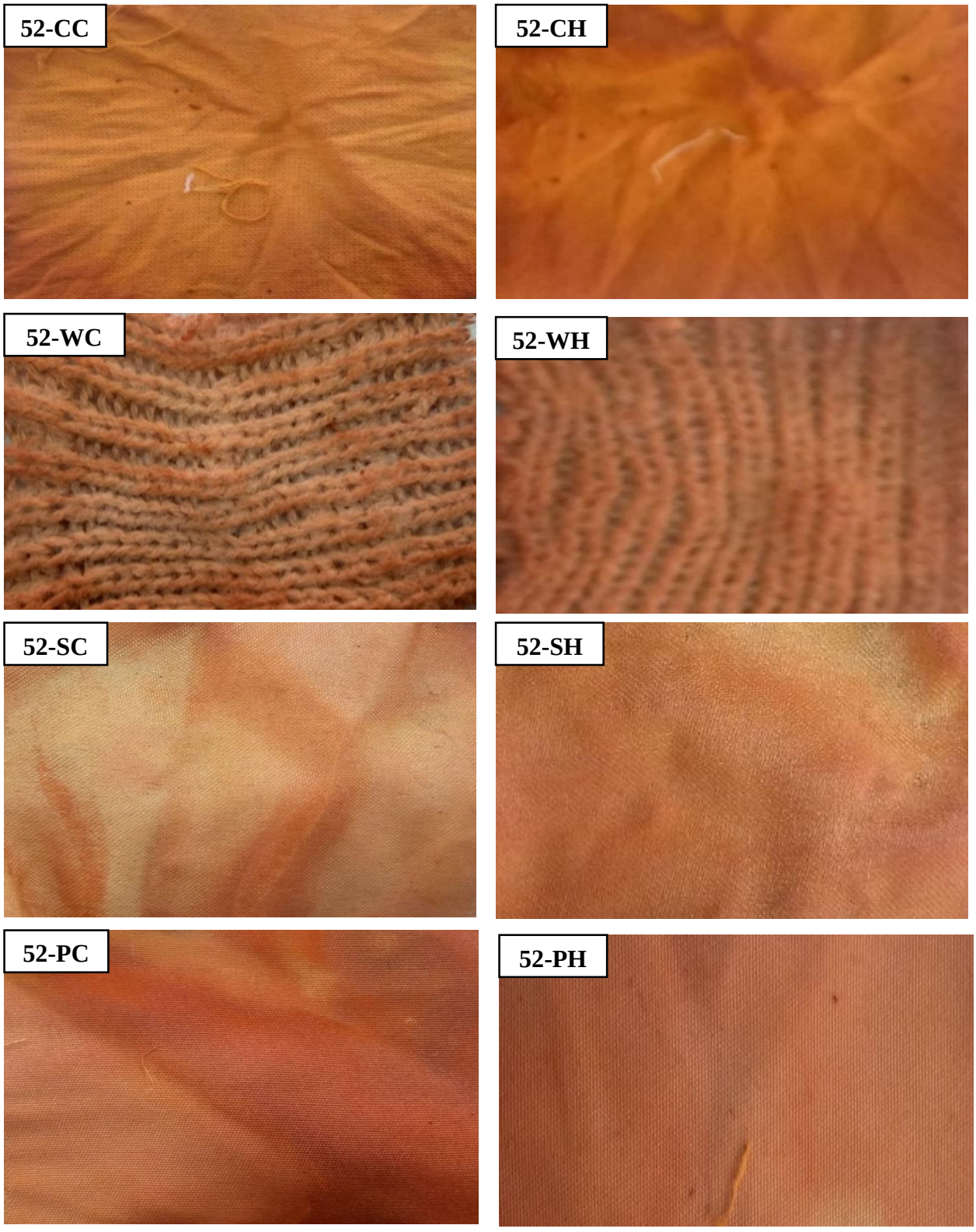

Figure 13: Fiber colors dyed with dye **52**

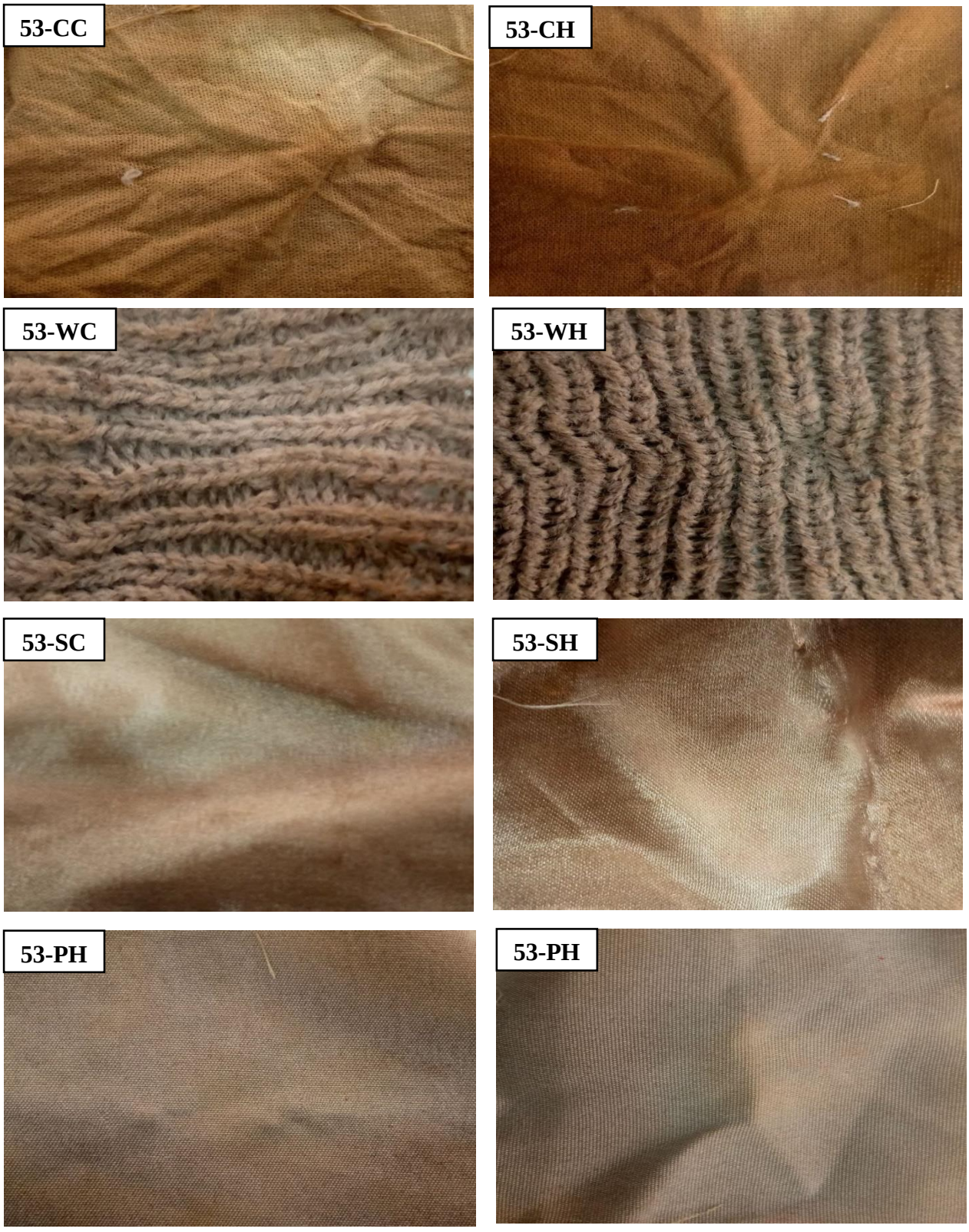

Figure 14: Fiber colors dyed with dye **53**

4.5. Antibacterial activity of synthesized compounds

The antibacterial activities of all synthesized compounds were evaluated *in vitro* following disk diffusion method against *S. aureus* and *E. coli* using Penicillin as a reference. The results revealed that all synthesized compounds exhibiting good to moderate activities. Among synthesized compounds, compound **48**, **50** and **53** showed potent inhibitory activity against Gram-positive, *S. aureus* with zone of inhibition of 14 ± 0.5, 11.5 ± 0.5, and 15 ± 0 mm compared to zone of inhibition of standard drug Penicillin (16 ± 0.5) at 100 mg/mL. The rest synthesized compounds **46**, **47**, **49**, **51** and **52** also showed good inhibitory activity against Gram- negative, *E.coli* with 13.1± 0.76, 12 ± 0, 14 ± 0.5, 12 ± 0.5 and 13 ± 0 mm zones of inhibition compared to standard drug Penicillin (19.8 ± 0.28) at 100 mg/mL. In contrast **52** and **53** were not active against *S.aureus* and *E.coli* respectively (**Table 18**).

Table 32: Zone of bacterial growth inhibition diameter (mm).

Samples	Concentrations in mg/Ml	Inhibition diameter (mm)	
		E.coli	*S.aureus*
46	50	10.1 ± 0.76	9.8 ± 0.28
	75	12.6 ± 0.57	12.1 ± 0.28
	100	13.1± 0.76	13 ± 0
47	50	9.5 ± 0.5	7 ± 1.1
	75	11.1 ± 0.28	7 ± 1.1
	100	12 ± 0	11.5 ± 0.5
48	50	10 ± 0.5	10.5 ± 0.5
	75	11 ± 0.5	12.6 ± 0.76
	100	12 ± 0	14 ± 0.5
49	50	12 ± 0	10 ± 1.1
	75	12.6 ± 0.5	10.6 ± 0.57
	100	14 ± 0.5	11.5 ± 0.5
50	50	8 ± 0	9.8 ± 0.76
	75	9.1± 0.2	10.5 ± 0.5
	100	10.3± 0.2	11.5 ± 0.5
51	50	8.8 ± 0.78	8.6 ± 0.76
	75	9.8 ± 0.78	9.6 ± 0.76
	100	12 ± 0.5	10.5 ± 0.5
52	50	8.5 ± 0.5	6 ± 0
	75	9.5 ± 0.5	6 ± 0
	100	13 ± 0	6 ± 0
53	50	6 ± 0	10.5 ± 0.5
	75	6 ± 0	13.1 ± 0.28
	100	6 ± 0	15 ± 0
Penicillin	100	19.8 ± 0.28	16 ± 0.5

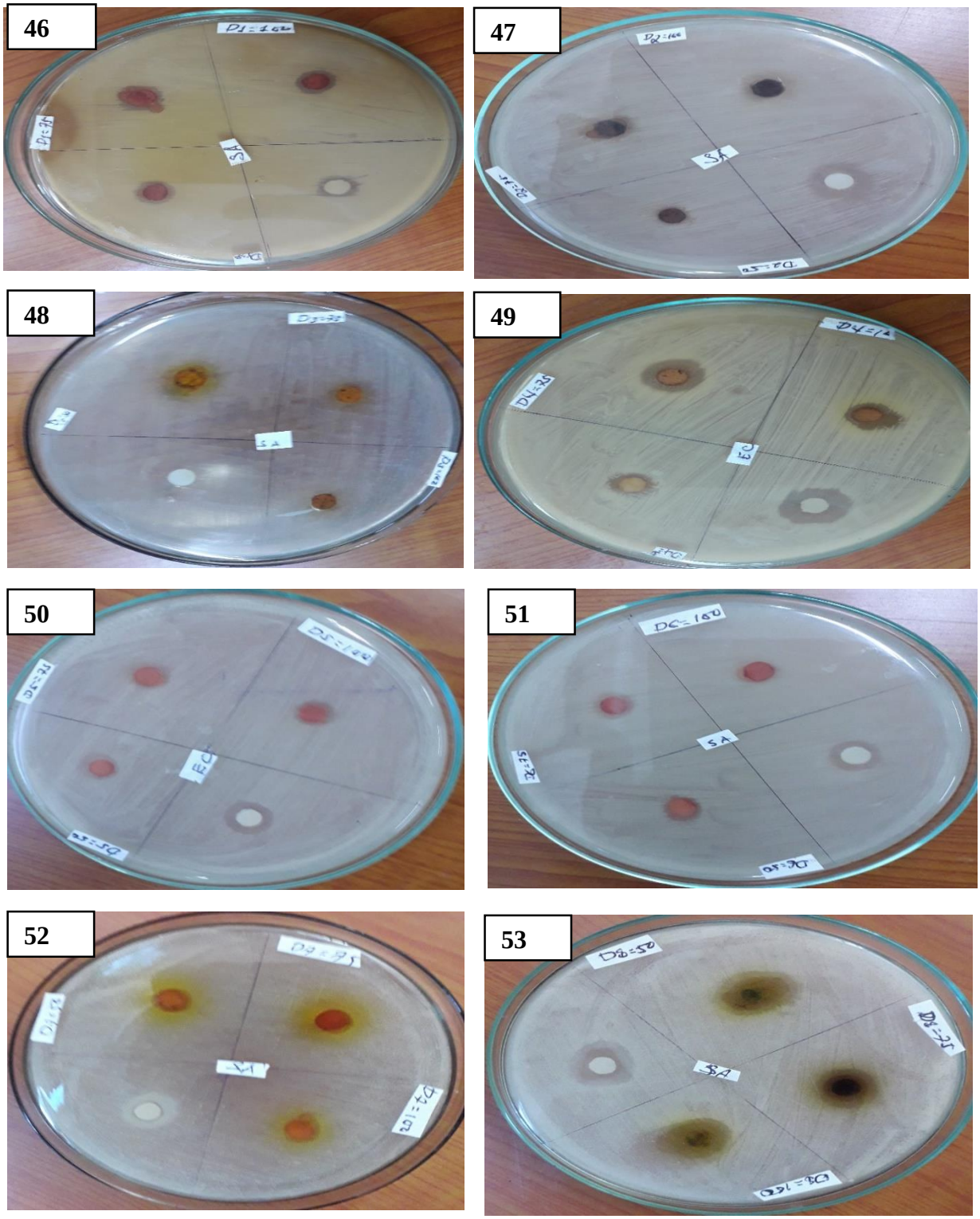

Figure 15: Bacterial growth inhibition of (**46- 47**).

4.5. Molecular docking study of synthesized compounds against DNA gyrase

In association with in vitro antimicrobial activity, it is useful to carry out *in silico* studies to predict the orientation and binding affinity at the active site of the receptor. The molecular docking of NMR identified ligand molecules **46- 53** with bacterial enzyme DNA gyrase is shown in **Figure 16**.

Among the investigated ligands, compound **46** and **47** exhibited better docking efficiency with DNA gyrase. **46** formed one hydrophobic interactions with amino acids Phe-160, hydrogen bond with Ser-62, Asn-308, Ser-306, Arg-171 and van-der wall interaction with Ser-420, Leu-359, Cys-159, Lys-65 in the active site of the target protein with the least binding affinity -7.2. **47** formed two hydrophobic interactions with amino acids Phe-160 and Cys-159, hydrogen bond with Ser-62, Ser-306, Asn-308, Arg-171 and van-der wall interaction with Ser-420, Leu-359 in the active site of the target protein with the least binding affinity -7.2. Hence two compounds were considered as the best dock conformation among the investigated ligands (**Table 19**). Compound **48** formed four hydrogen bonds with Ser-62, Asn-308, Ser-306 and Arg-171 amino acids, hydrophobic interaction with Phe-160 and Ser-420 and van-der wall interaction with Lys-65, Leu-421, Cys-159 and Leu-359 with least binding affinity -6.6. Both **49** and **50** formed hydrophobic interactions with Phe-160 and Lys-65, hydrogen bond with Ser-306, Ser-420, Lys-417 and Thr-418 and Ser-62, Ser-306, Asn-308 and Lys-305 respectively and van-der wall interaction with Ser-62, Leu-359, Leu-421, Arg-361, Gln-422 and Gly-419 and Ser-420 and Leu-359 of target protein with the least binding affinity of -6.1 and -6.4 respectively.

While **51** formed hydrophobic interaction with Phe-160, Lys-305 and Asn-308, hydrogen bond with Ser-62 and Ser-306 and van-der wall interaction with Ser-420, Leu-359, Lys-65, Arg-171 and Asp-307 with binding affinity of – 6.2. **52** formed hydrophobic interaction with Phe-160 and Lys-65, hydrogen bond with Ser-62, Ser-420 and Asn-308and van-der wall interaction with Ser-306, Leu-359 and Gly-419 with binding affinity of – 5.8. **53** formed hydrophobic interaction with Phe-160, Lys-305 and Asn-308, hydrogen bond with Ser-420 and Lys-65and van-der wall interaction with Ser-62, Leu-359, Ser-306, Asp-307 and Leu-421with binding affinity of – 6.3.

However, all these docked molecules exhibited more hydrophobic interaction than th standard drug Penicillin of binding affinity -6.9. The binding affinity, H-bond, hydrophobic interaction and van-der wall interaction of selected ligands were summarized in **Table 19**.

Table 33: Molecular docking results of isolated compounds against penicillin binding protein 4 (dacB) from *E. Coli*, complexed with penicillin-G (PDB ID 2EX8).

S. No.	Ligands	Affinity (kcal/ mol)	H-bond	Residual Hydrophobic/Pi-Cation/Pi-Anion/ Pi-Alkyl interactions	Van-der Walls interactions
1	**46**	– 7.4	Ser-62, Asn-308, Ser-306, Arg-171	Phe-160	Ser-420, Leu-359, Cys-159, Lys-65
2	**47**	– 7.4	Ser-62, Ser-306, Asn-308, Arg-171	Phe-160, Cys-159	Ser-420, Leu-359
3	**48**	– 6.6	Ser-62, Asn-308, Ser-306, Arg-171	Phe-160, Ser-420	Lys-65, Leu-421, Cys-159, Leu-359
4	**49**	– 6.1	Ser-306, Ser-420, Lys-417, Thr-418	Phe-160	Ser-62, Leu-359, Leu-421, Arg-361, Gln-422, Gly-419
5	**50**	– 6.4	Ser-62, Ser-306, Asn-308, Lys-305	Phe-160, Lys-65	Ser-420, Leu-359
6	**51**	– 6.2	Ser-62, Ser-306	Phe-160, Lys-305, Asn-308	Ser-420, Leu-359, Lys-65, Arg-171, Asp-307
7	**52**	– 5.8	Ser-62, Ser-420, Asn-308	Phe-160, Lys-65	Ser-306, Leu-359, Gly-419
8	**53**	– 6.3	Ser-420, Lys-65	Phe-160, Lys-305, Asn-308	Ser-62, Leu-359, Ser-306, Asp-307, Leu-421
	Penicilin-G	– 6.9	Ser-62, Ser-398, Lys-305, Thr-418	Phe-160	Ser-306, Asn-308, Leu-359, Leu-421

Crystal structure of penicillin binding protein 4 (dacB) from Escherichia coli, complexed with Penicillin-G.

P

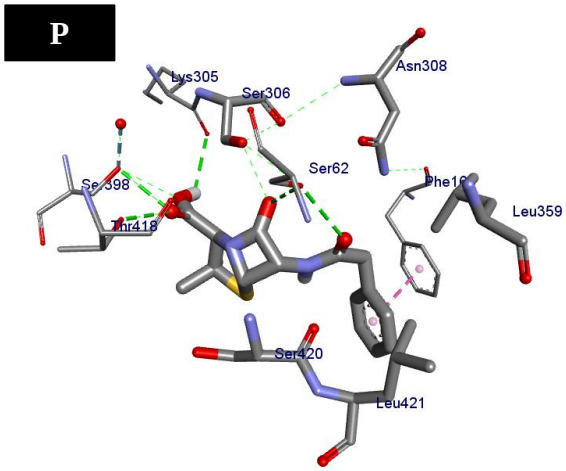
Lys305
Ser306
Asn308
Ser62
Ser398
Thr418
Leu359
Ser420
Leu421

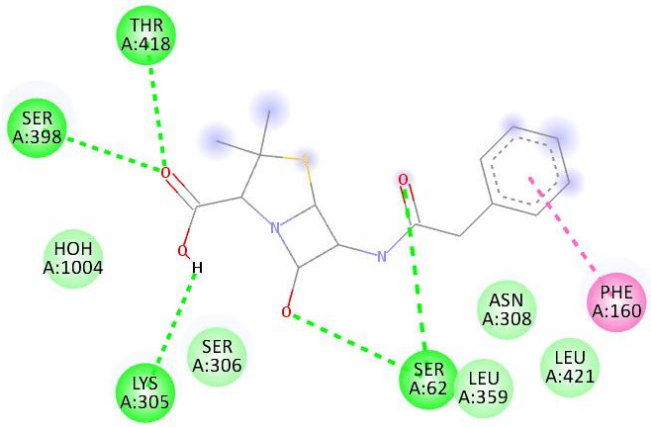
THR A:418
SER A:398
HOH A:1004
SER A:306
LYS A:305
SER A:62
LEU A:359
ASN A:308
PHE A:160
LEU A:421

46

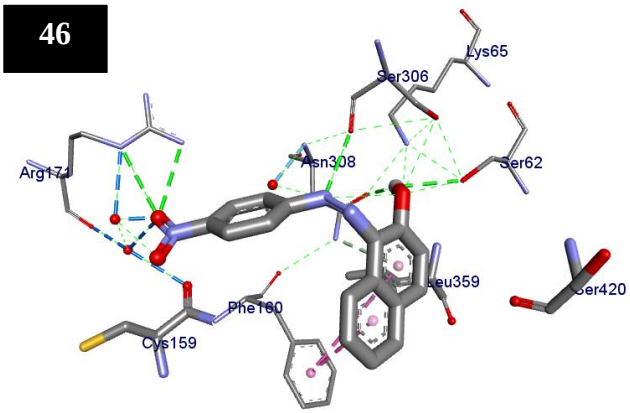
Lys65
Ser306
Asn308
Ser62
Arg171
Leu359
Ser420
Phe160
Cys159

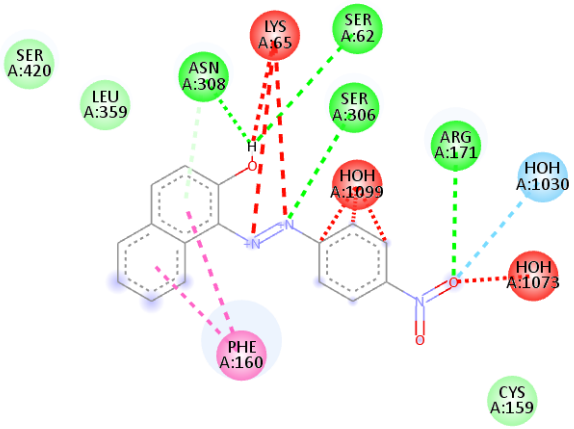
SER A:420
LYS A:65
SER A:62
ASN A:308
LEU A:359
SER A:306
ARG A:171
HOH A:1099
HOH A:1030
HOH A:1073
PHE A:160
CYS A:159

47

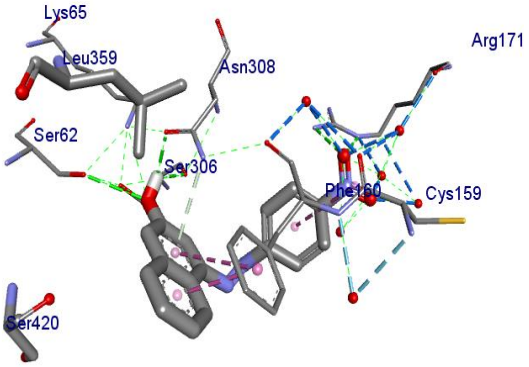
Lys65
Leu359
Asn308
Arg171
Ser62
Ser306
Phe160
Cys159
Ser420

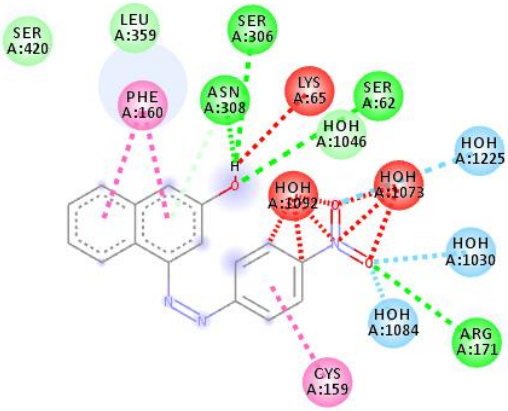
SER A:420
LEU A:359
SER A:306
PHE A:160
ASN A:308
LYS A:65
SER A:62
HOH A:1046
HOH A:1225
HOH A:1092
HOH A:1073
HOH A:1030
HOH A:1084
ARG A:171
CYS A:159

48

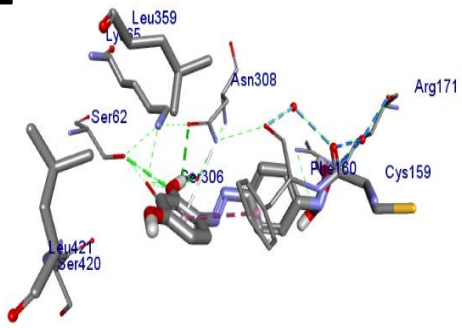
Leu359
Asn308
Arg171
Ser62
Ser306
Phe160
Cys159
Leu421
Ser420

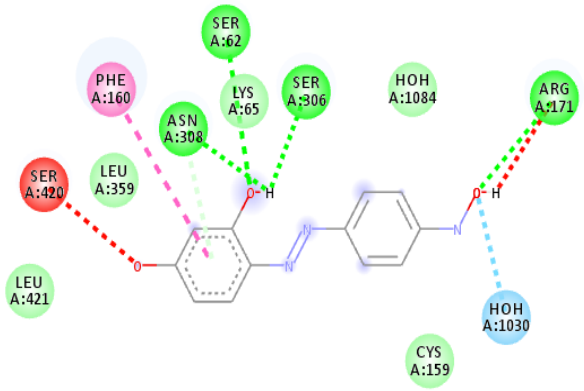
SER A:62
PHE A:160
LYS A:65
SER A:306
HOH A:1084
ARG A:171
ASN A:308
SER A:420
LEU A:359
LEU A:421
HOH A:1030
CYS A:159

49

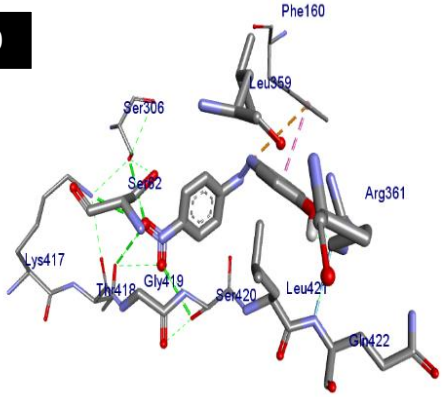
Phe160
Leu359
Ser306
Ser62
Arg361
Lys417
Thr418
Gly419
Ser420
Leu421
Gln422

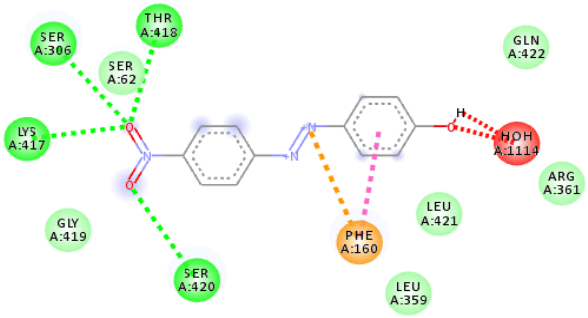
SER A:306
THR A:418
SER A:62
GLN A:422
LYS A:417
HOH A:1114
ARG A:361
LEU A:421
GLY A:419
PHE A:160
SER A:420
LEU A:359

50

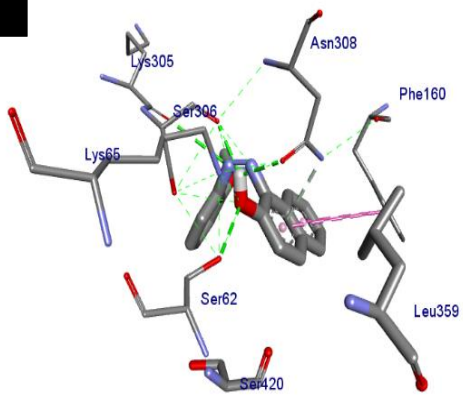
Asn308
Lys305
Phe160
Ser306
Lys65
Ser62
Leu359
Ser420

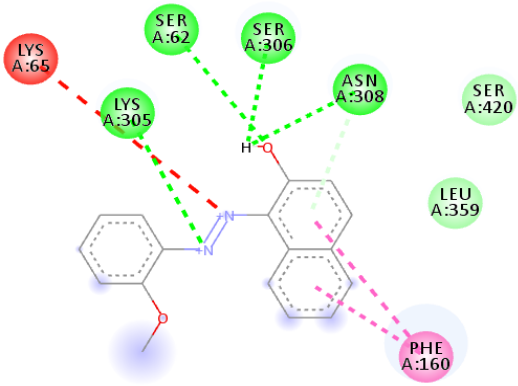
SER A:62
SER A:306
LYS A:65
ASN A:308
SER A:420
LYS A:305
LEU A:359
PHE A:160

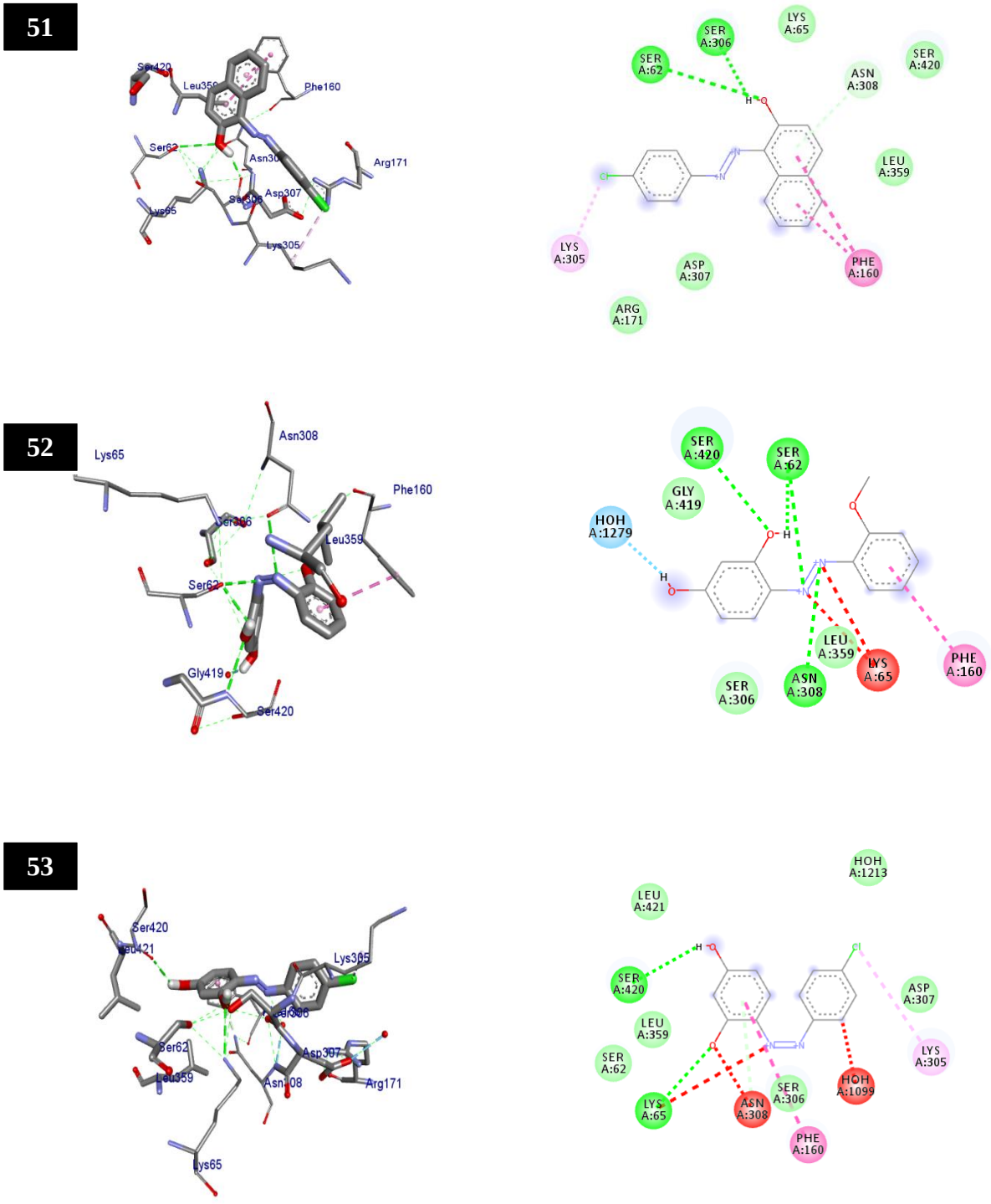

Figure 16: 2D and 3D protein ligand interaction of DNA gyrase with selected ligand figures on left are 3D and right are 2D.

5. CONCLUSION AND RECOMMENDATION

5.1. Conclusion

Azo dye compounds were successfully synthesized and their *in vitro* antibacterial activity evaluated. Diazotization of aniline and azo dye coupling undergoes smoothly to produce azo dye derivatives with good to excellent yield (68.3-97.7%). Purity of the synthesized products was tested using thin-layer chromatography. Their structural elucidation of the synthesized compounds was undergo using UV, ^{1}H, ^{13}C and Dept-135 NMR spectra.

Dyeing abilities of eight azo dyes were investigated in terms of their exhaustion and fixation on cotton, polyester, silk and wool fibers in cold and hot conditions. Results showed that all the eight dyes are better exhausted and fixed on the all types of fibers in cold dyeing condition than hot condition. Higher value of dyes fixation on cotton and polyester, cellulose fibers, than silk and wool, protein fibers on the basis of availability of reactive groups of dyes with the fiber substrate. Azo dyes are reactive dyes in which the compounds and the substrates of fibers react to form covalent bonds, therefore such dyes are more advantageous than other types of dyes in color fastness, variety of hue, high applicability, duration etc.

Azo dye compounds were evaluated in vitro for antimicrobial activities S. *aurous* and *E.coil* bacteria by using the paper disc diffusion method. Azo dyes have shown better antibacterial activities. Among synthesized compounds, compound **48**, **50** and **53** showed potent inhibitory activity against Gram-positive, *S. aureus* and **46**, **47**, **49**, **51** and **52** also showed potent inhibitory activity against Gram- negative, *E.coli*. All synthesized azo dyes exhibited promising docking efficiency with DNA gyrase and **46** and **47** are best among them.

5.2. Recommendations

Based on the present study the following recommendations were forwarded:

- ✓ In synthetic organic chemistry these compounds may be used as starting materials for further synthesis of other important heterocyclic compounds by their derivatives.
- ✓ Synthesis of more azo dye derivatives should be carried out.
- ✓ Some of the tested compounds displayed potent antibacterial activity; therefore, the mechanism of action should be studied.
- ✓ The antibacterial activity was carried out on two strain (*S. aureus* and *E. coli*), therefore the synthesized compounds should be investigated on other strain.
- ✓ Further biological activities such as antiviral, anticancer and anti-inflammatory should be studied.
- ✓ All synthesized dyes have good dyeing potential on fibers; therefore, the mechanism of action should be studied.

Research Fund Acknowledgment

This research project is funded by Adama Science and Technology University under the grant number ASTU/SM-R/013/19, Adama, Ethiopia.

6. REFERENCES

Ajani, O. O., Akinremi, O. E., Ajani, A. O., Edobor-Osoh, A., & Anake, W. U. (2013). Synthesis and spectroscopic study of naphtholic and phenolic azo dyes. *Physical Review and Research International*, ***3***(1), 24-41.

Al-Rubaie, L. A. A. R., & Mhessn, R. J. (2012). Synthesis and characterization of azo dye para red and new derivatives. *E-Journal of Chemistry*, ***9***(1), 465-470.

Aziz, M. S., & El-Mallah, H. M. (2009). Electrical and optical properties of azo dye. *Indian Journal of Pure & Applied Physics*, ***47****(7),* 530-534

Bamoniri, A., Mirjalili, B. B. F., & Moshtael-Arani, N. (2014). Environmentally green approach to synthesize azo dyes based on 1-naphthol using nano $BF_3 \cdot SiO_2$ under solvent-free conditions. *Green Chemistry Letters and Reviews*, ***7***(4), 393-403.

Bamoniri, A., Mirjalili, B. B. F., & Moshtael-Arani, N. (2014). Nano $BF_3 \cdot SiO_2$: A green heterogeneous solid acid for synthesis of formazan dyes under solvent-free condition. *Journal of Molecular Catalysis A: Chemical*, ***393***, 272-278.

Beale, J. M., Block, J. H., & Hill, R. A. (2011). *Organic medicinal and pharmaceutical chemistry*, 501.

Bradshaw, T. D., Stevens, M. F. G., & Westwell, A. D. (2001). The discovery of the potent and selective antitumour agent 2-(4-amino-3-methylphenyl) benzothiazole (DF 203) and related compounds. *Current medicinal chemistry*, ***8***(2), 203-210.

Caldarelli, M., Baxendale, I. R., & Ley, S. V. (2000). Clean and efficient synthesis of azo dyes using polymer-supported reagents. *Green Chemistry*, ***2***(2), 43-46.

Chopde, H. N., Meshram, J. S., Pagadala, R., & Mungole, A. J. (2010). Synthesis, characterization and antibacterial activity of some novel azo-azoimine dyes of 6-bromo-2-naphthol. *International Journal of ChemTech Research*, ***2***(3), 1823-830.

Christoforou, I. C., & Koutentis, P. A. (2006). New regiospecific isothiazole C–C coupling chemistry. *Organic & biomolecular chemistry*, ***4***(19), 3681-3693.

Dabbagh, H. A., Teimouri, A., & Chermahini, A. N. (2007). Green and efficient diazotization and diazo coupling reactions on clays. *Dyes and pigments*, ***73***(2), 239-244.

Eissa, F., & Mohamed, N. (2018). Azo Dyes: Preparation Via Environmentally Benign Way. *Journal of Chemical Engineering & Process Technology*, ***9*** *(4),* 2157-7048.

El Harfi, S., & El Harfi, A. (2017). Classifications, properties and applications of textile dyes: A review. *Applied Journal of Environmental Engineering Science*, ***3***(3), 0-3.

Fernández, C., Larrechi, M. S., & Callao, M. P. (2010). An analytical overview of processes for removing organic dyes from wastewater effluents. *TrAC Trends in Analytical Chemistry*, ***29***(10), 1202-1211.

Garel, L., & Saint-Jalmes, L. (2006). One-pot fluoro-de-diazoniation of anilines in organic medium. *Tetrahedron letters*, ***47***(32), 5705-5708.

Geng, J., Dai, Y., Qian, H. F., Wang, N., & Huang, W. (2015). 2-Amino-4-chloro-5 formylthiophene-3-carbonitrile derived azo dyes. *Dyes and Pigments*, ***117***, 133-140.

Habermann, J., Ley, S. V., & Smits, R. (1999). Three-step synthesis of an array of substituted Benzofurans using polymer-supported reagents. *Journal of the Chemical Society, Perkin Transactions* ***1***, (17), 2421-2423.

Hooker, J., Hinks, D., Montero, G., & Conlee, C. (2002). Synthesis of N, N-diethyl-N-{4-[(E)-(4-nitrophenyl) diazenyl] phenyl} amine via in situ diazotisation and coupling in supercritical carbon dioxide. *Coloration technology*, ***118***(6), 273-276.

Hutchinson, I., Chua, M. S., Browne, H. L., Trapani, V., Bradshaw, T. D., Westwell, A. D., & Stevens, M. F. (2001). Antitumor benzothiazoles. 14. Synthesis and in vitro biological properties of fluorinated 2-(4-aminophenyl) benzothiazoles. *Journal of medicinal chemistry*, ***44***(9), 1446-1455.

Iftikhar, M., Jamil, N. A., & Shahbaz, B. (2001). Rubbing, Ironing and Dry Cleaning Fastness of Reactive Dyed Cotton Knitted Fabric as Influenced by Salt, Alkali and Dye. *International Journal of Agriculture & Biology*, ***3***(1), 109-12.

Jortner, J., & Rao, C. N. R. (2002). Nanostructured advanced materials. Perspectives and directions. *Pure and applied chemistry*, ***74***(9), 1491-1506.

Kiran, V. M., & Mehta, M. (2012). Studies on some isoxazoline-azo compounds and their colourant performance and fastness evaluation on synthetic fabric. *International Journal of Chem Tech Research*, ***4***(1), 409-414.

Kucharski, S., Janik, R., Motschmann, H., & Radüge, C. (1999). Trans-cis isomerisation of azobenzene amphiphiles containing a sulfonyl group. *New Journal of Chemistry*, ***23***(7), 765-771.

Li, M., Zhang, K., & Hou, A. (2015). Crystallographic study of two monoazo disperse dyes with a D–π–A system. *Coloration Technology*, ***131***(1), 38-42.

Mahran, M. A., William, S., Ramzy, F., & Sembel, A. M. (2007). Synthesis and in vitro evaluation of new benzothiazole derivatives as schistosomicidal agents. *Molecules*, ***12***(3), 622-633.

Mamhidir, A. G., Karlsson, I., Norberg, A., & Mona, K. (2007). Weight increase in patients with dementia, and alteration in meal routines and meal environment after integrity promoting care. *Journal of clinical nursing*, ***16***(5), 987-996.

Maradiya, H. R. (2012). Disperse dyes based on 2-aminothiazole derivatives for cellulose triacetate fabric. *Journal of Saudi Chemical Society*, ***16***(1), 69-74.

Matyjas, E., & Rybicki, E. (2003). Novel reactive red dyes. *Autex Res. J*, ***3***(9095), 21- 27.

Merrington, J., James, M., & Bradley, M. (2002). Supported diazonium salts—convenient reagents for the combinatorial synthesis of azo dye. *Chemical communications*, (2), 140-141.

Mirjalili, B. B. F., Bamoniri, A., and Akbari, A. (2008). $BF_3 \cdot SiO_2$: an efficient alternative for the synthesis of 14-aryl or alkyl-14H-dibenzo [a, j] xanthenes. *Tetrahedron Letters*, ***49***(45), 6454-6456.

Mobaraki, A., Movassagh, B., & Karimi, B. (2014). Hydrophobicity-enhanced magnetic solid sulfonic acid: a simple approach to improve the mass transfer of reaction partners on the surface of the heterogeneous catalyst in water-generating reactions. *Applied Catalysis A: General*, ***472***, 123-133.

Morgan, K. J. (1961). 409. Infrared spectra and structure of arylazonaphthols. *Journal of the Chemical Society (Resumed)*, 2151-2159.

Mustafa, A., & Turner, C. (2011). Pressurized liquid extraction as a green approach in food and herbal plants extraction: A review. *Analytica chimica acta*, ***703***(1), 8-18.

Ogoleva, L.N.; Stepanov, B.I. (1965). The Isomer Ratio in Azo Coupling.ž. *Organic Chemistry*. **1**, 2083–2086.

Okuhara, T. (2002). Water-tolerant solid acid catalysts. *Chemical reviews*, ***102***(10), 3641-3666.

Padmavathi, D. G., & Shanmugapriya, M. (2009). A survey of attacks, security mechanisms and challenges in wireless sensor networks. *International Journal of Computer Science and Information Security*, ***4***, 1-2.

Padmavathi, V., Reddy, G. S., Padmaja, A., & Kondaiah, P. (2009). Synthesis, antimicrobial and cytotoxic activities of 1, 3, 4-oxadiazoles, 1, 3, 4-thiadiazoles and 1, 2, 4-triazoles. *European journal of medicinal chemistry*, ***44***(5), 2106-2112.

Parimi, U., & Kolli, D. (2012). Antibacterial and free radical scavenging activity of Michelia champaca Linn. flower extracts. *Free Radicals and Antioxidants*, ***2(***2), 58-61.

Qiu, J., Tang, B., Ju, B., Xu, Y., & Zhang, S. (2017). Stable diazonium salts of weakly basic amines—convenient reagents for synthesis of disperse azo dyes. *Dyes and Pigments*, ***136***, 63-69.

Raghavendra, K. Ajay Kumar. (2013). Synthesis of Some Novel Azo Dyes And Their Dyeing, RedoxSynthesis Of Some Novel Azo Dyes And Their Dyeing, Redox. *International Journal of ChemTech Research, **5**(4),* 1756-1760.

Rahimizadeh, M., Eshghi, H., Shiri, A., Ghadamyari, Z., Matin, M. M., Oroojalian, F., & Pordeli, P. (2012). Fe $(HSO_4)_3$ as an Efficient Catalyst for Diazotization and Diazo Coupling Reactions. *Journal of the Korean Chemical Society*, ***56***(6), 716-719.

Raposo, M. M. M., Fonseca, A. M. C., Castro, M. C. R., Belsley, M., Cardoso, M. F. S., Carvalho, L. M., & Coelho, P. J. (2011). Synthesis and characterization of novel diazenes bearing pyrrole, thiophene and thiazole heterocycles as efficient photochromic and nonlinear optical (NLO) materials. *Dyes and Pigments*, ***91***(1), 62-73.

Rizk, H. F., S. A. Ibrahim, and M. A. El-Borai (2015). Synthesis, fastness properties, color assessment and antimicrobial activity of some azo reactive dyes having pyrazole moiety. *Dyes and Pigments* **112**, 86-92.

Safari, J., & Zarnegar, Z. (2015). An environmentally friendly approach to the green synthesis of azo dyes in the presence of magnetic solid acid catalysts. *RSC advances*, ***5***(23), 17738-17745.

Shridhar, A. H., Keshavayya, J., Peethambar, S. K., & Hoskeri, H. J. (2016). Synthesis and biological activities of Bis alkyl 1, 3, 4-oxadiazole incorporated azo dye derivatives. *Arabian Journal of Chemistry*, ***9***, 1643-1648.

Shridhar, B. S. (2012). Nitrogen fixing microorganisms. *International journal of microbial research* , ***3***(1), 46-52.

Sousa, M. M., Miguel, C., Rodrigues, I., Parola, A. J., Pina, F., de Melo, J. S. S., & Melo, M. J. (2008). A photochemical study on the blue dye indigo: from solution to ancient Andean textiles. *Photochemical & Photobiological Sciences*, ***7***(11), 1353-1359.

Stanková, M., & Lebl, M. (1996). Library generation through successive substitution of trichlorotriazine. *Molecular diversity*, ***2***(1), 75-80.

Stolz, A. (2001). Basic and applied aspects in the microbial degradation of azo dyes. *Applied microbiology and biotechnology*, ***56***(1), 69-80.

Tacic, A., Nikolic, V., Nikolic, L., & Savic, I. (2017). Antimicrobial sulfonamide drugs. *Advanced technologies*, ***6***(1), 58-71.

Tskhovrebov, A. G., Naested, L. C., Solari, E., Scopelliti, R., & Severin, K. (2015). Synthesis of azoimidazolium dyes with nitrous oxide. *Angewandte Chemie*, ***127***(4), 1305-1308.

Upadhyay, R. K., Seema, A., Sanidhya, U., & Tiwari, H. K. (2011). Synthesis and dyeing action of novel thioindigoid reactive dyes. *Asian Journal of Chemistry*, ***23***(7), 3127-3220.

Valizadeh, H., & Shomali, A. (2012). A new nitrite ionic liquid (IL-ONO) as a nitrosonium source for the efficient diazotization of aniline derivatives and in-situ synthesis of azo dyes. *Dyes and Pigments*, ***92***(3), 1138-1143.

Valizadeh, H., Amiri, M., & Hosseinzadeh, F. (2012). Nanoparticles of organosilane-based nitrite ionic liquid immobilized on silica for the diazotization of aniline derivatives and subsequent synthesis of azo dyes. *Dyes and pigments*, ***92***(3), 1308-1313.

Valizadeh, H., Shomali, A., Nourshargh, S., & Mohammad-Rezaei, R. (2015). Carboxyl and nitrite functionalized graphene quantum dots as a highly active reagent and catalyst for rapid diazotization reaction and synthesis of azo-dyes under solvent-free conditions. *Dyes and Pigments*, ***113***, 522-528.

Vina, A. (2010). Improving the speed and accuracy of docking with a new scoring function, efficient optimization, and multithreading Trott, Oleg; Olson, Arthur J. *Journal of Computational Chemistry*, ***31***(2), 455-461.

Wadia, D. N., & Patel, P. M. Synthesis and Application of Monofunctional Reactive Dyes Based on 3-(4-amino phenyl)-5-Benzylidene-2-Substituted Phenyl-3, 5-Dihydro-Imidazol-4-One. *Arabian journal of chemistry*, **4**, 279-185.

Yadav, S. S., Redden, R. J., Hatfield, J. L., Lotze-Campen, H., & Hall, A. J. (2011). *Crop adaptation to climate change* ,507-521.

Yasuda, K., & Ley, S. V. (2002). The simultaneous use of immobilised reagents for the one-pot conversion of alcohols to carboxylic acids. *Journal of the Chemical Society, Perkin Transactions **1*** (8), 1024-1025.

Yazdanbakhsh, M. R., & Moradi-e-Rufchahi, E. (2009). Synthesis, characterization and spectroscopic properties of some new azo dyes derived from 6-aminopyrimidine-2, 4 (1H, 3H) Dione. *Oriental Journal of Chemistry*, ***25***(1), 41-45.

Yazdanbakhsh, M. R., Abbasnia, M., Sheykhan, M., & Ma'mani, L. (2010). Synthesis, characterization and application of new azo dyes derived from uracil for polyester fibre dyeing. *Journal of Molecular Structure*, ***977***(1-3), 266-273.

Yazdanbakhsh, M. R., Yousefi, H., Mamaghani, M., Moradi, E. O., Rassa, M., Pouramir, H., & Bagheri, M. (2012). Synthesis, spectral characterization and antimicrobial activity of some new azo dyes derived from 4, 6-dihydroxypyrimidine. *Journal of Molecular Liquids*, ***169***, 21-26.

Appendix 1: UV-Vis (200-600 nm, MeOH: H_2O) spectrum of compound **46**.

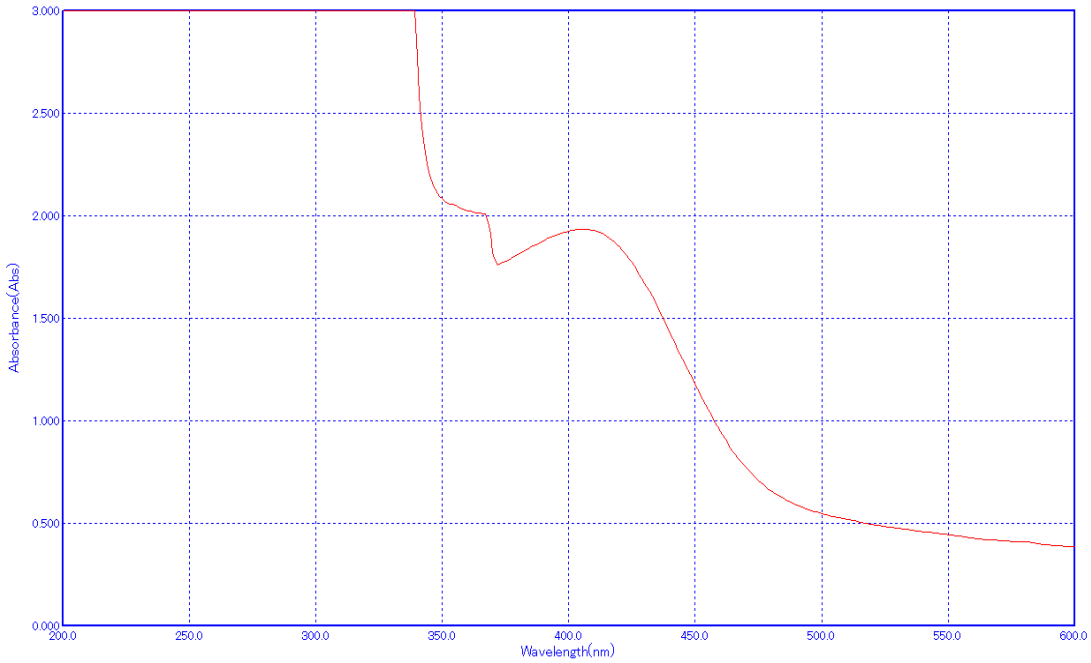

Appendix 2: ^1H NMR (400 MHz, $CDCl_3$) spectrum of compound **46**.

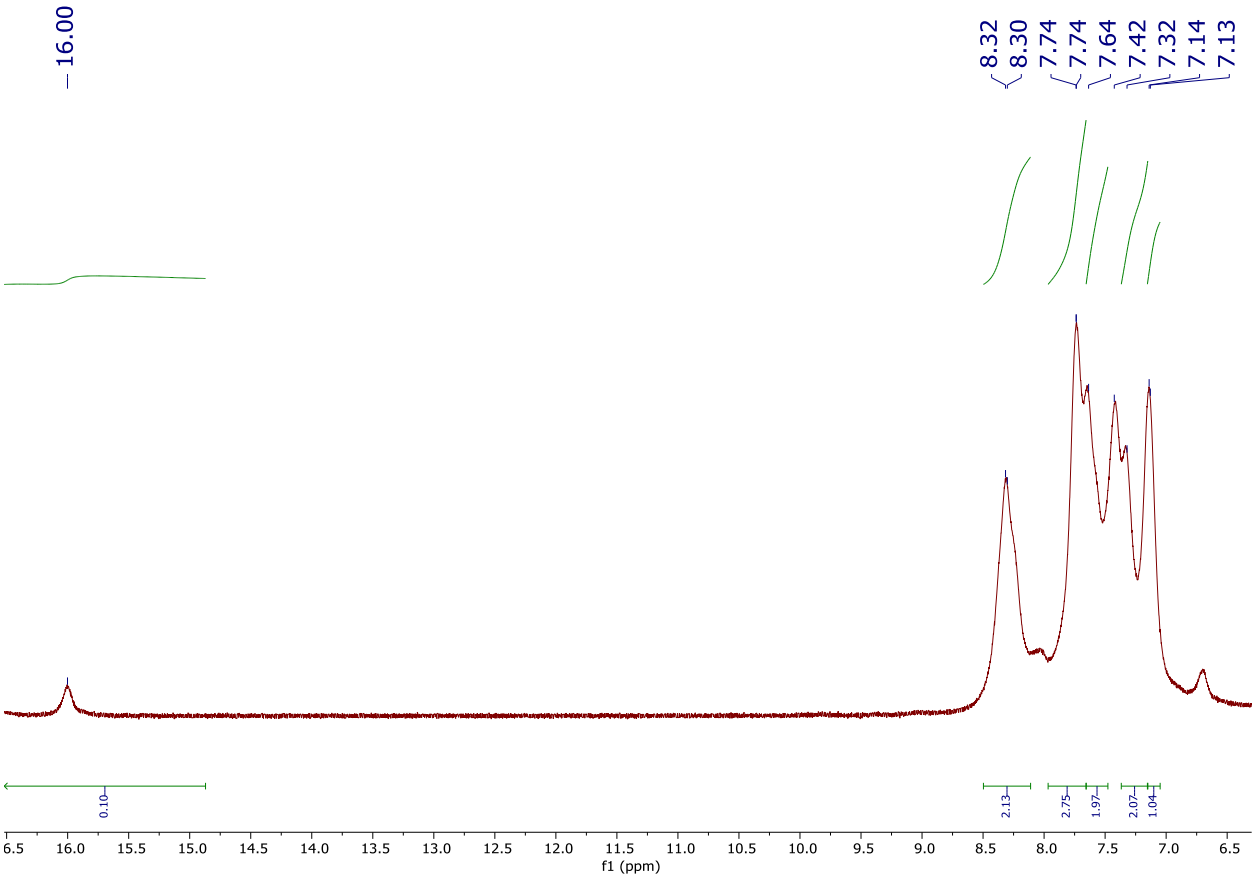

Appendix 3: ^{13}C NMR (100 MHz, $CDCl_3$) spectrum of compound **46**.

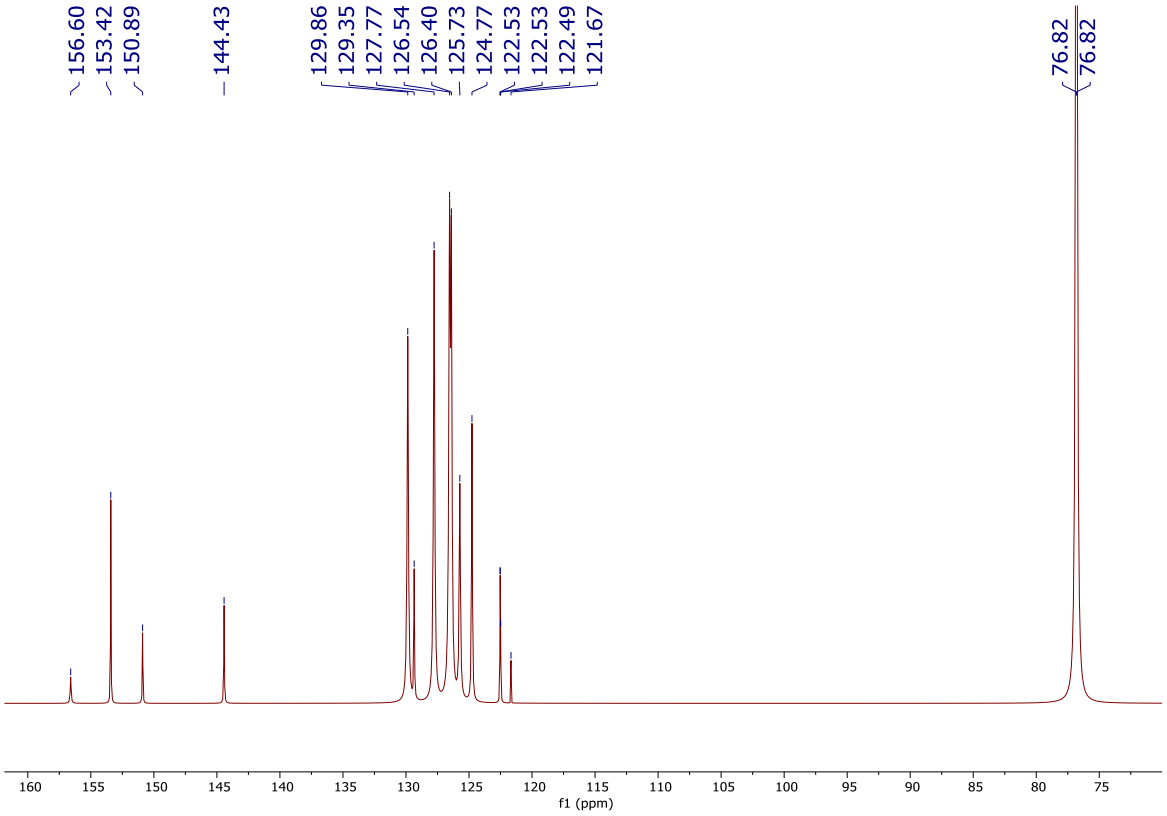

Appendix 4: DEPT-135 NMR (100 MHz, $CDCl_3$) spectrum of compound **46.**

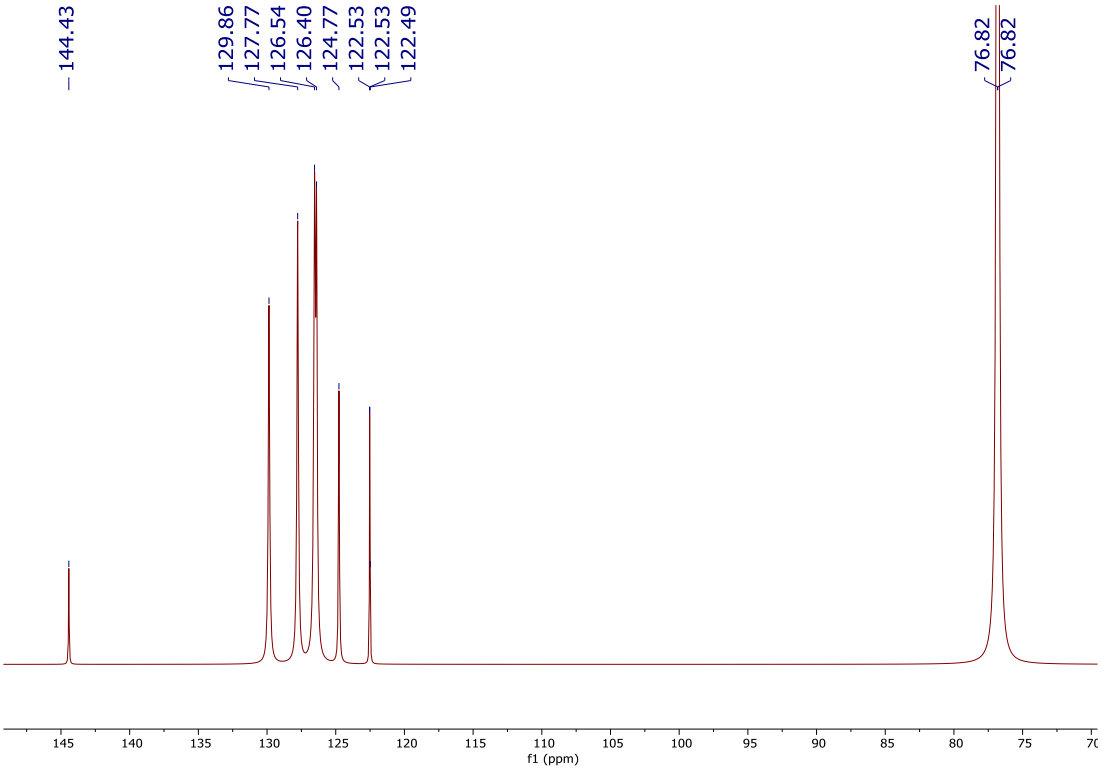

Appendix 5: UV-Vis (200-600 nm, MeOH: H_2O) spectrum of compound **47**.

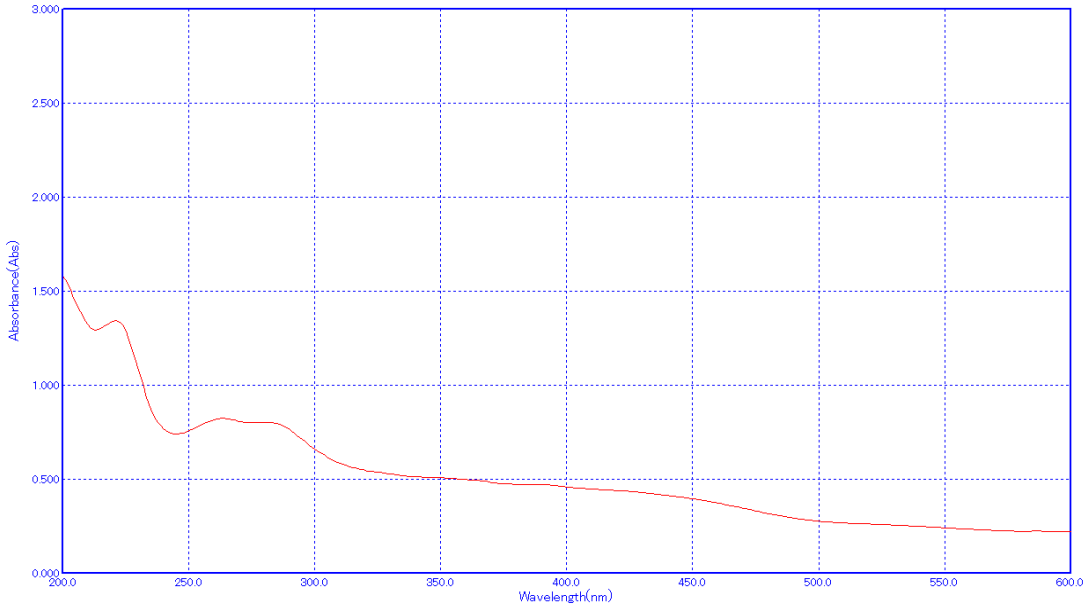

Appendix 6: ^1H NMR (400 MHz, $CDCl_3$) spectrum of compound **47**.

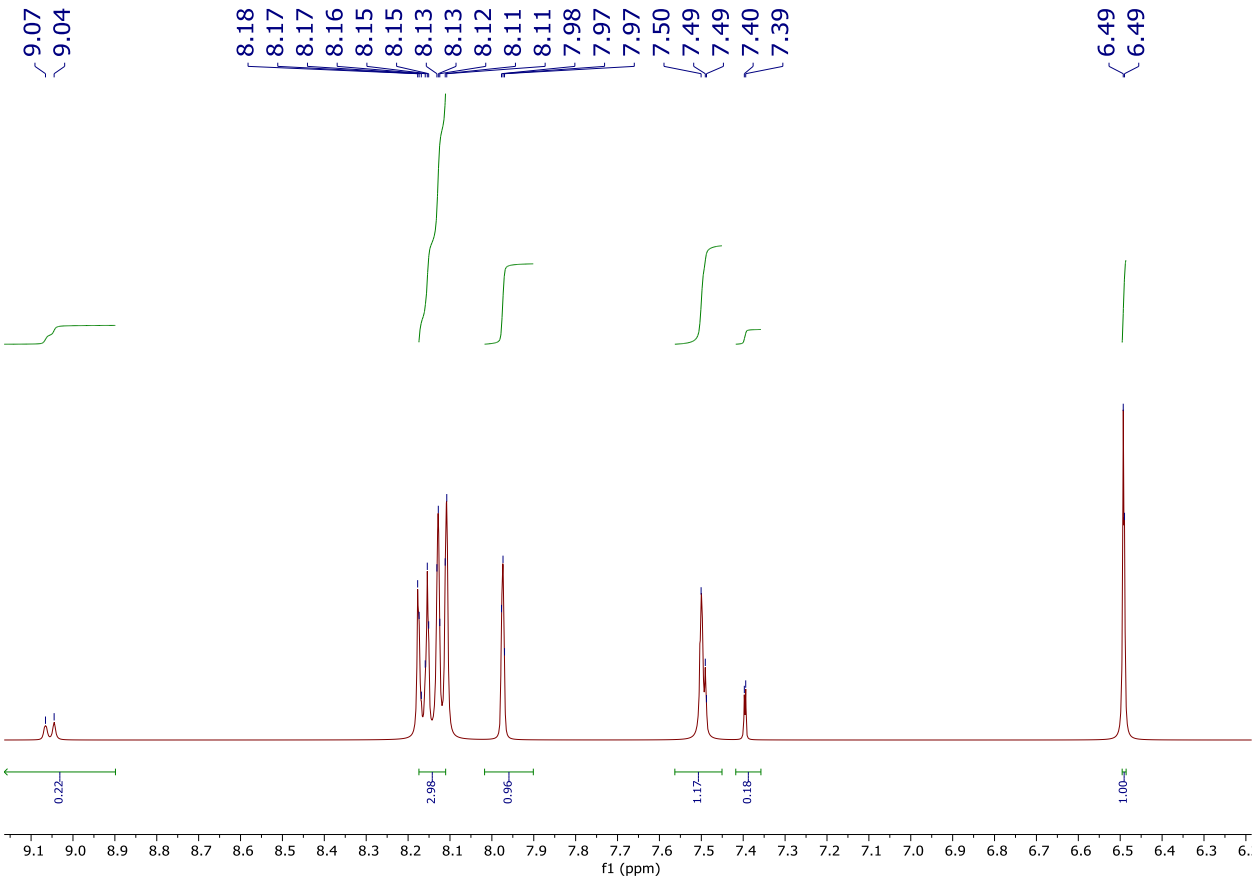

Appendix 7: ^{13}C NMR (100 MHz, $CDCl_3$) spectrum of compound **47.**

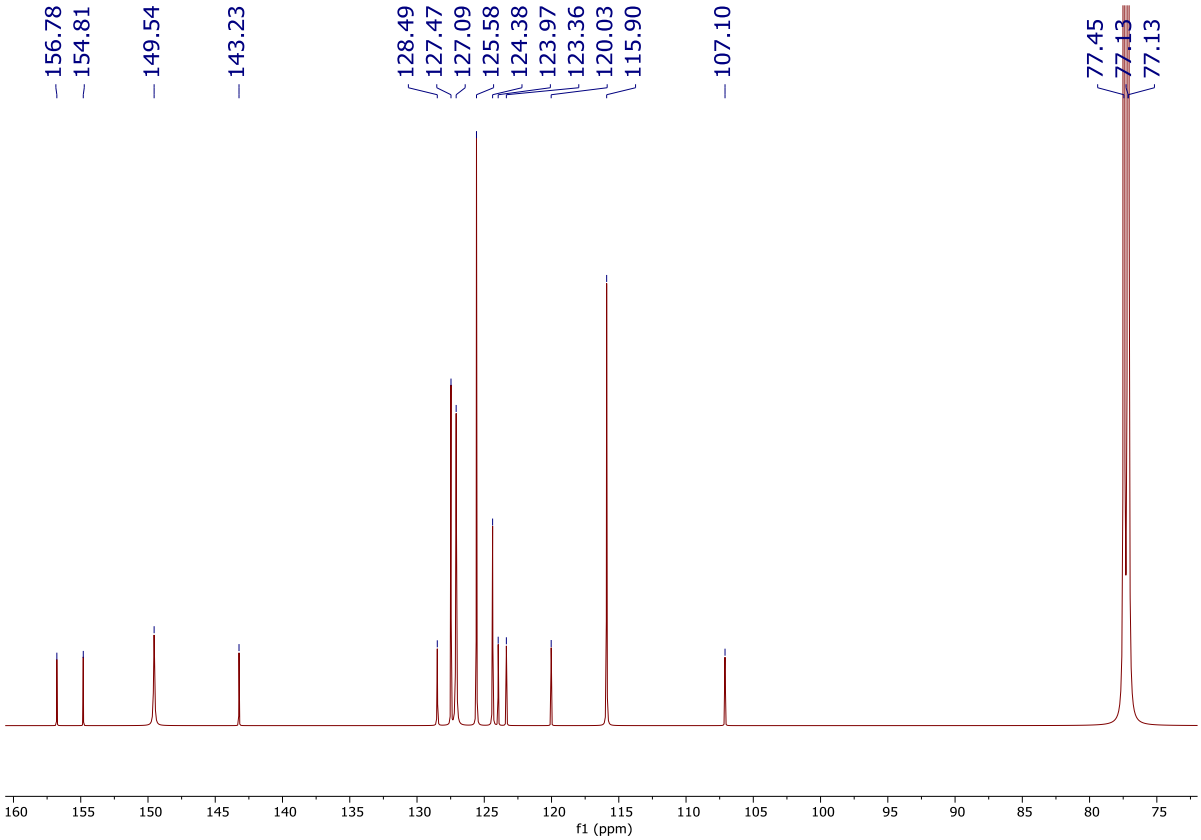

Appendix 8: DEPT-135 NMR (100 MHz, $CDCl_3$) spectrum of compound **47**.

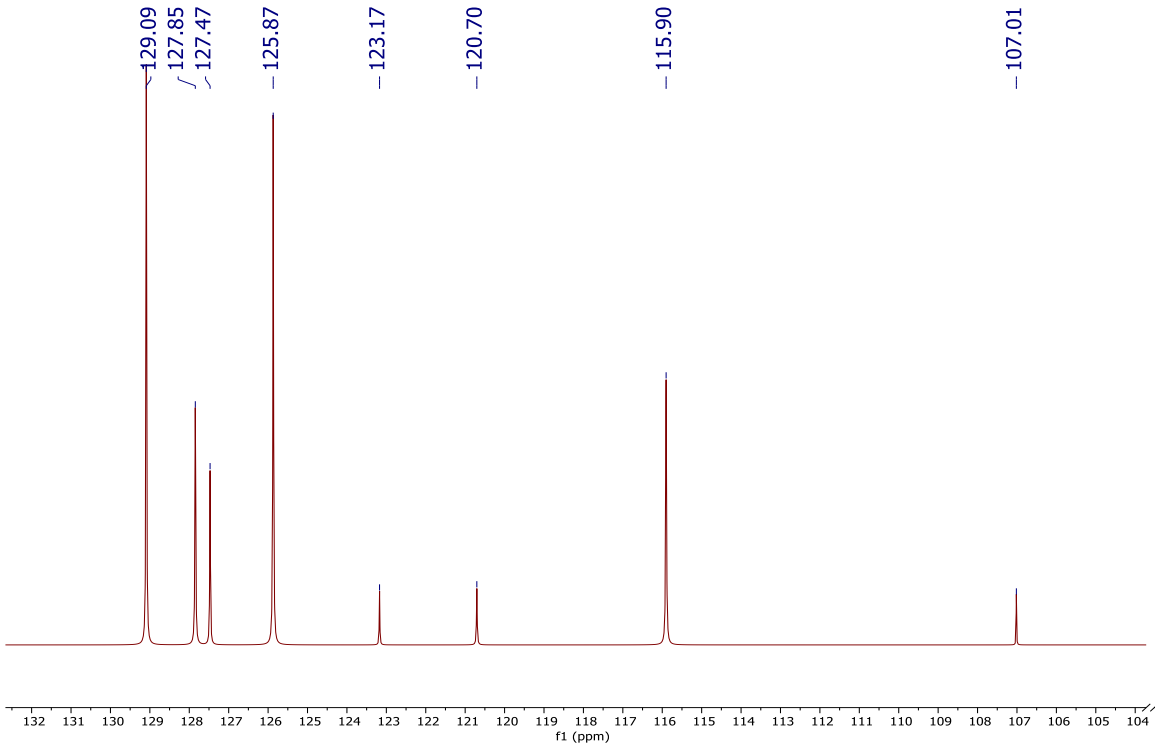

Appendix 9: UV-Vis (200-600 nm, MeOH: H_2O) spectrum of compound **48**.

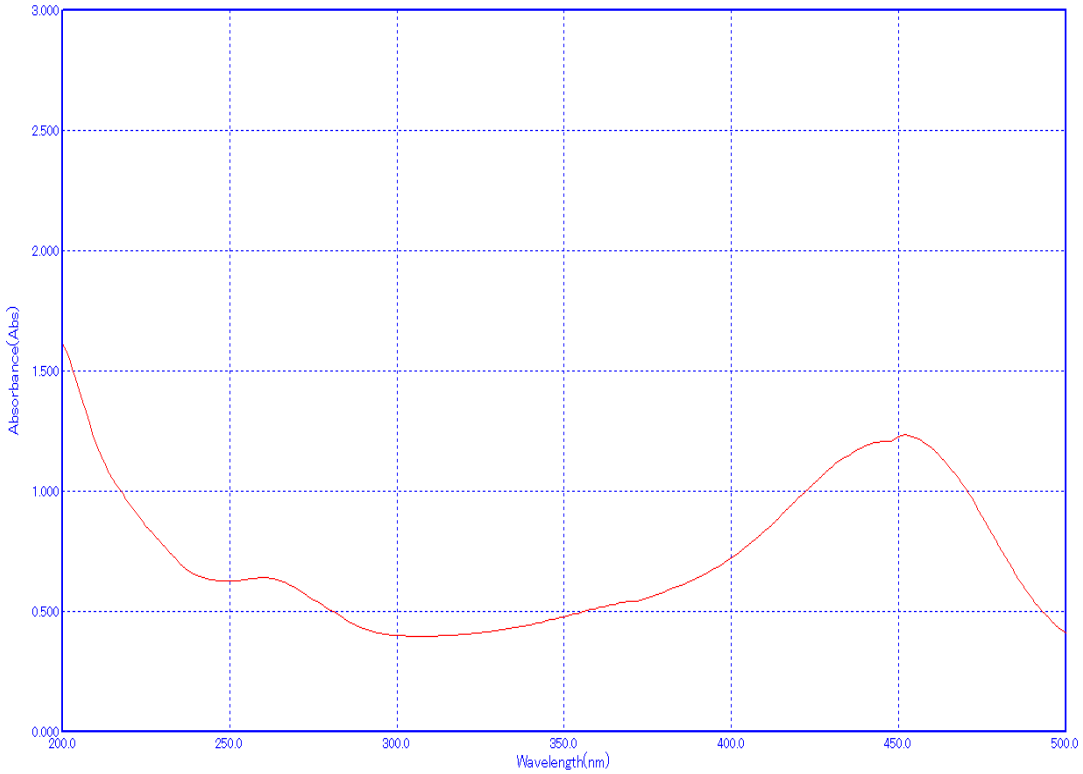

Appendix 10: ^1H NMR (400 MHz, $CDCl_3$) spectrum of compound **48**.

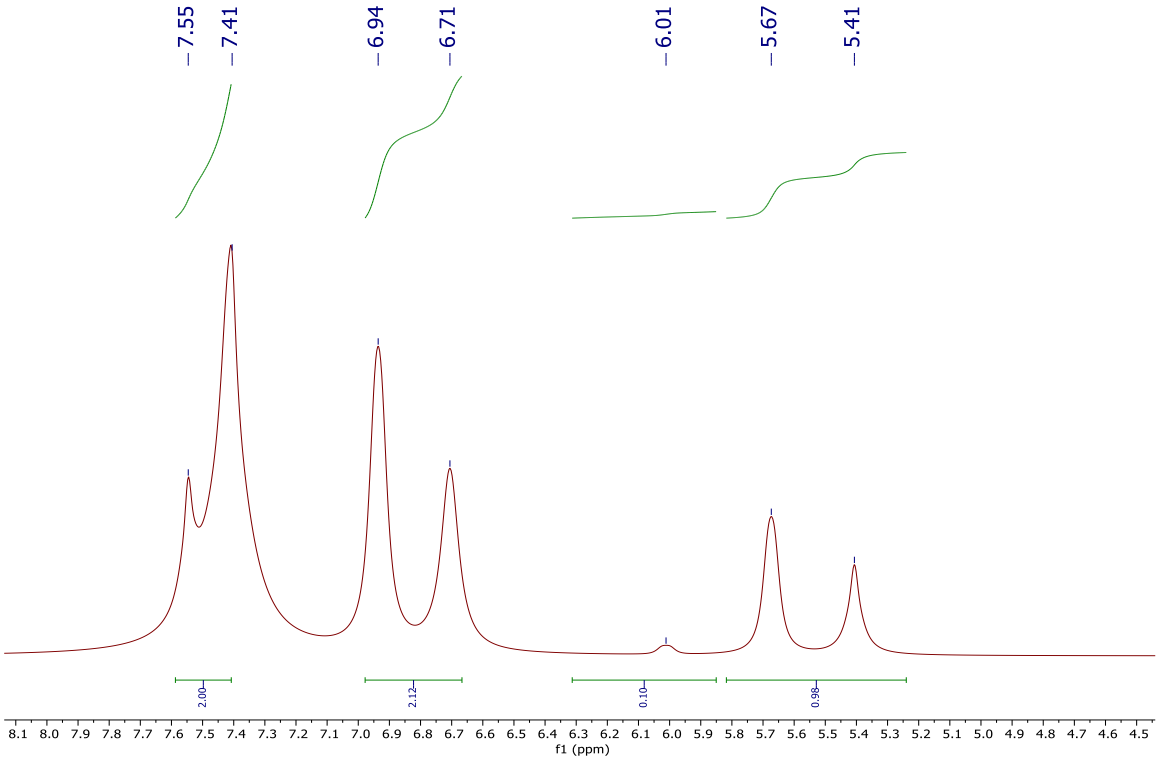

Appendix 11: ^{13}C NMR (100 MHz, $CDCl_3$) spectrum of compound **48**.

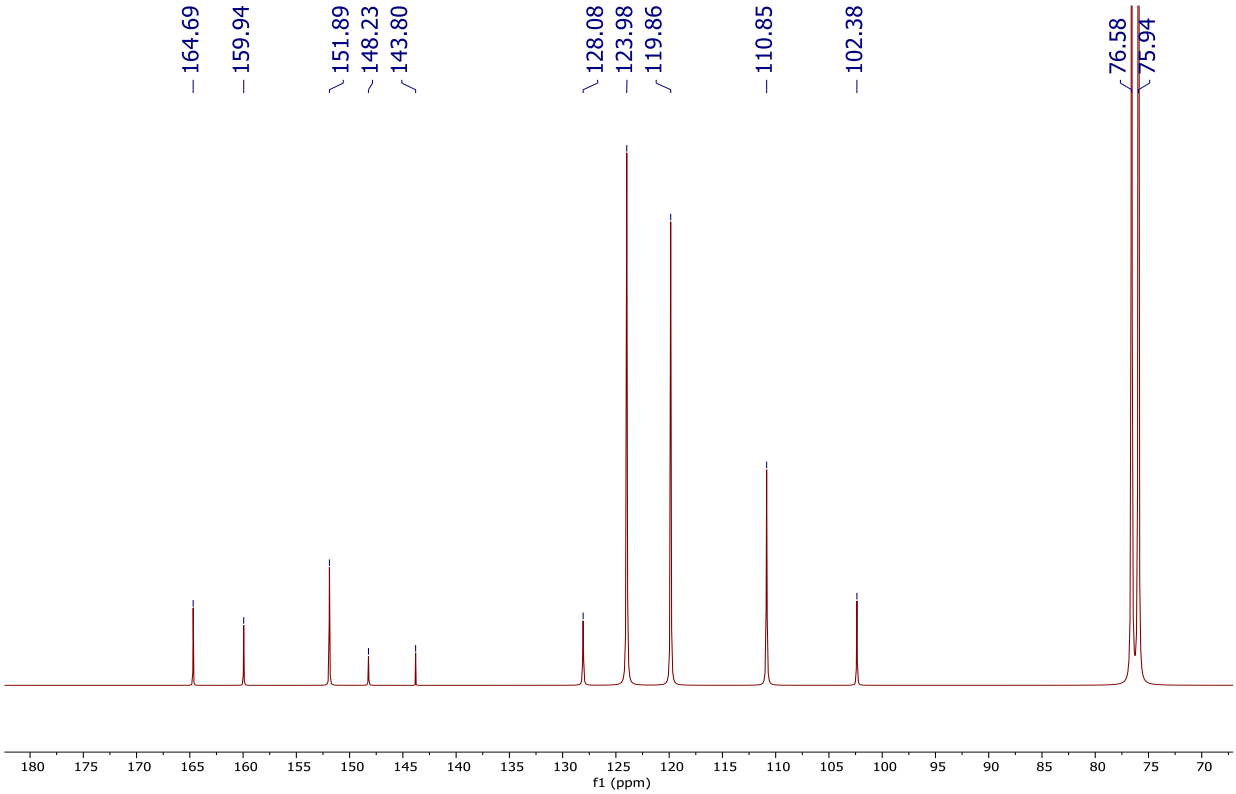

Appendix 12: DEPT-135 NMR (100 MHz, $CDCl_3$) spectrum of compound **48**.

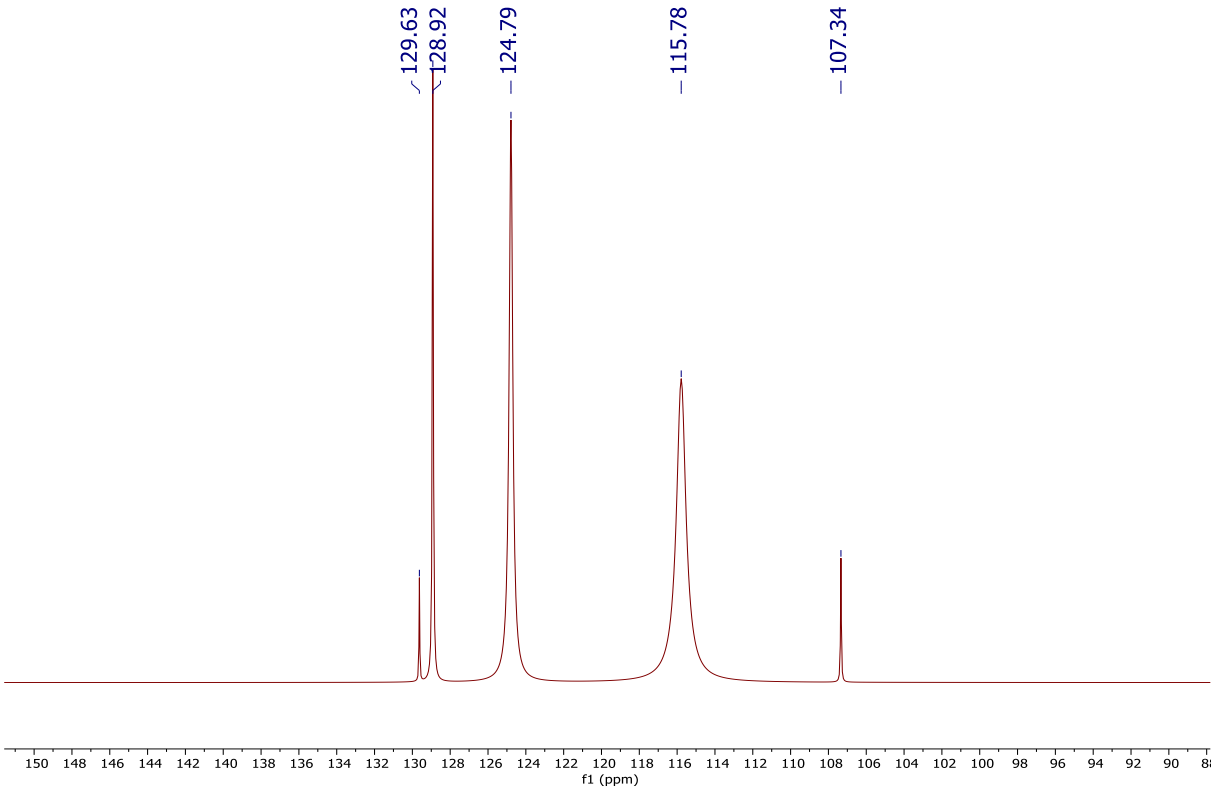

Appendix 13: UV-Vis (200-600 nm, MeOH: H_2O) spectrum of compound **49**.

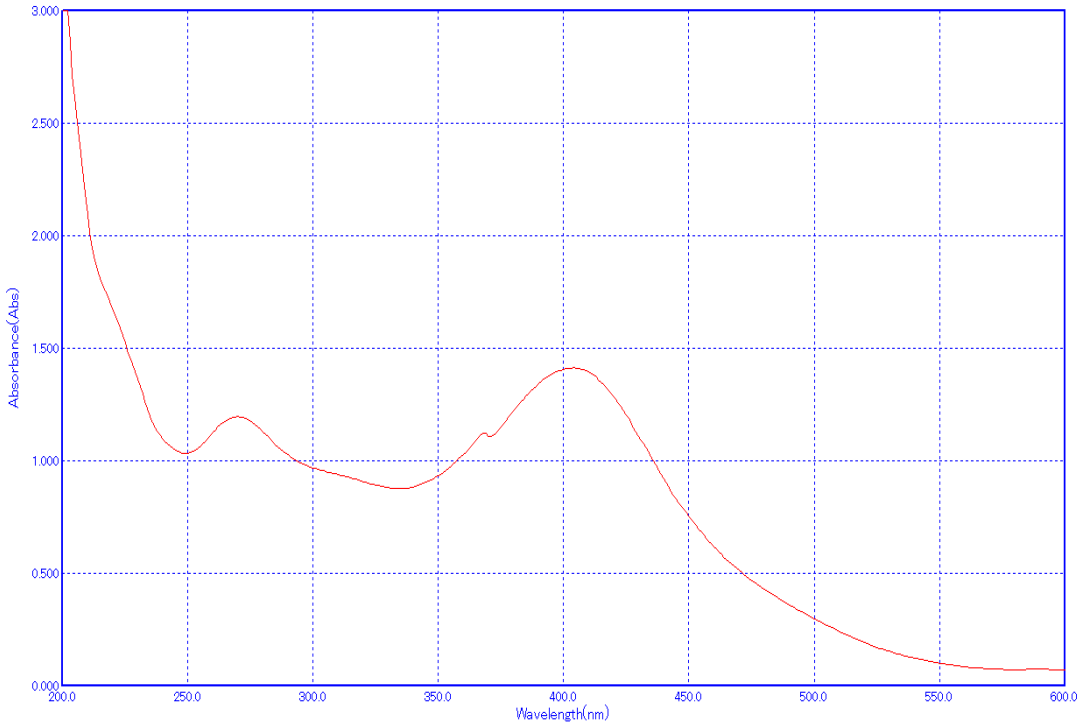

Appendix 14: ^{1}H-NMR (400 MHz, MeOD) spectrum of compound **49.**

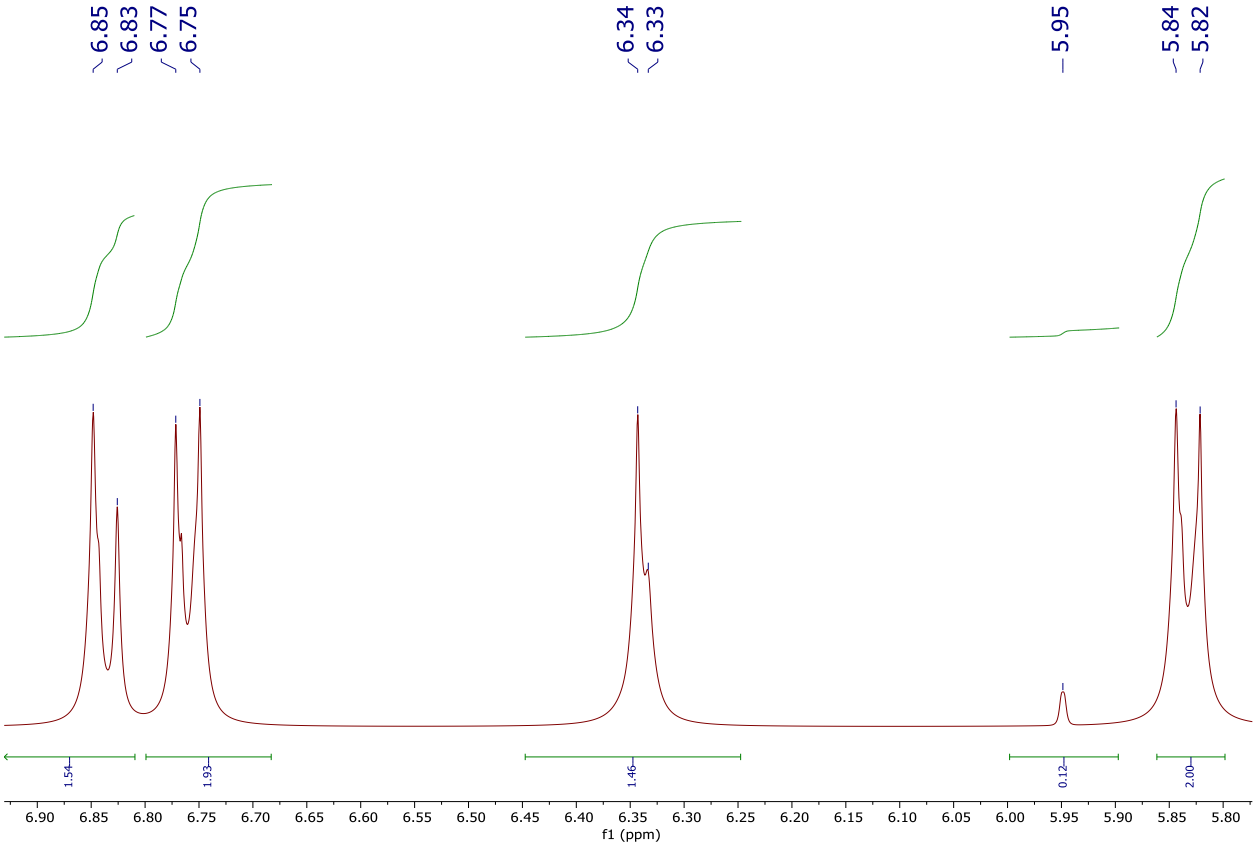

Appendix 15: ^{13}C-NMR (100 MHz, MeOD) spectrum of compound **49.**

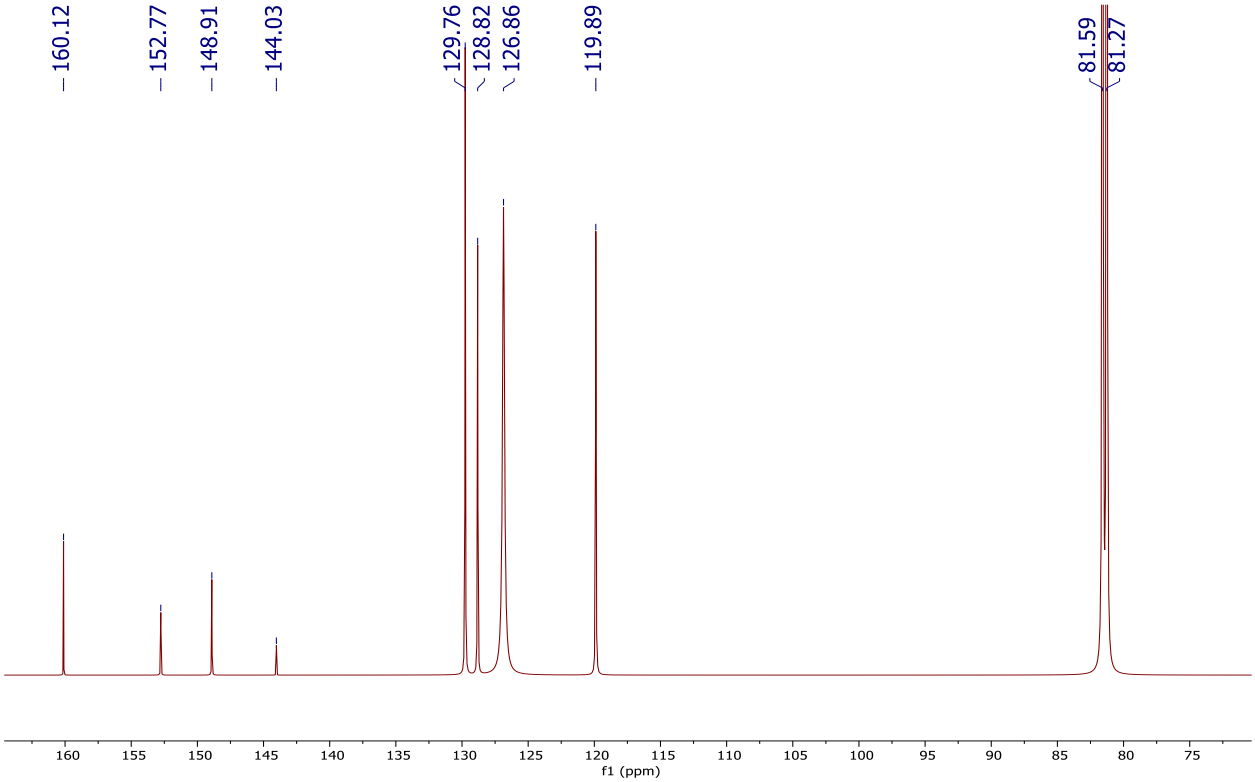

Appendix 16: DEPT-135 NMR (100 MHz, $CDCl_3$) spectrum of compound **49**.

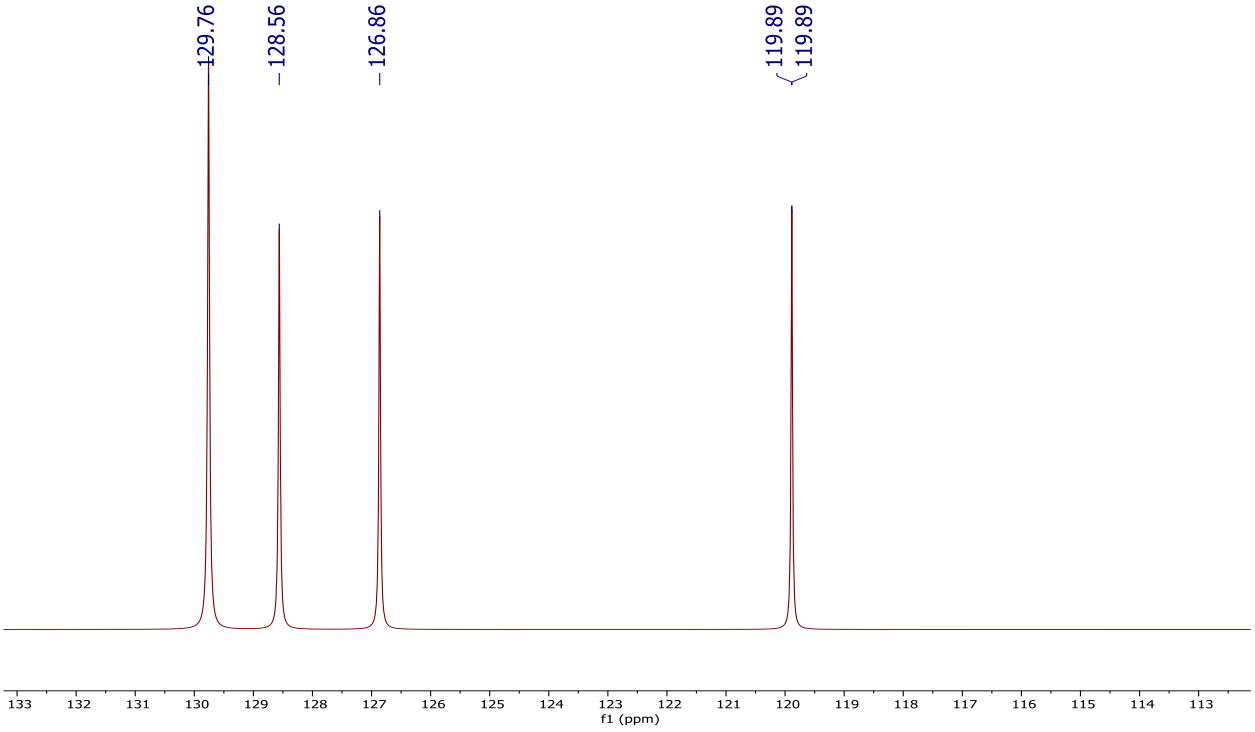

Appendix 17: UV-Vis (200-600 nm, MeOH: H_2O) spectrum of compound **50**.

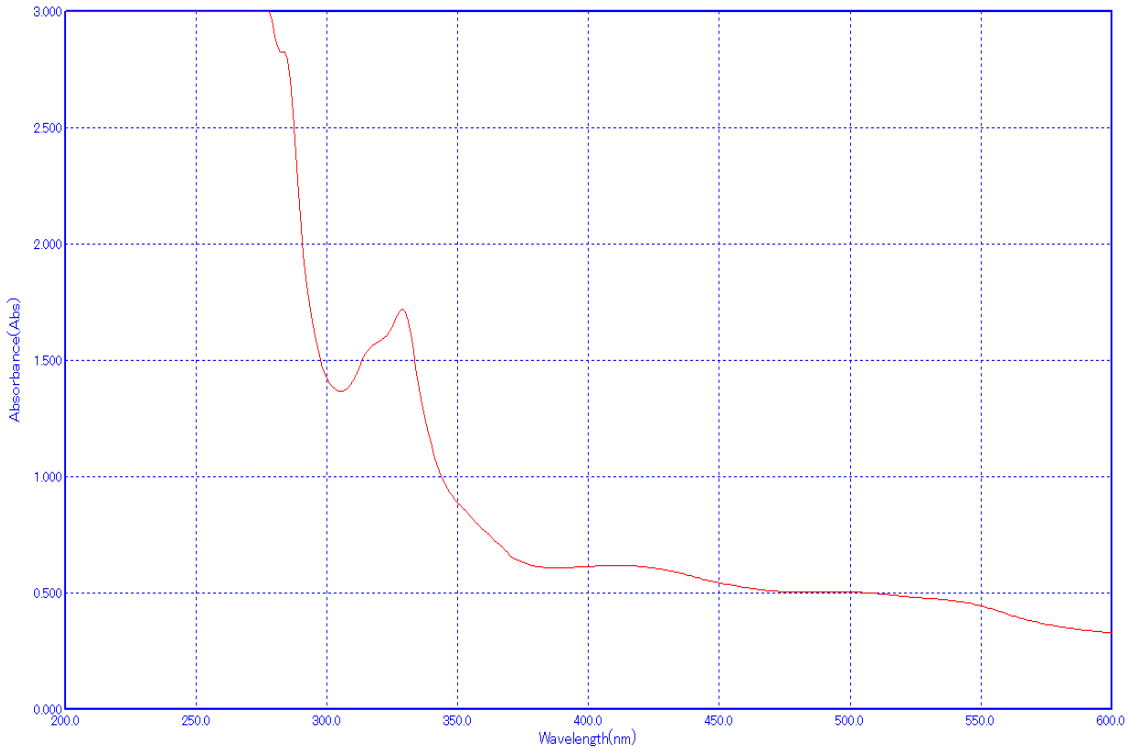

Appendix 18: ^{1}H-NMR (400 MHz, MeOD) spectrum of compound **50.**

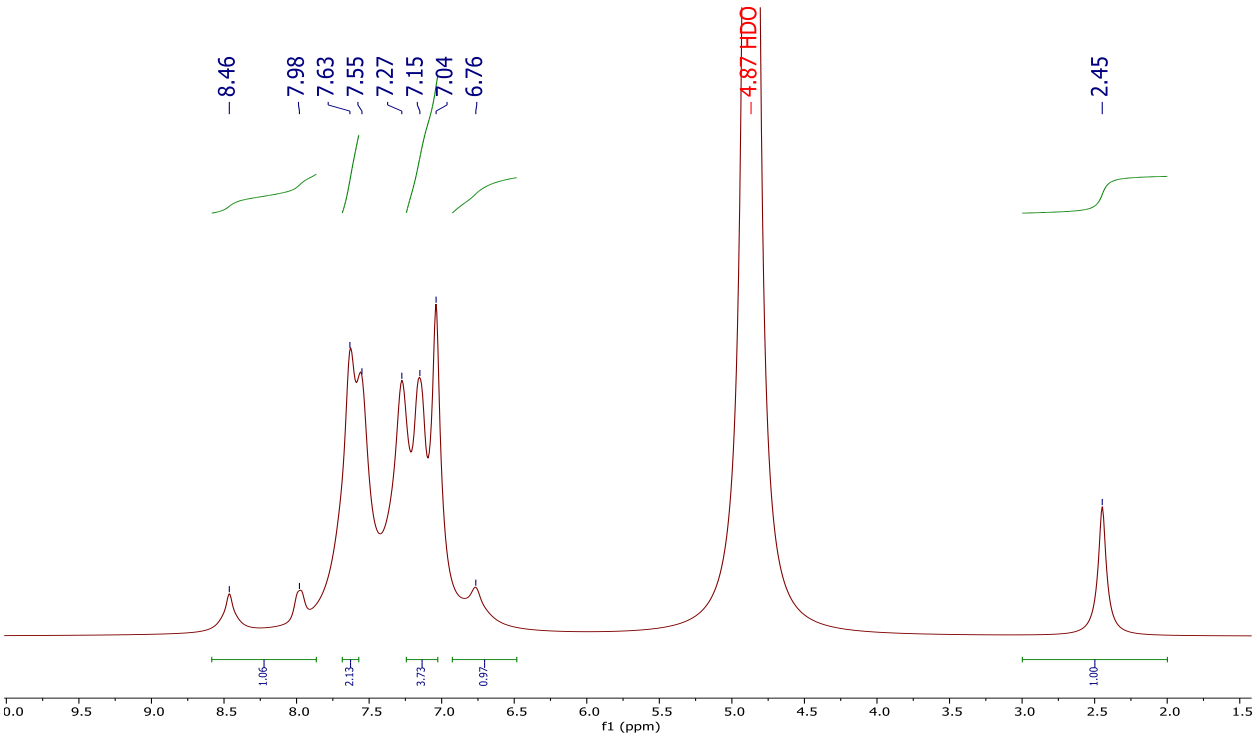

Appendix 19: ^{13}C-NMR (100 MHz, MeOD) spectrum of compound **50.**

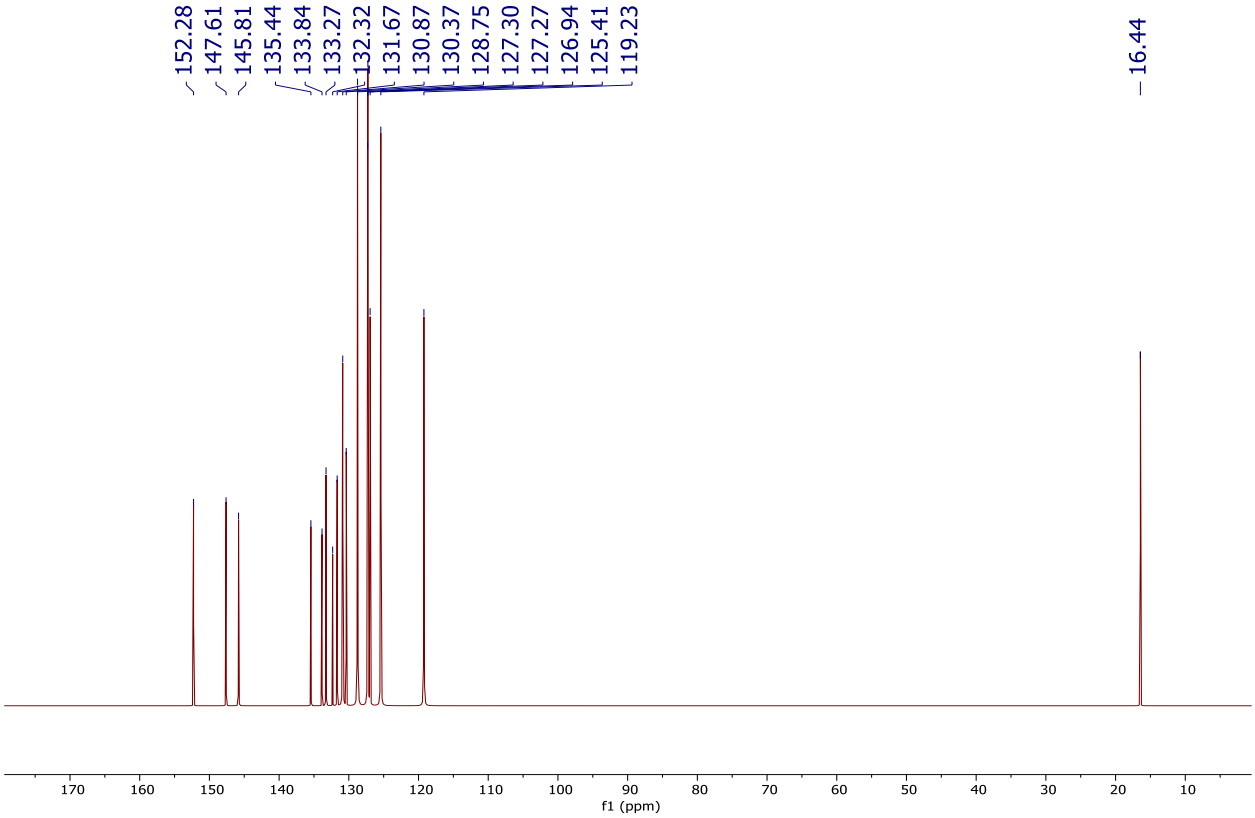

Appendix 20: DEPT-135 NMR (100 MHz, MeOD) spectrum of compound **50**.

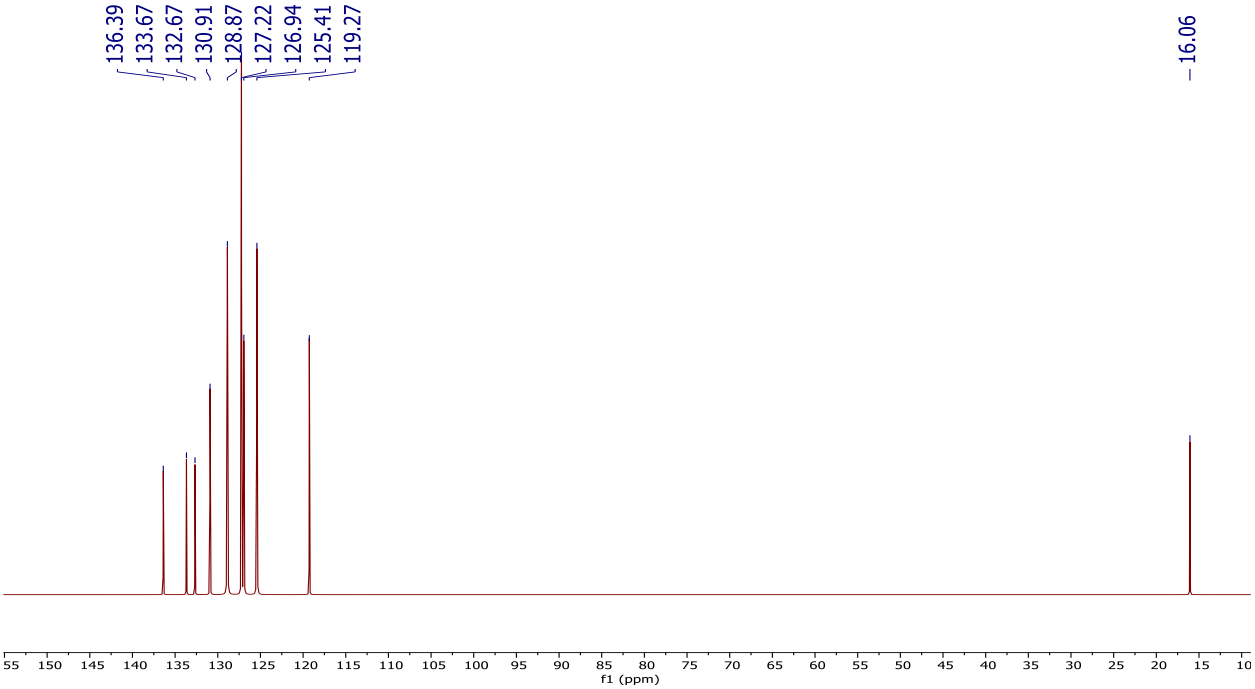

Appendix 21: UV-Vis (200-600 nm, MeOH: H_2O) spectrum of compound **51**.

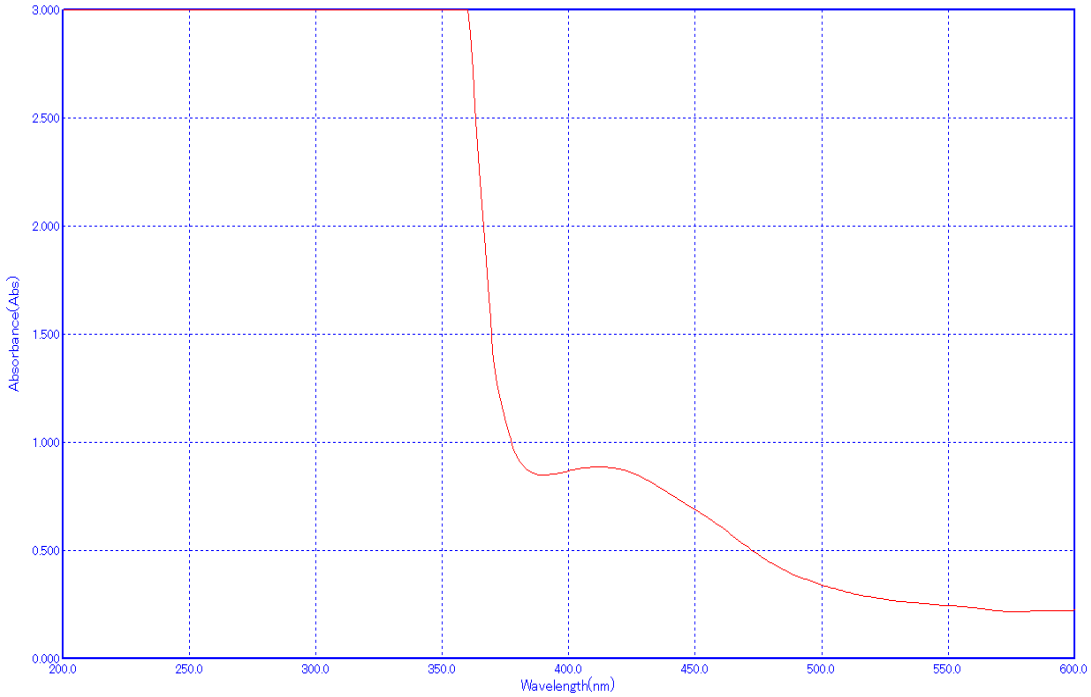

Appendix 22: ^{1}H-NMR (400 MHz, MeOD) spectrum of compound **51.**

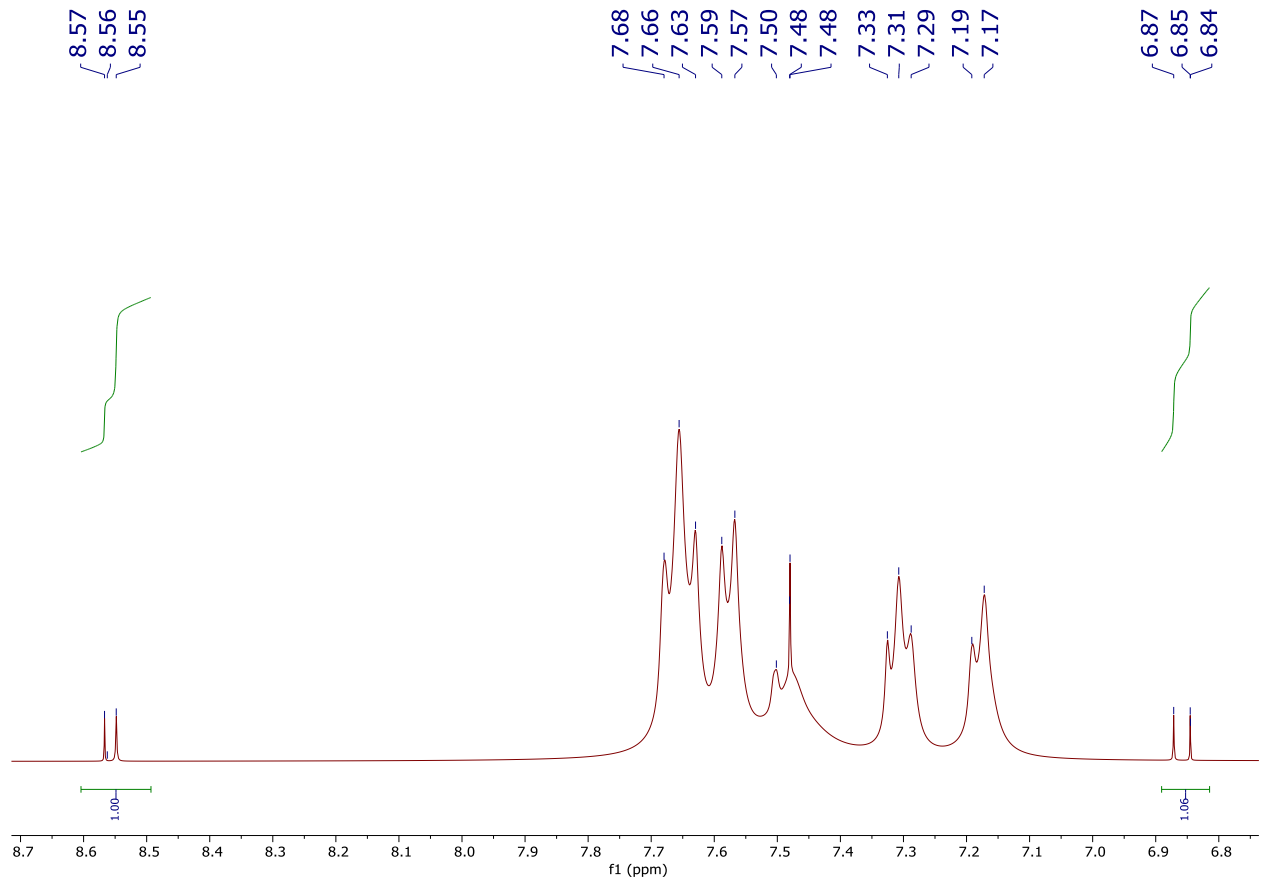

Appendix 23: ^{13}C-NMR (100 MHz, MeOD) spectrum of compound **51.**

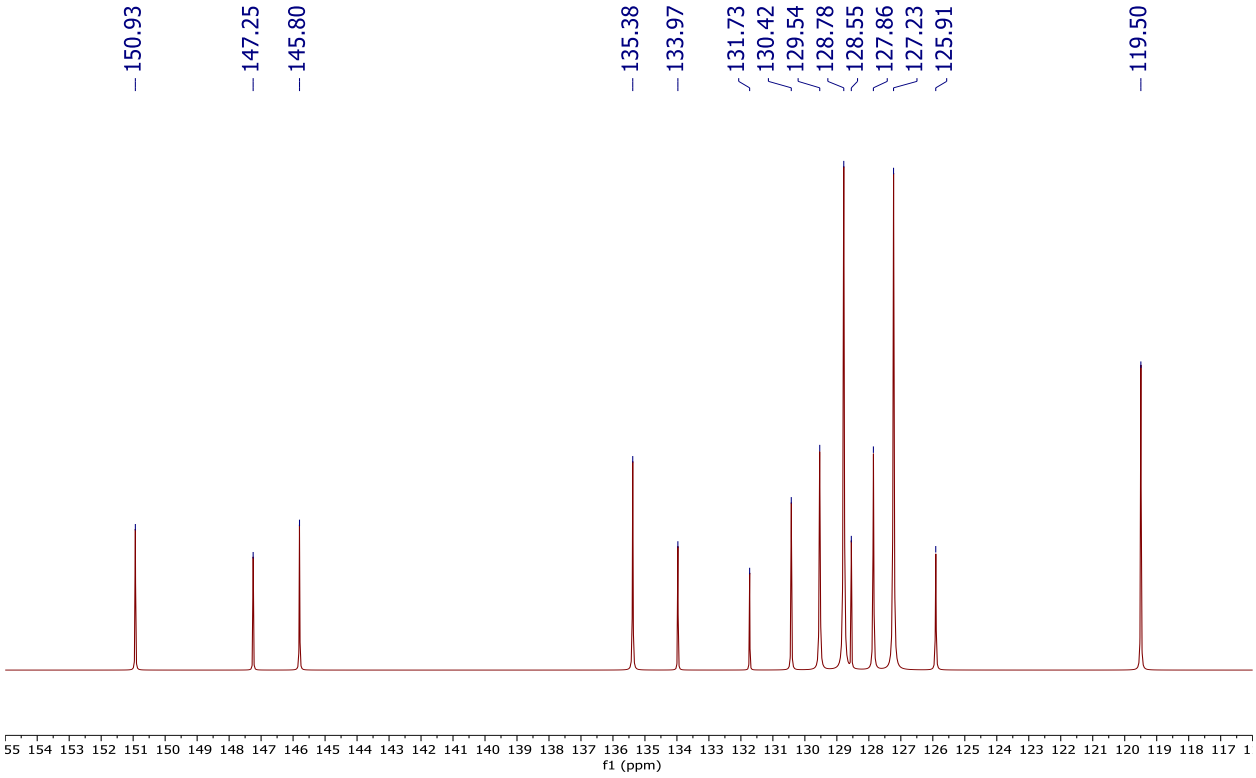

Appendix 24: DEPT-135 NMR (100 MHz, MeOD) spectrum of compound **51**.

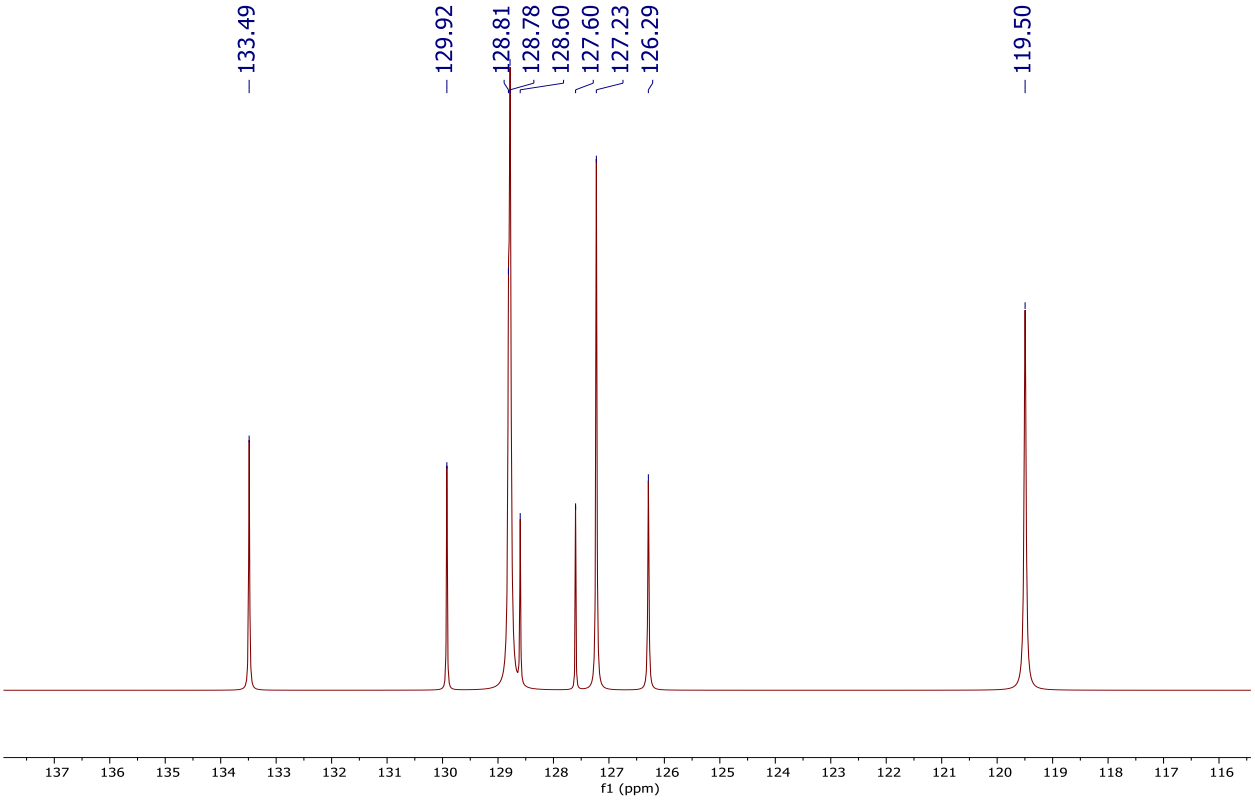

Appendix 25: UV-Vis (200-600 nm, MeOH: H_2O) spectrum of compound **52**.

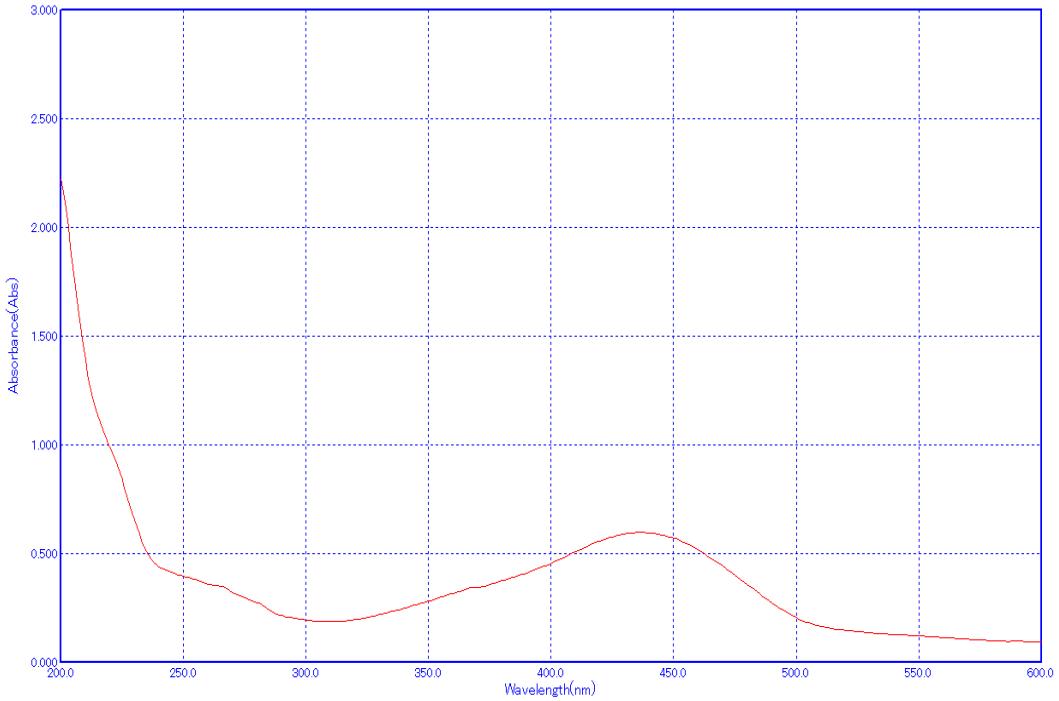

Appendix 26: ^{1}H-NMR (400 MHz, MeOD) spectrum of compound **52.**

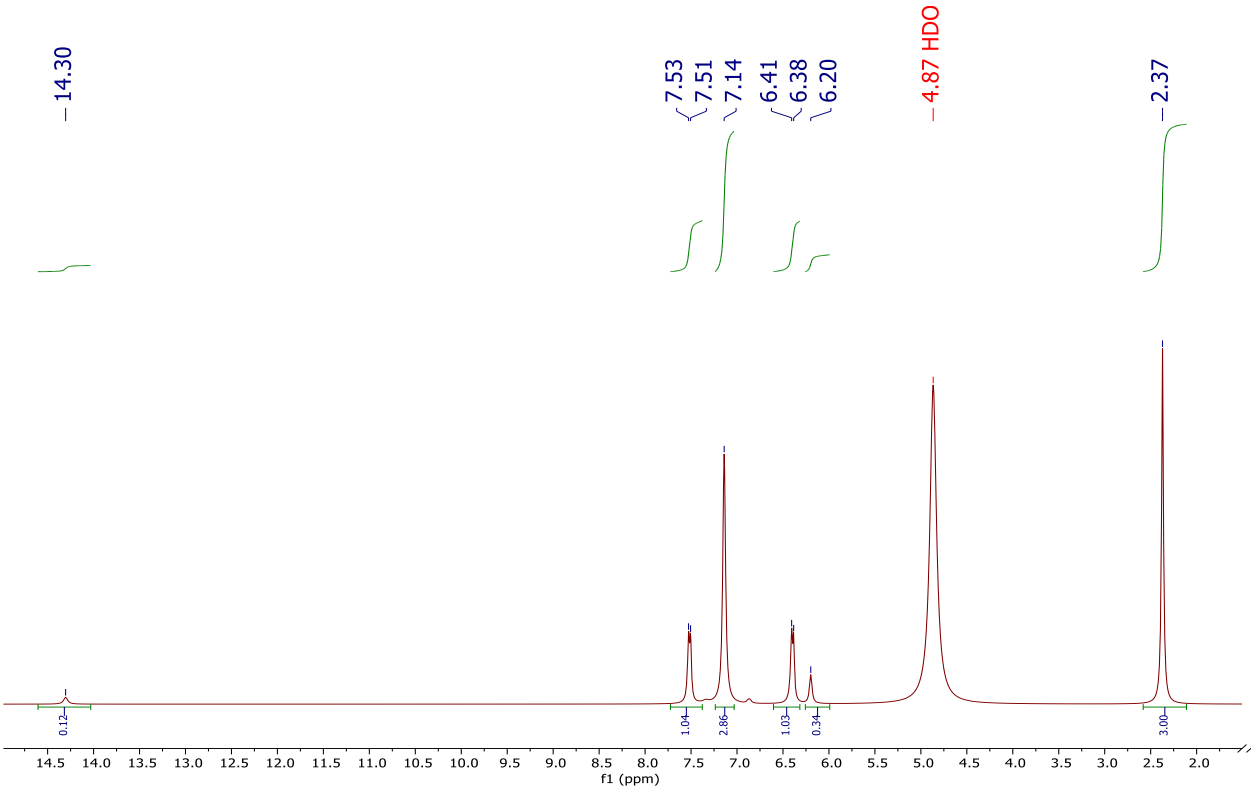

Appendix 27: ^{13}C-NMR (100 MHz, MeOD) spectrum of compound **52.**

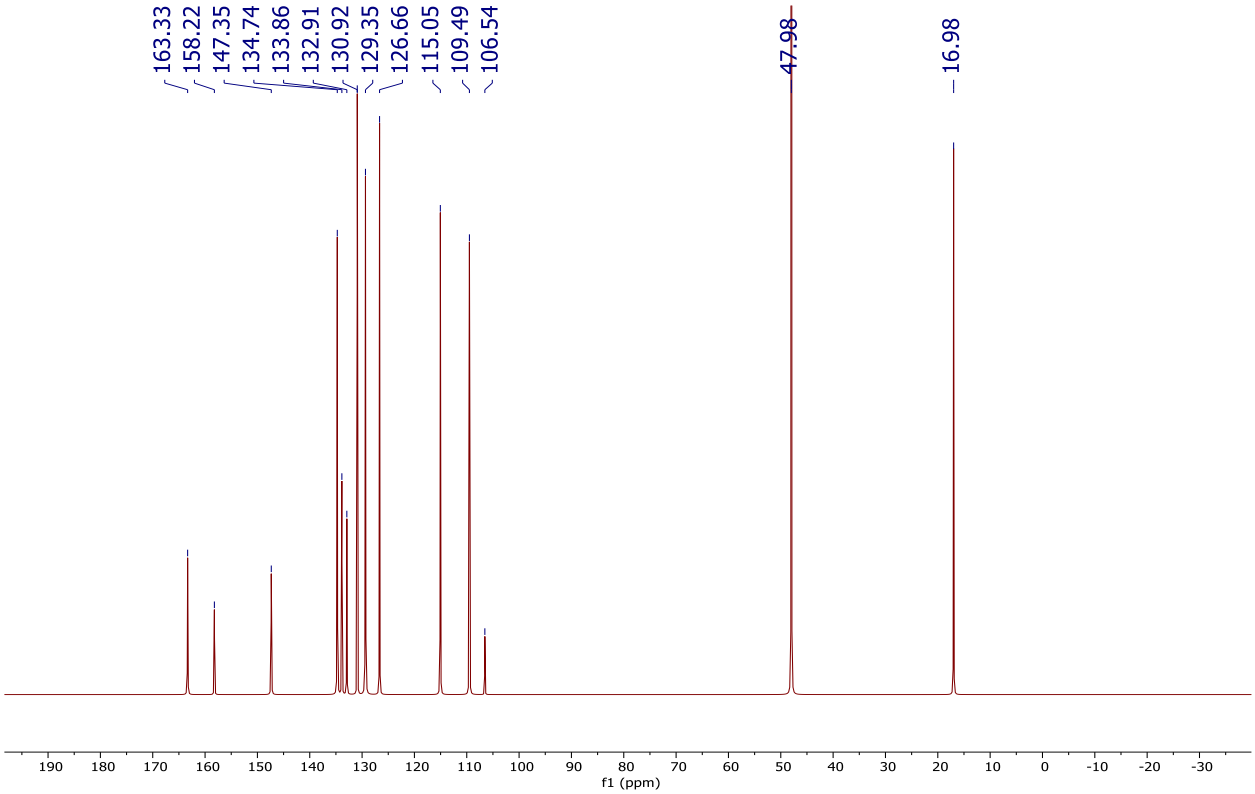

Appendix 28: DEPT-135 NMR (100 MHz, MeOD) spectrum of compound **52.**

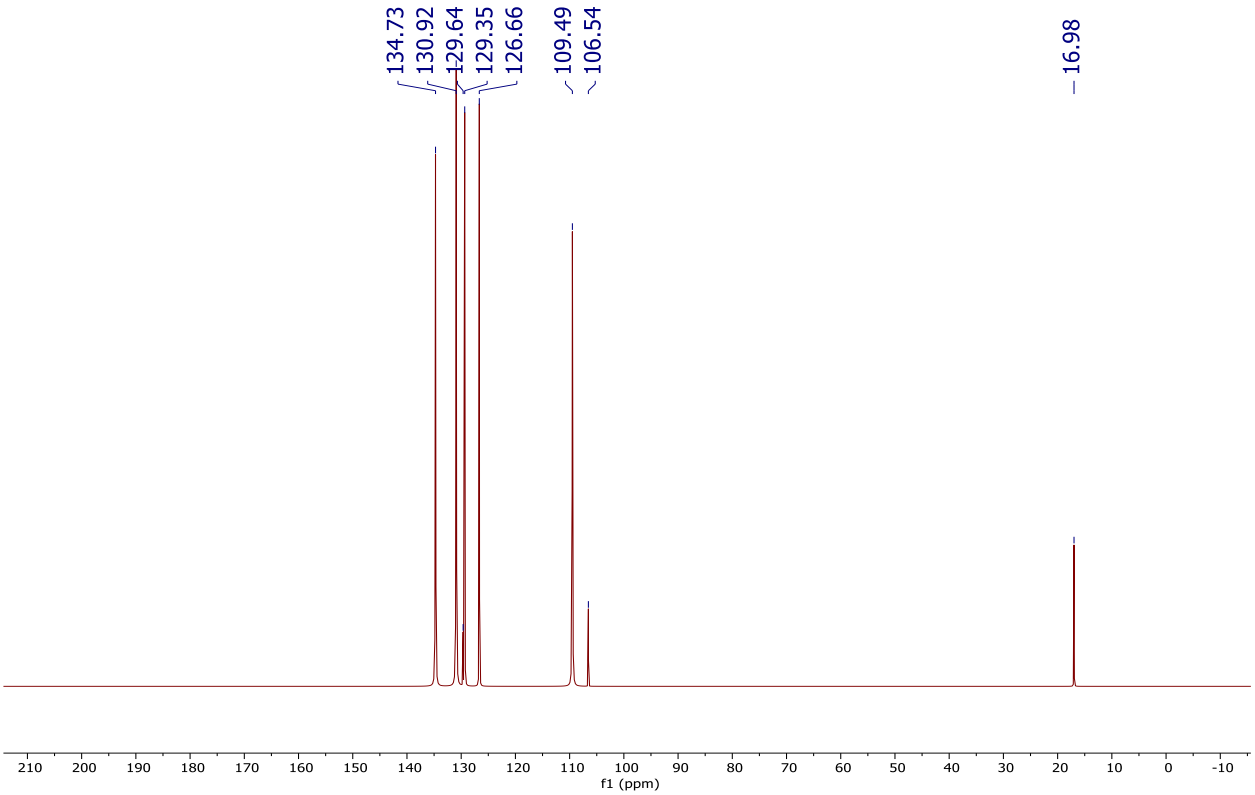

Appendix 29: UV-Vis (200-600 nm, MeOH: H_2O) spectrum of compound **53**.

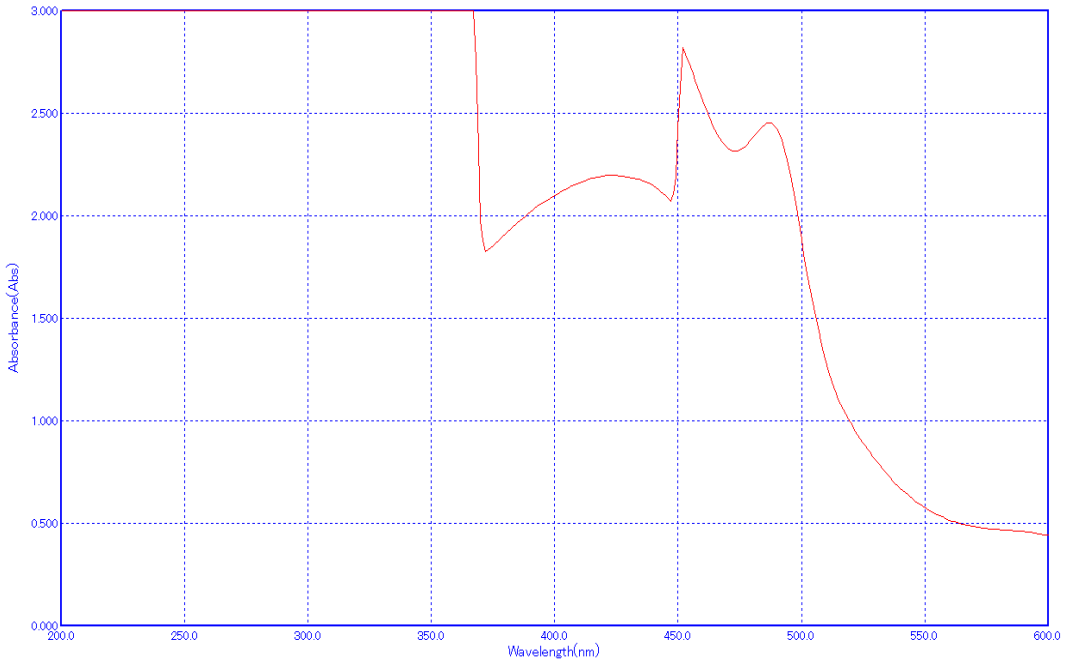

Appendix 30: ^{1}H-NMR (400 MHz, MeOD) spectrum of compound **53.**

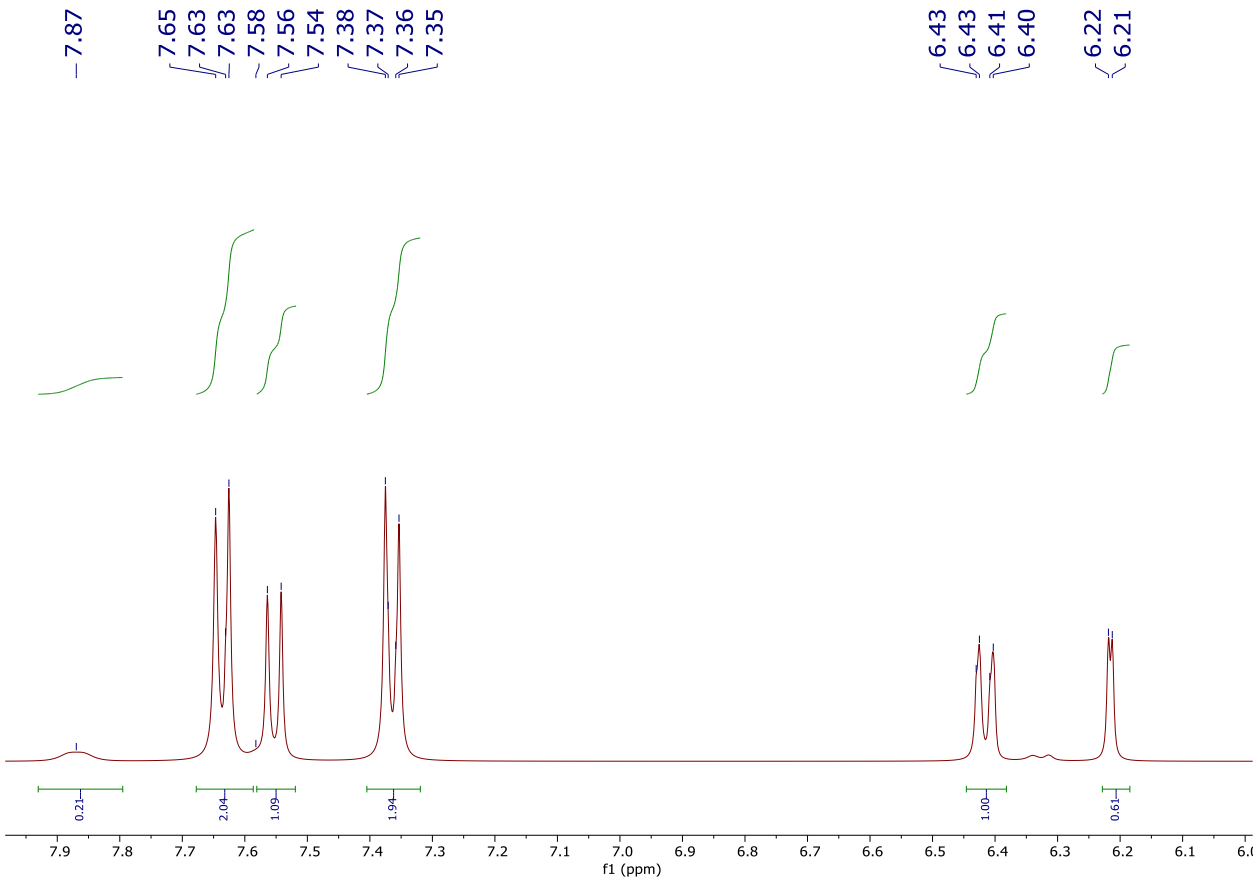

Appendix 31: ^{13}C-NMR (100 MHz, MeOD) spectrum of compound **53.**

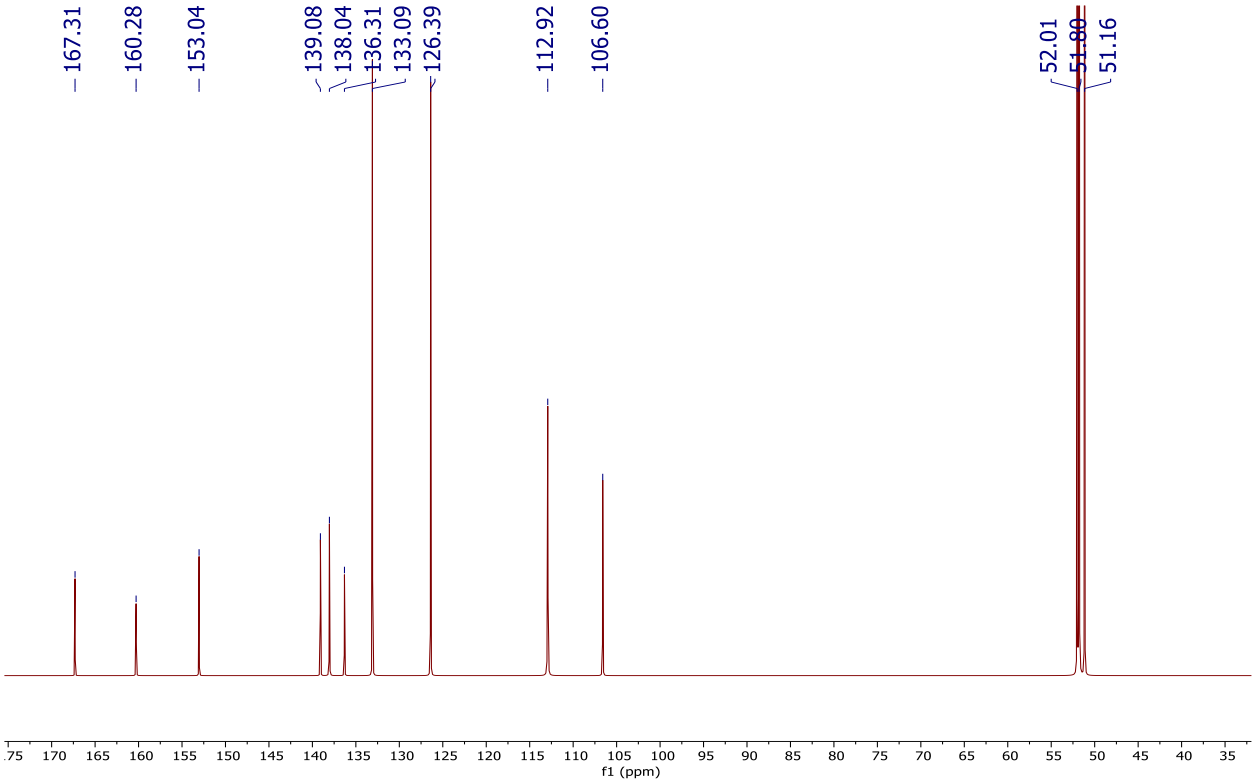

Appendix 32: DEPT-135 NMR (100 MHz, MeOD) spectrum of compound **53.**